TECHNISCHE UNIVERSITÄT MÜNCHEN

Lehrstuhl für Siedlungswasserwirtschaft

Diversities and activities of three sulfidogenic biofilms originated from oil-field water tanks-control strategies to reduce corrosion by application of novel surfactants

Ahmed Ibrahim Mahmoud Sayed Labena

Vollständiger Abdruck der von der Fakultät für Bauingenieur- und Vermessungswesen der Technischen Universität München zur Erlangung des akademischen Grades eines Doktors der Naturwissenschaften (Dr. rer. nat.)
genehmigten Dissertation.

Vorsitzende: Univ. - Prof. Dr. rer. nat. B. Helmreich
Prüfer der Dissertation:

1. Univ. - Prof. Dr. rer. nat. H. Horn, Karlsruher Institut für Technologie
2. Univ. - Prof. Dr. rer. nat. R. F. Vogel

Die Dissertation wurde am 17.10.2012 bei der Technischen Universität München eingereicht und durch die Fakultät für Bauingenieur- und Vermessungswesen am 30.11.2012 angenommen.

Abstract

Three water samples with different salinities (0.23 %, 3.19 % and 5.49 % NaCl) were collected from the Qarun Petroleum Company (QPC) water tanks, Egypt. The water samples were enriched three times and used as an inoculum for biofilm cultivation. Dissimilatory sulfite reductase-β subunit (dsrβ) based on denaturing gradient gel electrophoresis (DGGE) was used to identify the sulfidogenic community's composition directly from the original water samples and from their cultivated biofilms. The three samples showing different microbial diversity composition. The most often detected sulfidogenic bacteria were *Desulfovibrio* spp. (phylum *Proteobacteria*, class *Deltaproteobacteria*) and the *Desulfotomaculum* spp. (phylum *Firmicutes*, class *Closdtridia*). No *Archaea* species were detected by DGGE using the functional gene dsrβ. Therefore, the 16S rRNA cloning technique was used to detect the presence of other *Archaea* such as methanogens that induce corrosion of metal. Only one water sample with low salinity and sulfate content had a positive result with *Archaea* primers. Methanogens were the dominant species in the water sample. The activity of the sulfidogenic biofilms was detected by measuring sulfide production in the bulk phase, the metal corrosion rate and biofilm structure and constituent analyses. The sulfidogenic biofilm cultivated with the highest medium salinity had the highest corrosion rate. These results gave an indication of severe metal corrosion when high chloride anions concentration was present beneath the sulfidogenic biofilm matrix. However, the sulfidogenic biofilm cultivated with the lowest medium salinity and the highest sulfide production showed low metal surface corrosion. The metal corrosion rate in this case was related to the sulfidogenic bacterial activities over the metal surface. Scanning electron microscopy (SEM) and energy dispersive X-ray spectroscopy (EDX) confirmed the effects of salinity and activity on the metal surface by detecting the chloride and the sulfide ions beneath the biofilm matrices. The fully hydrated cultivated biofilms were analyzed by applying the confocal laser scanning microscopy (CLSM) to determine their structure with respect to distribution of extracellular polymeric substance (EPS glycoconjugates and proteins) and microbial population over the metal surface. In order to protect the metal surface from the effects of salinity and activity of sulfidogenic bacteria a novel cationic monomeric surfactant (CMS-I) and two novel cationic gemini surfactants (CGS-II, CGSIII) were synthesized and characterized. Sulfidogenic activities were determined based on sulfide production, redox potential, bio-

film constituents and metal corrosion rate. Comparison of the inhibitory effect of CMS-I and CGS-II was done on the basis of protecting the metal surface from the salinity (3.18 % NaCl) and the activity of sulfidogenic bacteria. The lowest corrosion rate was achieved for sulfidogenic-bacteria at concentration of 10 mM and 1 mM with inhibitory efficiencies of 92 and 94 % for CMS-I and CGS-II, respectively. CGS-II was also applied to inhibit the sulfidogenic bacteria growing at low salinity (0.23 % NaCl). A high inhibitory efficiency of 95 % of the sulfidogenic bacteria was achieved at 1 mM CGS-II. Additionally CGS-III was used to protect the metal surface from the high salinity (5.49 % NaCl) and the activity of sulfidogenic bacteria. The lowest corrosion rate was detected for the sulfidogenic bacteria at concentration of 5 mM CGS-III with an inhibition efficiency of 97 %. The gemini surfactants (CGS-II, CGS-III) showed high ability to inhibit the sulfidogenic-biofilm formation over the metal surface at a concentration of 0.1 mM in comparison to CMS-I at the same concentration. The inhibition efficiency of the synthesized surfactants was discussed in terms of protecting the metal surface from the medium salinity and strong inhibition of the environmental-sulfidogenic communities on the metal surface and in the bulk phase. This efficiency can be achieved by adsorption of the synthesized surfactant molecules on the metal surface and formation of a protective film. The biocide effect of the synthesized surfactants was attributed to an electrostatic interaction between the negatively charged bacterial cell membrane (lipoprotein) and the positively charged ammonium group (NH_4^+) of the synthesized surfactants. In addition, physical disruption also occurs as a result of the penetration of the hydrophobic chains (alkyl groups) of the synthesized surfactants into the cell membrane which leads to damage of the selective permeability of the cell membrane and hence inactivation of the cells occurs.

Keywords: Microbial influenced corrosion, sulfidogenic biofilms, dissimilatory sulfite reductase-β subunit, denature gradient gel electrophoresis, methanogenic *Archaea*, confocal laser scanning microscopy, microbial corrosion inhibition, cationic monomeric surfactant, cationic gemini surfactant.

Kurzfassung

Drei Wasserproben mit verschiedenen Salzkonzentrationen (0,23 %, 3,19 %, und 5,49 % NaCl) wurden aus Wassertanks der Qarun Petroleum Company (QPC), Ägypten, entnommen. Die Wasserproben wurden dreimal angereichter und das Inokulum für die Biofilmkultiverung verwendet. Um die Zusammensetzung der sulfidogenen, mikrobiellen Gemeinschaft zu identifizieren verwendete man das Gen für die β-Untereinheit der dissimilatorischen Sulfitreductase (dsrβ) kombiniert mit der denaturierenden Gradienten-Gelelektrophorese (DGGE). Diese Analyse erfolgte sowohl für die originalen Wasserproben als auch für die kultivierten Biofilme. Diese drei Proben zeigten unterschiedliche Zusammensetzungen in ihrer mikrobiellen Diversität. Dabei wurden am häufigsten die Bakterien *Desulfovibrio* spp. (Familie *Proteobakterien*, Klasse *Deltaproteobakterien*) und *Desulfotomaculum* spp. (Familie *Firmicutes*, Klasse *Clostridien*) gefunden, jedoch keine *Archaeen* mittels DGGE über das funktionelle dsrβ-Gen detektiert. Deshalb wurde versucht über Klonierung der 16S rRNA das Vorkommen anderer *Archaeen*, wie z.B. methanogener, welche für die Korrosion von Metall verantwortlich sind, nachzuweisen. Ein positives Ergebnis mittels archaeellen Primern zeigte nur eine Wasserprobe (geringer Salz- und Sulfatgehalt), in welcher methanogene *Archaeen* die dominierende Gruppe darstellten. Über Messung der Sulfidzunahme in der Flüssigphase, die Korrosion des Metalls und Veränderungen in der Struktur und Zusammensetzung des Biofilms auf der Metalloberfläche wurde die Aktivität des sulfidogenen Biofilms ermittelt. Dabei stellte sich heraus, dass der Biofilm im Medium mit dem höchsten Salzgehalt auch die stärkste Korrosion verursachte. Dieses Ergebnis gab einen Hinweis darauf, wie schwere Metallkorrosion unter Anwesenheit hoher Konzentrationen an Chlorid Ionen in der Matrix der sulfidogenen Biofilme verursacht werden könnte. Jedoch zeigte sich Korrosion auf der Metalloberfläche auch an jenem Biofilm die mit dem geringsten Salzgehalt im Medium und der höchsten Sulfid Produktion kultiviert wurden. In diesem Fall war die Korrosion des Metalls durch die Aktivität der sulfidogegen Bakterien über der Metalloberfläche bedingt. Die Effekte der Salinität und auch der mikrobiellen Aktivität auf der Metalloberfläche wurden durch Auswertung von rasterelektronen-mikroskopischen Daten (SEM) und dem Einsatz der Energie-Dispersions-Röntgen-Spektroskopie (EDX) bestätigt indem direkt die Chlorid und Sulfid Ionen unter den Biofilmen gemessen wurden. Zusätzlich wurden vollständig

hydratisierte Biofilme mit Hilfe der konfokalen Laser-Scanning-Mikroskopie (CLSM) mit dem Ziel untersucht deren Struktur hinsichtlich der Verteilung der extrazellulären, polymeren Substanzen (EPS Glykokonjugate und Proteine) und der mikrobiellen Population auf der Metalloberfläche zu analysieren. Zum Schutz der Metalloberfläche vor den Effekten des Salzgehaltes von 3,19 % NaCl und der Aktivität sulfidogenischer Bakterien kamen drei Tenside zum Einsatz: ein neues kationisches Monomer (CMS-I) und zwei neue kationische Gemini-Tenside (CGS-II, CGS-III) welche charakterisiert werden sollten. Die Bestimmung sulfidogenischer Aktivität erfolgte über die Suflid Produktion, das Redoxpotential, Bestandteile des Biofilms und die Korrosionsrate des Metalls. Der Schutz der Metalloberfläche vor den Einflüssen der Salinität und der Aktivität der sulfidogenischen Bakterien diente als Grundlage für den Vergleich der hemmenden Effekte von CMS-I mit dem von CGS-II. Die geringste Korrosionsrate wurde dabei für sulfidogenische Bakterien bei 10 mM und 1 mM, mit einer effektiven Hemmung von 92 % bei CMS-I und 94 % bei CGS-II, erreicht. CGS-II wurde zudem benutzt um das Wachstum sulfidogenischer Bakterien bei niedrigem Salzgehalt von 0,23 % NaCl zu inhibieren. Ebenso wurde eine hohe Hemmungseffizienz von 95 % bei einer Konzentration von 1 mM CGS-II bei den sulfidogenischen Bakterien erzielt. Zum Schutz der Metalloberfläche vor hoher Salzkonzentration von 5,49 % NaCl und sulfidogenischen Bakterien wurde für das Benetzungsmittel CGS-III verwendet. Dabei reichte 5 mM CGS-III aus um eine Hemmung von 97 % zu erreichen. Die zwei Gemini-Tenside CGS-II und CGS-III zeigten, verglichen mit CMS-I und bei gleicher Konzentration von 0,1 mM eine hohe Hemmung der Biofilmbildung auf der Metalloberfläche. Es wurde vermutet, dass die hohe Effizienz der synthetisierten Benetzungsmittel einerseits auf den Schutz der Metalloberfläche vor dem Salzgehalt des Mediums zurück zu führen ist, andererseits diese Substanzen das Wachstum der sulfidogenischen Bakteriengemeinschaft stark hemmen, sowohl auf dem Metall als auch in der Flüssigphase. Dieser Effekt entsteht dadurch, dass die Moleküle dieser Benetzungsmittel an die Metalloberfläche adsorbieren und einen Schutzfilm bilden. Die biozide Wirkung dieser Benetzungsmittel beruht auf der elektrostatischen Wechselwirkung der positiv geladenen Ammonium-Gruppe (NH_4^+) mit der negativ geladenen bakteriellen Zellmembran (Lipoproteine). Zusätzlich entsteht eine „aktive“ Störung in der selektiven Permeabilität der Zellwand als Ergebnis der Durchdringung dieser durch die hydrophoben Ketten (Alkylgruppen) der synthetischen

Benetzungsmittel was schließlich zur Beschädigung der Zellwand und damit dem Tod der Zelle führt.

Schlüsselbegriffe: Mikrobiell beeinflusste Korrosion; Sulfidogenische Biofilme; dissimilatorische Sulfitreduktase β-Untereinheit; denaturierende Gradienten-Gelelektrophorese; methanogene Archaeen; konfokale Laser-Scanning Mikroskopie; Hemmung mikrobieller Korrosion; kationisches, monomeres Benetzungsmittel; kationisches Gemini-Tensid.

Acknowledgments

With immense pleasure, I would like to express my heartfelt gratitude to my advisor Prof. Dr. Harald Horn for his guidance during the course of this work at Water Quality Control institute, Technical University of Munich. I render my appreciation to him for giving me a simulating research environment, valuable comments (that I will never forget). Prof Horn, thanks a lot for your trust and enthusiasm. I would like also to express my deepest gratitude to Dr. Elizabeth Müller for the informative and helpful discussion as well as showing me the molecular biology world through provision of support and valuable advices. She learned me how I can write a good scientific paper, thanks a lot Dr Müller. I would like to express my deepest gratitude to Prof. Rudi Vogel for his kindly acceptance to review my thesis. I am deeply indebted to Prof. Dr. Brigitte Helmreich for her support especially at the first days. I would like to express my thanks to Dr. Hocin Arab, Dr. Tomas Neu, Dr. Michael Wagner, Dr. Christoph Haisch, Dr. Andrea Hille-Reichel and Mrs. Christine Sternkopf for their kind suggestion and Microscopy analysis help. I would like to express my gratefully acknowledge the invaluable help and cooperation of Ms. Ursula Wallentits, Ms. Susanne Thiemann, Ms. Stephanie West, Mr. Wolfgang Shröder, Mr. Hubert Moosrainer, and Mr. Claus Lindenblatt. Thanks a lot for your support, your kind suggestions and help. They were always ready to help me and give me the feeling that i am at home and between my family. I am extremely grateful to the secretary teamwork Ms. Susanne Wieseler, Ms. Marianne Lochner, Ms. Therese Puchall for their kind help and friendly dealing. I am highly obliged and gratefully acknowledge to my friends and colleagues at Water quality control institute, Dr. Danial Taherzadeh, Dr. David Martinez, Dr. Hoa Kieu, Dr. Liu Sitong, Dr. Konrad Koch, Yang Li, Evelyn Walter, Kehl Oliver, Christina Klarmann, Tobias Rocktäschel, Bastian Herzog, Riccardo Matruglio, Mohamed Rajab, and Mateo Urena. Many thanks for my friends and colleagues at the Egyptian Petroleum Institute, Egypt for their kind support. Especial thanks for Dr. Mamoun and his teamwork at Qarun Petroleum Company (QPC), Egypt for their support and help. Last and not least I wish to dedicate my entire thesis to my family, my wife, lovely daughters, father, mother and brothers for their encouragement and support.

(Ahmed Labena)

List of abbreviations

AFM	Atomic force microscopy
AH2	Hydrogen as electron donor
AMP	Adenosine monophosphate
APB	Acid-producing bacteria
APS	Adenosine phosphosulfate
ATP	Adenosine triphosphate
Blast	Basic local alignment search tool
CB	Cultivated biofilm
C_{cmc}	Critical micelle concentration
CGS	Cationic gemini surfactant
CLSM	Confocal laser scanning microscopy
CMS	Cationic monomeric surfactant
DANN	Deoxyribonucleic acid
DDBJ	DNA Data Bank of Japan
DGGE	Denaturing gradient gel electrophoresis
DSMZ	Deutsche Sammlung von Mikroorganismen und zellkulturen GmbH, Braunschweig, Germany
dsrβ	Dissimilatory sulfite reductase-β subunit
EDS or EDX	Energy dispersive X-ray spectroscopy
EMBL	European Molecular Biology Laboratory, UK
EPS	Extracellular polymeric substance
ESEM	Environmental scanning electron microscopy
FITC	Fluorescein-isothiocyanate
FTIR	Fourier transforms infrared spectroscopy
GC	Mole percent of guanine and cytosine
HSLs	N-acyl homoserine lactones
LB	Luria broth
MDB	Metal-depositing bacteria
Me	Metal ion
MIC	Microbially influenced corrosion
MPN	Most probable number
MRB	Metal-reducing bacteria

List of abbreviations

NCBI	National Center for Biotechnology
NMR	Nuclear magnetic resonance spectroscopy
NR-SOB	Nitrate-reducing/sulfide-oxidizing bacteria
NUB	Nitrate-utilizing bacteria
PAPS	Phosphoadenosine-5’-phosphosulfate
PCR	Polymerase chain reaction
QPC	Qarun Petroleum Company (QPC), Egypt
rDNS	Ribosomal deoxynucleic acid
rRNA	Ribosomal ribonucleic acid
SEM	Scanning electron microscopy
SRB	Sulfate-reducing bacteria
SRP	Sulfate-reducing prokaryotes
TAE	Tris-Acetate-EDTA buffer
TEM	Transmission electron microscopy
VDU	Visual display unit
W	Water sample
XRD	X-ray diffraction

Table of contents

CHAPTER 1

State of knowledge

1.1. An overview on economic impacts and principal reactions during corrosion process

The term “corrosion” refers to a process of material deterioration due to reactions with its surroundings (Davis, 2000). Materials exposed to corrosion include metals, polymers, ceramics, and even our own teeth.

Iron as a base metal is the cheapest and most widely used material in industry. It is usually unstable without protection and can corrode in aqueous environments. This corrosion process implies chemical or electrochemical reactions and metabolic activities of microorganisms in a process termed microbially influenced corrosion (MIC). MIC of iron materials leads to a lot of economic and environmental problems such as plugging of injection and disposal systems, corrosion of facilities and souring of fluids and reservoirs (Flemming, 1996).

The total estimated cost of metallic corrosion in the United States represented approximately $276 billion per year occurred in different industrial fields (Figure 1–1). Specifically, in the oil and gas industries the estimated cost of metallic corrosion is $13.4 billion per year, with MIC, alone accounted for about $2 billion per year (Koch et al., 2002).

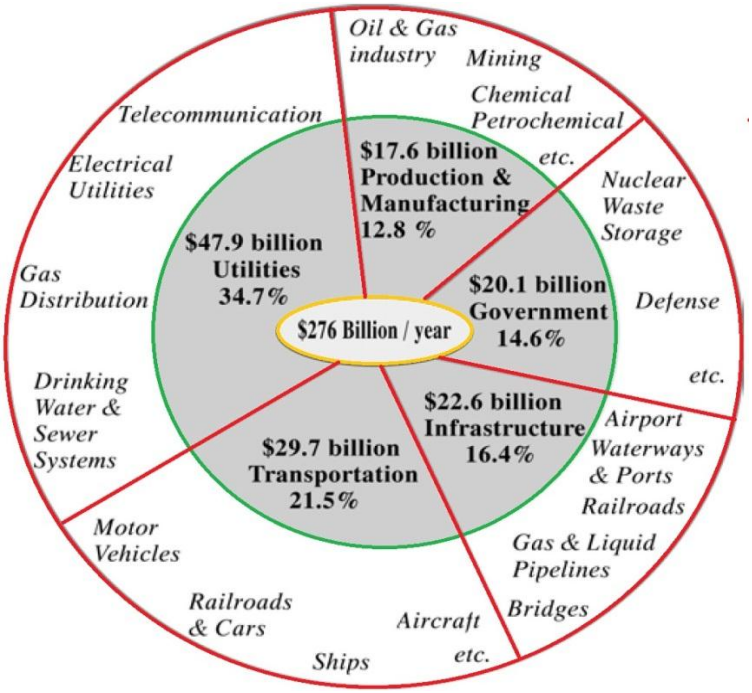

Figure 1–1. Cost caused by corrosion in USA (www.corrosion .com; assessed 01.01.2012).

When metal contacts water, positive metal ions are released into the surrounding medium and free electron remains in the metal surface (eq. 1).

$$Me \leftrightarrow Me^{n+} + ne^{-} \quad (1)$$

The reaction shifts to the right if the released electrons are continuously removed, resulting in a net dissolution of the metal. The free electrons can be consumed by reactions with oxidizing substances (electron acceptor) from the aqueous phase at the metal-water boundary. Such electron acceptors are protons, oxygen, undissociated weak acids or water. Areas on the metal surface where metal dissolution and electron uptake reactions occur are termed anodic and cathodic sites, respectively. If the anodic and cathodic corrosion products accumulate at the metal/water interface, the corrosion rate will slow down. This process termed polarization which might collapse by continuously removing of corrosion products, causing depolarization processes and continuous corrosion.

Microorganisms are known to have the ability to depolarize both anodic and cathodic sites either indirectly by excretion of chemically reactive products or directly by their metabolic activities over the metal surface. The main species of microorganisms associated with microbial corrosion on the metals surface are sulfate-reducing bacteria (SRB), metal-reducing bacteria (MRB), metal-depositing bacteria (MDB), slime-producing bacteria and acid producing bacteria (APB) (Beech et al., 2002).

In natural habitat, it is difficult to find single bacterial species existing in isolation, and commonly, bacterial communities act synergistically to induce corrosion of the metals through co-operative metabolism. These microorganisms can induce corrosion either in the presence of oxygen (aerobic) or in the absence of oxygen (anaerobic). The most aggressive microbial corrosion is usually observed where both aerobic and anaerobic microorganisms are involved (Videla, 2001).

1.2. Aerobic microbial corrosion

Under aerobic conditions MIC processes take place by using oxygen as a final electron acceptor which is removed by iron oxidation. The ferrous ions (Fe^{2+}) formed might be oxidized chemically or by biologically (iron-oxidizing bacteria) to ferric oxide. The best studied iron-oxidizer is *Thiobacillus ferrooxidans*, which is cultivated at a low pH and a high redox potential. This microorganism promotes the corrosion on the metal surfaces as a result of its high ability to produce sulfuric acid by oxidizing sulfur compounds (Gu and Mitchell, 2000).

Pseudomonas species are commonly found also in connection with aerobic microbial corrosion. They colonize the metal surfaces, thereby creating oxygen-free environment for anaerobic bacteria especially sulfate-reducers (Hunter, 2001).

Fungi and algae species might be also involved in the aerobic microbial corrosion process. Fungi species such as *Aspergillus, Penicillium,* and *Fusarium* grow on fuel components and produce organic acids which induce localized corrosion on metal surface (Little et al., 2001). Algae are also able to produce organic acids and decrease the pH of the environment in the presence of light favoring corrosion of the metals (Mara and Williams, 1972).

1.3. Anaerobic microbial corrosion

Iron and steel also corrode severely under anaerobic conditions (Cord-Ruwisch, 2000). Pipelines, tanks, marine platforms and underground structure have been assumed to be mediated by different groups of anaerobic microorganisms respiring with oxidized compounds such as sulfate, nitrate, ferric iron or carbon dioxide (Iverson, 1987).

Sulfate-reducing prokaryotes (SRP) are considered a large and heterogeneous group of anaerobic prokaryotes comprising both *Bacteria* and *Archaea*. SRP share the ability of anaerobic respiration using organic compounds or hydrogen as electron donor and sulfate as a terminal electron acceptor (Thauer and Badziong, 1980).

1.3.1. Sulfate-reducing bacteria (SRB)

Sulfate-reducing bacteria (SRB) represent a diverse group within the SRP. They are abundant in many ecosystems such as soil, marine and fresh water sediments, brackish water, artesian water, hot spring, oil and natural gas wells, sulfur deposits, sludge, acid main drainage, rice fields, deep-see hydrothermal vent, rumen of sheep and gut of insects and can even be related to human diseases (Postgate, 1984).

SRB are anaerobic bacteria which gain energy for growth by oxidizing organic compounds or hydrogen with sulfate being reduced to hydrogen sulfide (Rabus et al., 2006). They are ubiquitous in anoxic environments and play an important role in many industrial processes. In addition to their important role in the global sulfur cycle, SRB are important regulators of a variety of processes including mercury methylation, biodegradation of chlorinated aromatic pollutants in anaerobic soil and sediments, organic matter turnover and removing of heavy metals, sulfate or sulfur com-

pounds from wastewater (Ach and Hintelmann, 2011, Barton and Tomei, 1995). SRB are proposed to be mainly responsible for MIC (Cord-Ruwisch, 1995). SRB lead to many of economic and environmental problems such as corrosion of pipelines and tanks, plugging of injection or disposal wells and souring of oil reservoirs (Brennenstuhl and Doherty, 1990).

The mechanism by which sulfate reducers facilitate corrosion of metals has attracted many investigators, but details of the process are still inadequately understood (Cord-Ruwisch, 2000).

1.3.1.1. Taxonomy of SRB

SRB classification has traditionally been based on morphological, physiological, and biochemical characteristics (see Table 1–1). The cellular morphology of SRB is highly diverse, and still used as a taxonomic feature. The common shapes of SRB are vibrio, rods, spheres, and oval. SRB can also be divided into two main groups according to their oxidation of organic substrates (Widdel and Bak, 1992). The first group carries out an incomplete oxidation of substrates to acetate and CO_2, while the second one completely oxidizes its substrates to CO_2.

The final step in the sulfate reduction reaction by SRB is the reduction of sulfite (SO_3^{2-}) to sulfide (S^{2-}). This reduction reaction is catalyzed by dsr. The dsr studied is composed of a multi subunit complex (α, β, γ, δ) (Steuber and Kroneck, 1998). The dsr is present in all prokaryotes capable of respiring sulfate. Four bacteria and one archaeal (*Archaeoglobus fulgidus*) dsr have been purified and their enzyme properties have been characterized Dahl et al., 1993, Lee et al., 1973). Characterized dsr bacterial enzyme can be identified according to the optical properties e.g. desulfoviridin, desulforubidin, desulfofuscidin and P582 compounds (LeGall and Fraque 1988) The optical properties of dsr are due to the presence of a prosthetic group (consisted of siroheme and iron-sulfur (Fe-S clusters). Minor variations in the structure and composition of these groups result in distinct spectral differences. Therefore the dsr can be used as a taxonomic marker (Birkeland, 2005). A number of additional properties, such as the electron donors pattern, fatty acid composition, electron transfer proteins (cytochromes of C_3 and b-types, flavodoxins, ferredoxins and hydrogenase), respiratory menaquinones, immunological similarity, mole percent of guanine and cytosine (GC) in DNA, optimal growth conditions and acetate

oxidation have also been used for the taxonomic classification of SRB (Caumette et al., 1991).

Table 1–1. Taxonomic Characteristics of some representative genera of sulfate-reducing microorganisms. Table has been taken from Ref. (Rabus et al., 2006).

				Electron donor (examples)							
Genus	**Morphology**	**Type of sulfite-reductase**	**Electron acceptors other than SO_4^{2-}**	**Complete oxidation**	**H_2**	**Lactate**	**Acetate**	**Propionate**	**Higher fatty acids**	**Ethanol**	**Methanol**
Desulfovibrio	Vibrio	Desulfovirdin	SO_3^{2-}, $S_2O_3^{2-}$, Fumarate	-	+	+	-	-	-	+	±
Desulfomicrobium	Oval or rod	ND	SO_3^{2-}, $S_2O_3^{2-}$	-	+	+	-	-	-	±	-
Desulfobulbus	Oval	Desulforubdin	SO_3^{2-}, $S_2O_3^{2-}$, NO_3	-	+	+	-	+	-	+	-
Desulfobacter	Oval or vibrio	Desulforubdin	SO_3^{2-}, $S_2O_3^{2-}$	+	±	-	+	-	-	±	-
Desulfobacterium	Oval	Desulforubdin	$S_2O_3^{2-}$	+	±	±	(+)	±	±	±	±
Desulfococcus	Sphere	Desulfovirdin	SO_3^{2-}, $S_2O_3^{2-}$	-	-	+	(+)	+	+	+	-
Desulfosarcina	Oval (form aggregates)	ND	SO_3^{2-}, $S_2O_3^{2-}$	+	+	+	(+)	+	+	+	-
Desulfomonile	Rod	Desulfovirdin	$S_2O_3^{2-}$, 3Cl⁻ benzoate	+	+	-	-	ND	ND	-	-
Desulfonema	Multicellular filaments	(± Desulfovirdin)	SO_3^{2-}, $S_2O_3^{2-}$	+	±	±	(+)	+	+	-	-
Desulfotomaculum	Straight or curved rods, endospors	P582	$S_2O_3^{2-}$, Fumarate	±	±	±	±	±	±	+	±
Thermodesulfobacterium	Rod	Desulfofuscidin	$S_2O_3^{2-}$	-	+	+	-	-	-	-	-
Archaeoglobus	Sphere	Archaeal	SO_3^{2-}, $S_2O_3^{2-}$	+	±	+	-	ND	ND	ND	ND

[a]. +, utilized; -, not utilized; ±, utilized by some strains; (+), poorly utilized; ND, not determined; (± Desulfo- virdin), present in some strains.

Sulfate reducing microorganisms can be divided into seven phylogenetic lineages, five bacterial lineages and two archaeal based on 16S ribosomal RNA (16S rRNA) gene sequence analyses (Figure 1–2) (Muyzer and Stams, 2008). The majority of the identified SRB (around 23 genera) belongs to the phylum *Proteobacteria (*class *Deltaproteobacteria)* (Wingender et al., 1999). The phylum Firmicutes composes three endospore-forming SRB species affiliated within the class clostridia (*Desulfotomaculum, Desulfosporosinus and Desulfosporomusa*) (Birkeland, 2005). Three phyla lineages, Nitrospirae (*Thermodesulfovibrio* spp.), *Thermodesulfobacteria* (*Thermodesulfobacterium* spp.) and *Thermo-desulfobiaceae* (*Thermodesulfobium* spp.) represent thermophilic sulfate reducers. Within the *Archaea*, Sulfate reducers belong to the genus *Archaeoglobus* within the phylum *Euryarchaeota* and to the

genera *Thermocaldium* and *Caldirvirga* within the phylum Crenarchaeota (Muyzer and Stams, 2008).

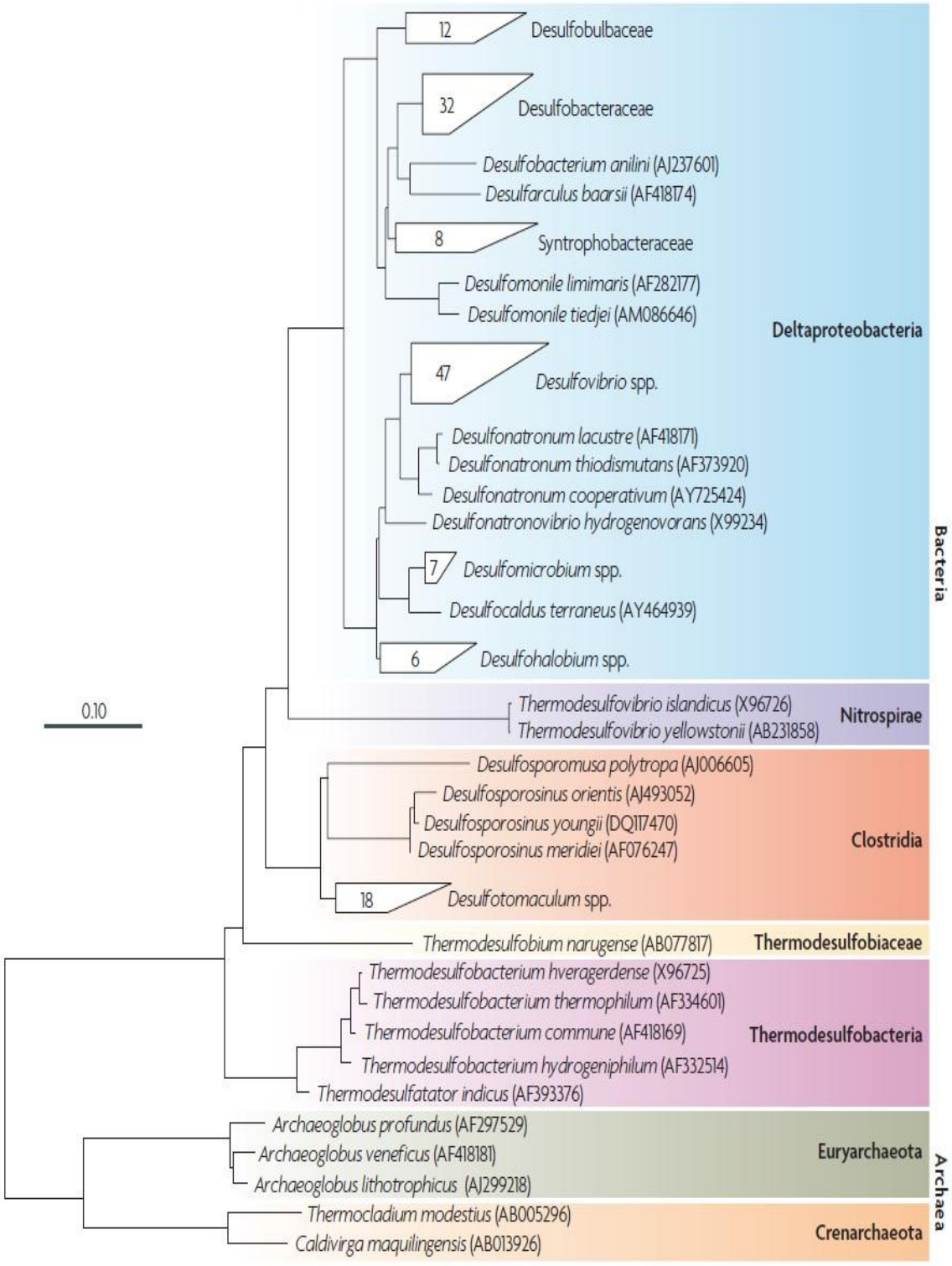

Figure 1–2. Phylogenetic tree based on nearly complete 16S ribosomal RNA (rRNA) sequence of described sulfate-reducing bacteria species. Figure has been taken from Ref. (Muyzer and Stams, 2008).

1.3.1.2. Biochemistry of SRB

In the process of anaerobic sulfate respiration, SRB reduce sulfate to sulfide in a reaction involving the transfer of eight electrons. This reaction occurs via several intermediates and is accomplished by number of enzymes. The sulfate anion is a chemically stable ion and cannot easily be reduced due to its low redox-potential (SO_4^{2-}/HS- anion pair $E_0' = -0.22$ V). Therefore sulfate cannot be reduced without being activated; SO_4^{2-} is activated by adenosine triphosphate (ATP). The enzyme ATP sulfurylase firstly catalyzed the binding of sulfate to a phosphate molecule of ATP, leading to the formation of adenosine phosphosulfate (APS) as shown in Figure 1–3. Sulfate reduction process can be achieved either by dissimilative or assimilative reactions. In the dissimilative sulfate reduction, the SO_4^{2-} ion in APS is reduced directly to sulfite (SO_3^{2-}) by the enzyme APS-reductase with releasing adenosine monophosphate (AMP). While in the assimilative sulfate reduction, another phosphorus (P) is added to APS forming phosphoadenosine phosphosulfate (PAPS) followed by the reduction of sulfate to sulfite with the release of phosphoadenosine 5`-phosphate (PAP). Once sulfite is formed, it is reduced to hydrogen sulfide by the activity of sulfite reductase enzyme in both cases. The sulfide formed is excreted to the environment during dissimilative sulfate reduction. While in case of assimilative sulfate reduction the sulfide formed is immediately converted into organic sulfur compounds such as sulfur-containing amino acids (Madigan et al., 2010). Sulfite is more reactive than sulfate as it contains free electron pairs. The redox potential of the HSO^{3-}/HS- anion couple is $E_0' = -0.116$ V. Therefore sulfite is reduced by dsr directly to sulfide. Two different pathways have been proposed. The simplest pathway is a six-electron reduction step directly without any free intermediates. The second pathway (called trithionate) postulates sequential sulfite reduction via trithionate ($S_3O_6^{2-}$) and thiosulfate ($S_2O_3^{2-}$) as intermediates. The latter pathway is based on the observation that trithionate and thiosulfate are formed as byproducts when sulfite is reduced in vitro by purified dsr and an artificial electron donor (Trudinger and Loughlin, 1981). In SRB, there is no unifying model for the transport mechanism of electron from donor to acceptor.

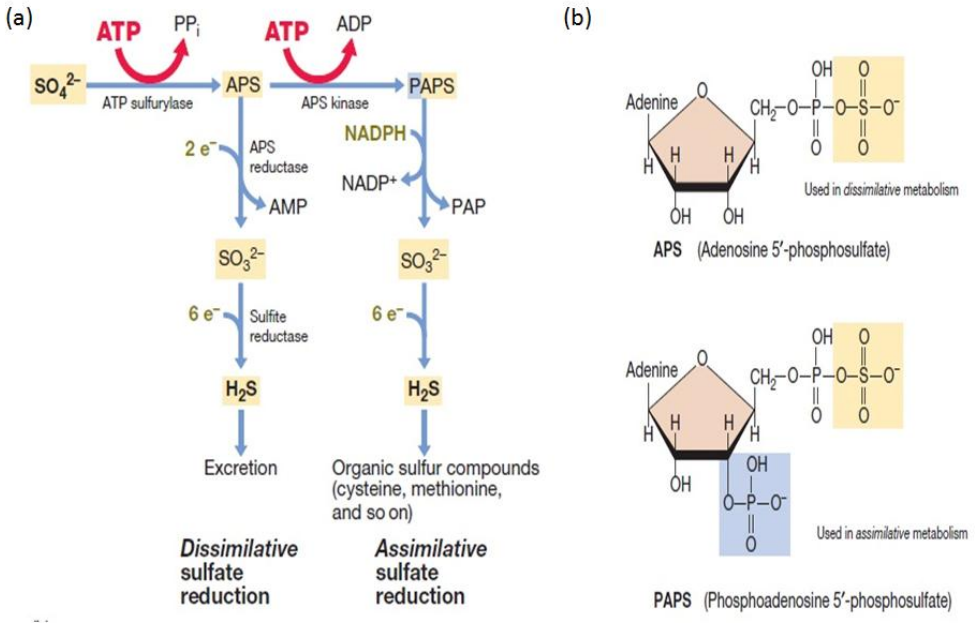

Figure 1–3. Biochemistry of sulfate reduction: (a) Two forms of active sulfate, adenosine 5'-phosphosulfate (APS) and phosphoadenosine 5'-phosphosulfate (PAPS). (b) Schemes of assimilative and dissimilative sulfate reduction. Figures have been taken from Ref. (Madigan et al., 2010).

- **Electron donor and acceptor metabolism**

SRB can utilize a variety of electron donors (Table 1–1). They have the ability to oxidize hydrogen and organic compounds such as lactate, propionate, succinate, format, ethanol, short chain fatty acid (e.g. acetate), long-chain fatty acids, aromatic compounds (benzoate, phenol, toluene) and short-chain hydrocarbon (ethane, propane, butane) (Nagpal et al., 2000, Rabus et al., 2006). Lactate is a ``classical`` electron donor for SRB and is utilized by a majority of species (Birkeland, 2005).

SRB oxidize organic compounds or hydrogen as an electron donor with sulfate being reduced to hydrogen sulfide (Table 1–1). The different SRB species can use many electron acceptors in addition to sulfate (SO_4^{2-}). They can use sulfur compounds such as elemental sulfur, organic sulfur compounds, thiosulfate, sulfite (Rabus et al, 2006), dimethylsulfoxides, and sulfonates (Jonkers et al., 1996, Lie et al., 1999). Few species of SRB can utilize non-sulfur compounds such as nitrate (Pietzsch and Babel, 2003). Although SRB are strict anaerobes, some sulfate reducers have the ability to tolerate oxygen at low concentrations and this oxygen tolerance is species-dependent. These SRB can use oxygen as terminal electron acceptor to oxidize the organic substrates or hydrogen and couple this reaction to ATP formation (Dolla et al., 2006).

- **Growth/activity at different environmental conditions**

SRB are a big group showing metabolic activity under many different environmental conditions. According to their optimal growth temperature SRB can be classified into, psychrophilic SRB isolated from permanently cold arctic marine sediments (optimal temperature between 7 and 10°C) (Knoblauch et al., 1999), mesophiles SRB (growth temperature < 40°C), moderate thermophiles SRB (growth temperature 40-60°C) and extreme thermophiles SRB (growth temperature > 60°C). (Rabus et al., 2000). The genus *Desulfotomaculum* (spore-forming species, phylum *Firmicutes*) grows optimally between 55 and 65°C and was isolated from hot North Sea oil reservoir (Nilsen et al., 1996). The thermophilic genera *Thermodesulfobacterium* and *Thermodesulfovibrio* as well as *Archaeoglobus* spp. have been reported to grow optimally between very high temperature of 70 and 90°C (Burggraf et al., 1990, Jeanthon et al., 2002).

SRB are also active over a wide range of pH values. SRB prefer a neutral pH environment (pH 7) and their growth is usually inhibited at pH values less than 5.5 or more than 9 (Widdel and Bak, 1992). Nevertheless, sulfate reduction activity has been observed in acid mine water having a pH of 2.5 (Tsukamoto et al., 2004). SRB isolated from these habitats, were grown in microniches, where higher and more favorable pH values could exist. Such microniches are maintained probably by the alkalization resulting from the production of bicarbonate (HCO_3^-) and proton scavenger ions (HS^-) (Widdel and Bak, 1992). High sulfate reduction activity was also observed at pH 10. Alkaliphilic *Desulfonatronum thiodismutans* sp. and *Desulfonatrovibrio hydrogenovorans* exhibit optimal pH values between 9.5 and 10 (Detkova et al., 2005).

Sulfate reduction activity is more often observed in marine habitat than in terrestrial environment because sulfate is more abundant in the seawater (28 mM). Marine SRB species are often completely inhibited in fresh water environment (Widdel and Bak, 1992). Halophilic sulfate reducers such as *Desulfovibrio halophilus* and *Desulfocella halophila* that were isolated from hypersaline environment with an optimum concentration of 4 - 5 % NaCl and can also tolerate the salinity up to 19 % NaCl (Brandt et al., 1999, Caumette at al., 1991). However, some SRB species have also been detected in fresh water environment (Castro et al., 2002).

SRB are strictly anaerobes and they need an anaerobic medium with a redox potential lower than -100 mV (Postgate, 1984). However it has been reported that

SRB are able to tolerate the oxygen and can grow with various negative redox potential or even with positive values. These phenomena can be explained by their ability to form favorable anoxic microniches environment (Neculita et al., 2007).

1.3.1.3. Mechanism of corrosion mediated by SRB

SRB are commonly detected where anaerobic corrosion of metal occurs. The corrosiveness of SRB is due to metabolites produced such as H_2S, supposed electrochemical effect termed cathodic depolarization, and microbial colonization (biofilm) over the metal surface.

- **Corrosion by H_2S.** It has been reported that the rate of chemical-induced corrosion was proportional to the concentration of H_2S added (Videla, 2000). H_2S can accelerate corrosion of metals by being source of bound protons and by precipitation of Fe^{2+} as FeS (Lee et al., 1995). It has also been proposed that the iron sulfide film that forms over the surface play an important role in the initiation of pitting corrosion (Rickard, 1969).
- **Corrosion by cathodic depolarization:** Cathodic depolarization is the most frequently theory of corrosion accelerated by SRB that has been proposed by Von Wolzogen Kuehr and van der Vlugt, 1934. This theory is based on the hydrogen consumption activity of SRB. Generally the corrosion reaction is an electrochemical reaction involves an anodic site and a cathodic site. The anodic reaction is the transfer of electrons from zero valent metal to an external electron acceptor causing the release of ferrous ions and electrons into the surrounding medium (Figure 1–4b, reaction 1). While at the cathode, the produced electrons at the anode can be consumed. In anaerobic environment, electrons at the cathode reduce the H^+ ions coming from water dissociation (Figure 1–4b, reactions 2 and 3), and consequently a hydrogen film is formed at the metal surface. The cathodic hydrogen film is consumed by SRB, and the cathode is depolarized continuously facilitating the transfer of the electrons from the anode to the cathode (Figure 1–4b, reaction 4) causing more iron dissolution. The metabolic end product of SRB is sulfide (S^{2-}) which deposited on the metal surfaces as FeS or $Fe(OH)_2$ (Figure 1–4, reaction 5).
- **Biofilm induced corrosion:** Microorganisms attached to the biological or non-biological surfaces embedded in an extracellular polymeric matrix form microbial layers, which are called ``biofilm``. Biofilms are layers composed of mul-tispecies microbial communities, extracellular polymeric substances (EPS),

inorganic material and water (Stoodeley and Kroneck, 1998). Biofilms are ecosystems organized by microorganisms protecting them from external forces influences once they are established. These ecosystems are characterized by a wide range of environmental conditions from aerobic to microaerophilic to anaerobic. Also, from copiotrophic to oligotrophic and from heterotrophic to chemolithotrophic. Biofilms provide a variety of potential growth niches for microorganisms by their ability to modify their surrounding medium. Modification of the biofilm surrounding medium results in a local gradient of many conditions such as oxygen, pH, redox potential, nutrients and flow rate (Sanders and Sturman, 2005). Sessile microorganisms and their planktonic counterpart are bio-functionally different with respect to gene regulation and protein synthesis (Stoodley et al., 2002). Over the past decades, it has become increasingly apparent that biofilms mode is the preferred growing way for most microorganisms Costerton et al., 1978). The biofilm formation process comprises of five major steps (Sanders and Sturman, 2005): initial attachment of microorganisms to the surface; biofilm initiation and EPS production; biofilm structural development; biofilm maturation and detachment of biofilm. Surface roughness and material composition of the substratum as well as hydrodynamic shear stress play an important role in the biofilm formation process. EPS typically account for about 50 % to 90 % (wt.) of organic matters in a biofilm (Wingender et al., 1999). Microbial EPS are biopolymers consisting of proteins, nucleic acids, polysaccharides, lipids and humic substances (Costerton, 1985). The content of EPS is varying depending on bacterial species and growth conditions (Sutherland, 1985, Horn and Morgenroth, 2006). EPS production serves to build a three dimensional structure (3D) in which microbial cells may occupy less than 15 % of the total biofilm volume (Costerton and Stoodley, 2003). This three-dimensional structure influences the movements of dissolved chemical compounds in and out of the biofilm matrix. In addition, it entraps particulate materials and cell clusters from the bulk phase create diffusion gradients. This diffusion gradient leads to localized conditions of chemical compounds dissolved in the water over the substratum (Lewandowski and Beyenal, 2003). Extracted EPS alone in seawater was found to accelerate the corrosion five times more than in the case of EPS free medium (Chan et al., 2002). A part from the direct EPS corrosive effect on the metal surfaces, EPS can help microbial communities in the biofilm matrix to

thrive under anaerobic conditions (even in aerobic environment) due to its adhesive and complex biofilm matrix structure. These conditions facilitate the growth and colonization of anaerobic bacteria such as SRB. Sulfidogenic biofilm facilitate corrosion by trapping corrosive metabolites products such as hydrogen sulfide in close proximity to metal surface and initialize localized corrosion (Geesey et al., 2000). It has been found that, EPS together with SRB species (*Desulfovibrio desulfuricans*) can induce more corrosion than that of EPS with none SRB species (*Pseudomonas fluorescence*) or a mixture culture of both strains (Beech and Campbell, 2008). It has been hypothesized that EPS has the ability to entrap metal ions by binding carboxylic groups of the exopolysaccharides and phosphate groups of the nucleic acids to the metal ions. Hence, it increased the overall metal-binding capacity of EPS (Beech and Gaylarde, 1999). This binding would influence the electrochemical behavior of a metal through formation of metal corrosion cells and galvanic coupling (Braissant et al., 2007). Sulfidogenic biofilms have been reported to be responsible for pitting and crevice corrosion on the metal surfaces (Beech, 2004) (Figure 1–4d). Corrosion rate increases especially in the presence of harmless anion such as chloride beneath biofilm matrix. The chloride anion increases the solubility of the corrosion products and also increases the conductivity of the electrolyte layer on the metal surface considerably. Thus it leads to destruction of the passive film existing on the metal surface and increases the corrosion rate (Giudice and Amo, 1996).

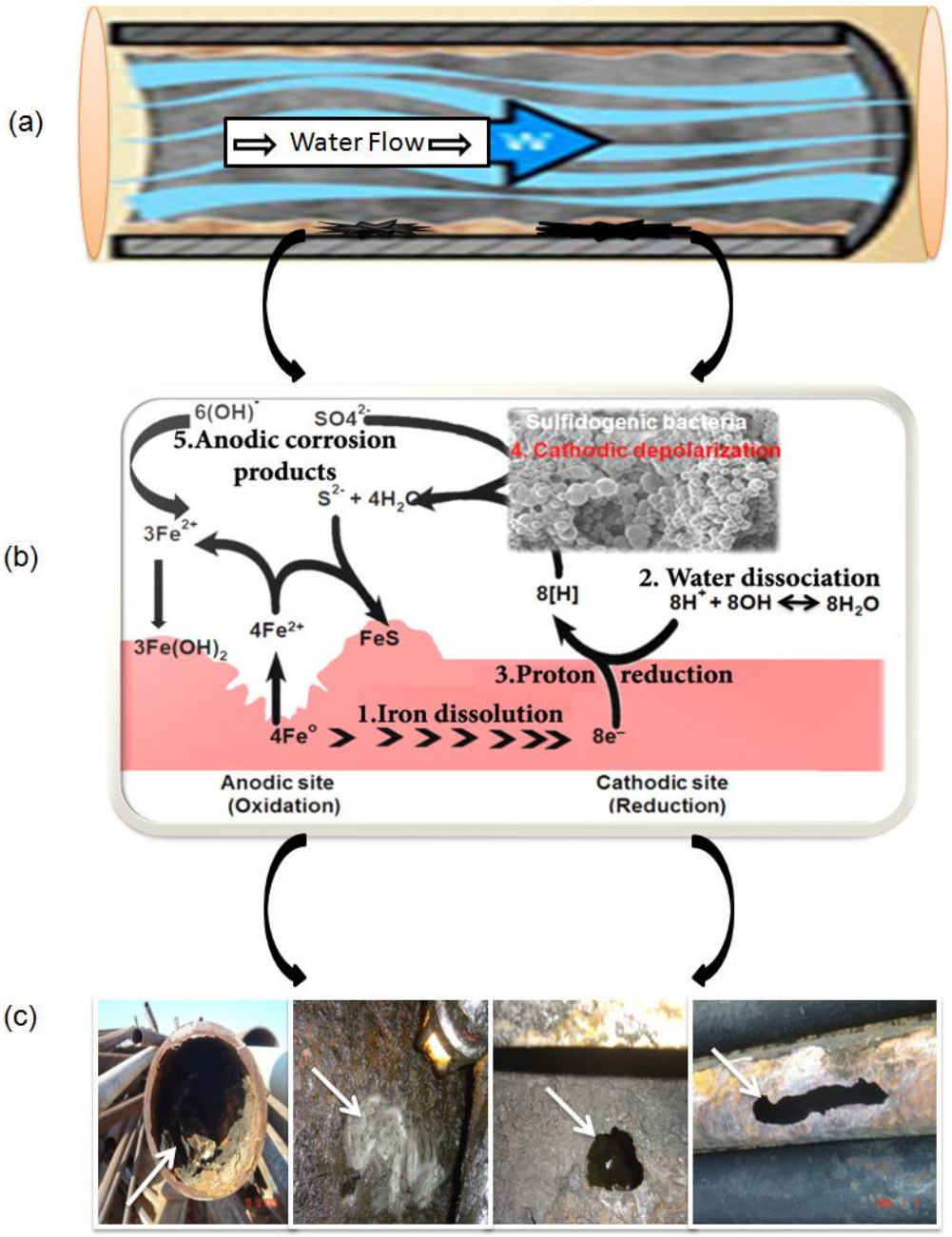

Figure 1–4 Mechanism of corrosion mediated by sulfate-reducing bacteria. (a) the flow of liquid over the pipeline surface, (b) schematic of anaerobic iron corrosion mediated by SRB (adapted from Ref. (Mori et al., 2010), and (c) the microbial corrosion problems in petroleum oil-field (Qarun company, Egypt).

1.3.1.4. Methanogenic Archaea and SRB

Based on 16S rRNA gene sequences, the domain *Archaea* composed of two main phyla: the *Euryarchaeota* and the *Crenarchaeota.* In addition to these two main phyla, the *Korarchaeota* (Elkins et al., 2008), the *Nanoarchaeota* (Huber et al., 2002), the *Thaumarchaeota* (Brochier-Armanet et al., 2008) and the *Aigarchaeota* (Nunoura

et al., 2011) have been proposed to be potential phylum-level taxonomic groups within the *Archaea.* However, the establishment of these phyla is still controversially discussed (Takai and Nakamura, 2011). Hyperthermophiles, in which most of them have the ability to metabolize sulfur, are the dominant group within phylum *Crenarchaeota.* The more physiologically diverse phylum *Euryarchaeota* is composed of extreme halophiles, *thermoacidophiles, methanogens, hyperthermophilic* sulfate and/or sulfite reducers and sulfur metabolizers (Garrity and Holt, 2001). Methanogens (methanogenic *Archaea*) are obligate anaerobes which are like SRB. Most methanogenic species are associated with fermentative and hydrogen-producing microorganisms (Whitman et al., 1992). According to the utilization of specific carbon sources, methanogens can be classified into three major groups: (i) the methylotrophic species using C_1-compounds with methyl groups such as trimethylamine or methanol; (ii) the acetoclastic methanogens using mainly acetate for methane production; and (iii) the hydrogenotrophic species using hydrogen, formate, or certain alcohol for reduction of CO_2 to methane (Garcia and Ollivier, 2000). The most favorable energetic reaction for methanogens is the reduction of CO_2 to CH_4 using H_2 as electron donor (eq. 2).

$$4H_2 + HCO_3^- + H^+ \rightarrow CH_4 + 3H_2O \qquad \Delta G_o = -135.5 \text{ KJ/mol methane} \qquad (2)$$

Under anaerobic conditions, methanogenic *Archaea* are competing SRB and other anaerobic bacteria for the available substrate. In contrast to sulfidogenic microorganisms, methanogens use a limited number of substrates for growth. Quantitatively, hydrogen, carbon dioxide and acetate are the most important and well-known substrates for methanogens. No methanogens have been reported to grow on organic matter, such as lactate, propionate and butyrate, which are common substrates for sulfidogenic microorganisms. Consequently, these compounds are degraded first by sulfidogenic bacteria and then the produce products can be used as substrates for methanogens. In the presence of excessively high concentration of sulfate compounds, sulfidogens compete with methanogens for hydrogen and acetate substrates (Schink and Stams, 2006). In this case sulfate reducers have a competitive advantage over methanogens as in marine environment (Ward and Winfrey, 1985). In contrast in freshwater environment where low sulfate concentration exists, methanogenesis is usually the dominant terminal process (Lovley and Phillips, 1987). When methanogens are present in contact with the metal surface, they are

inducing corrosion of metals by consuming cathodic hydrogen (cathodic depolarization) according to the following reaction (eq. 3)

$$4Fe + HCO_3^- + 9\,H^+ \rightarrow CH_4 + 4Fe_2^+ + 3H_2O \quad (3)$$

1.3.1.5. SRB recovered from oil field water

In early 1926 it was suggested that the sulfide detected in water originated from oil-fields was produced by microorganisms. This suggestion was based on the presence of SRB in water samples from a number of oil fields in United States (Bastin et al., 1926). Much later, it has been demonstrated that sulfide production can be caused by microorganisms growing under extreme physical conditions such as deep and hot petroleum reservoirs Rosnes et al., 1991). Hyperthermophilic SRB was recovered from a North Sea oil field (Beeder et al., 1995), and from a deep oil well in Alaska (stetter et al., 1993). A great diversity of SRB has been isolated from oil field all over the world and many of these isolates belong to new species and genera. A wide range of organic acids (such as lactate, acetate, propionate, butyrate pentanoate, and hexanoate) was detected in oil reservoirs (Barth and Riis, 1992, Barth, 1991) that might serve as substrate for SRB growth. Lactate is considered as a “classical” organic acid which is utilized by majority species of SRB as a substrate (Birkeland, 2005).

Results from cultivation-dependent experiments in produced water show a considerable difference. The German sulfide-rich reservoir wellhead water was characterized by using acetate as substrate for SRB (Cord-Ruwisch et al., 1986). While in African reservoirs, it was characterized by using lactate plus acetate as substrate (Tardy-Jacquenod et al., 1998).

Salinity of the oil field water is variable and is an important factor for in situ microbial diversity and activity. Voordouw and co-workers showed that cultivation from oil-field water with high and low salinity differed significantly in the SRB diversity. This result demonstrates that salinity is an important discriminating factor (Voordouw et al., 1996). The halophilic SRB isolates grow at optimum salinity between 5 and 6 % that being *Desulfovibrio vietnamensis* (Nga et al., 1996), *Desulfovibrio gracilis* (Magot et al., 1992) and *Desulfotomaculum halophilum* Tardy-Jacquenod et al., 1996). Oil field brines with salinity > 20 % have been detected, however most oil field formation water have a moderate salinity < 6 %.

1.3.1.6. Culture-independent detection of SRB

The application of molecular biological methods is a common technique to investigate the occurrence and distribution of bacteria in environmental samples. This technique has the advantage of providing direct information on community structure without cultivation. This method provides knowledge of the evolutionary relationship of microorganisms that allow grouping and characterizing microorganism through sequences of the obtained genes. The 16S rRNA sequence is the most tested taxonomic marker to study the prokaryotic taxonomy (*Bacteria* and *Archaea*). The 16S rRNA has these properties, (i) this gene is present in all bacteria; therefore it is a universal target for bacterial characterization, (ii) the 16S rRNA gene-function has remain constant over a long period of time, suggesting that sequence changes are more likely to reflect random changes (a more accurate measure of time) than selected changes, and (iii) the 16S rRNA genes (~ 1.500-bp) contain several regions of highly conserved sequence useful for proper sequence alignments determination. Therefore it can be used as taxonomic marker for phylogenetic analysis. The 16S rRNA gene (16S rDNA) is available in more than 200,000 bacterial sequences in the GenBank, implying the DNA Databank of Japan (DDBJ) (Miyazaki et al., 2004), GenBank at National Center for Biotechnology Information, USA (NCBI) (Benson et al., 2005) and the European Molecular Biology Laboratory, UK (EMBL) (Kulikova et al., 2004). The comparison of new sequences with the available sequences in the databank reveals information about the identity or relatedness of the new sequences to known species. 16S rRNA comparative sequence analysis has affiliated the major SRB genera into a number of distinct lineages (Devereux et al., 2005). Cloning and sequencing of 16S rRNA genes showed a large diversity of SRB Proteobacteria found in a shallow low-temperature oil field in Canada (Voordouw et al., 1992). A limited number of clones representing fermentative microorganism were detected, indicating that SRB constitute a major component of the bacterial community in this reservoir. In contrast by using the same approach, a very small number of SRB clones have been detected from high-temperature reservoirs in California. This results demonstrating that a high in situ temperature favors the growth of other microbial groups (Orphan et al., 2000). 16S rRNA based-denaturing gradient gel electrophoresis (DGGE) was used to determine the bacterial and archaeal diversity in the environmental samples. A total of 106 bacterial 16S rRNA sequences were obtained from DGGE bands and classified within three major groups: class beta and

gamma of phylum *Proteobacteria* and also class Clostridia of phylum *Firmicutes* (Zhu et al., 2003). Phylogenetic analysis based on 16S rRNA does not provide information about the metabolic capabilities of the microorganisms (Castroet al., 2002). Hence, a functional encoding gene approach has been implemented to characterize bacteria responsible for particular biogeochemical process (Fukuba et al., 2003, Scala and Kerkhof, 1999). Dsr-gene is the best studied example of such approach and has been used to discriminate between SRB in diverse communities (Wagner et al., 2005). For a long time, cloning and sequencing of dsr-gene libraries was the only available molecular approach for studying the functional diversity and dynamics of SRB communities. Although this is an effective method, a need exists for alternative approaches such as dsr gene-based DGGE to rapidly assess the SRB communities in different environments (Geets et al., 2006, Miletto et al., 2007).

1.3.1.7. SRB-biofilm assessment methods and surface monitoring

It is very important to monitor biofilm in oil-field (pipelines and tanks) in order to understand the interaction between microorganisms and metal surfaces. Tradition-al approaches rely on sampling of defined surface areas of pipeline or tanks or on exposure of test surfaces (“coupons”) with subsequent analysis in the laboratory. Coupons should provide with the same material as the pipeline itself. Classical example of such approach is the “Robbins device” (Ruseska et al., 1982). After a given periods of time coupons are removed and analyzed in laboratory to monitor biofilms. Biofilm monitoring techniques can be classified into three categories, depending on the level of information they provide (Flemming, 2003):

- **Level 1:** Monitoring devices such as optical sensors, ultrasound, heat transfer resistance and quartz microbalances detect the buildup of surface in general and cannot distinguish between biomass and inorganic deposits.
- **Level 2**: Monitoring devices such as biochemical probes and confocal scanning laser microscopy (CLSM) with staining protocols differentiate between organisms and/or biomass and inorganics fractions.
- **Level 3**: The application of specific genetic, chemical and enzymatic methods.

To detect the biofilm structure over the metal surfaces, there are several methods available (Surman et al., 1996). Basically the biofilm can be qualitatively analyzed in three different ways: dehydrated, partly dehydrated and hydrated.

Biofilm analysis using transmission electron microscopy (TEM) required different pretreatment steps, the sample has to be fixed, embedded dehydrated,

stained and sectioned. The results received from TEM will be cross section including cell location within the biofilm and internal cell structure (Costerton, 1985). Scanning electron microscopy (SEM) needs only fixation and dehydration steps to visualize the biofilm. Both TEM and SEM are able to use high magnification that is not achieved by classical light microscopy. In addition, there is additional option of elemental surface-microanalysis with either microscopic technique when combined with X-ray diffraction (XRD) or energy dispersive X-ray spectroscopy (EDS) (Marquis, 1989, Rajaseker et al., 2010). Nevertheless both techniques (TEM and SEM) shrink the biofilm sample due to necessity of fixation and dehydration, causing a loss of 3D structure which might give false information. Partly dehydrated biofilm can be characterized by applying environmental scanning electron microscopy (ESEM) which is a descendant of conventional SEM. This technique minimizes sample damage and changes in biological morphology that SEM and TEM pretreatment procedure induces. Biofilm sample do not require extensive manipulation, fixation, dehydration, air drying and metal coating (Sutton et al., 1994). Combination of X-ray microanalysis with the ESEM provides a potentially useful complement to conventional procedures (Darkin et al., 2001). The result received from ESEM give information closer to the real hydrated situation as has been shown for SRB biofilm (Castaneda and Benetton, 2008). However the electron beams will still damage the biological biofilm after a short period of time. Atomic force microscopy (AFM) is another technique using partly hydrated samples. AFM shows a high-resolution of biofilms and surfaces (Beech et al., 1991). Nevertheless, it cannot elucidate internal structure of biofilms.

Completely hydrated biofilms can be examined by light microscopic technique and light microscopy can be used to investigate biofilm samples with a few micrometers thickness. However, when biofilm thickness increases to hundred micrometers, CLSM is preferred (Hille et al., 2005). Combination of CLSM with different staining protocols allows visualization and quantification of biofilm constituents such as EPS and microbial populations. This technique allows sequential examination of serial images on a visual display unit (VDU). This gives a three dimensional structure of different biofilm constituents. The application of Fluorescein isothiocyanate (FITC)-labeled lectins allowed the detection of EPS glycoconjugates fraction of a biofilm system (Neu, 2000). FITC has been applied to stain protein fraction in the sludge floc (Schmidtova and Baldwin, 2011). In recent years,

there is an increased interest in multicolor fluorescence experiments for exploring the distribution of EPS and/or microbial cells in the biofilm system. The idea of using multiple fluorochromes experiments is to apply highly specific fluorochromes with minimum spectral peak interference (Table 1–2). The minimum spectral peak interference between two channels (bleed-through) can be significantly achieved when the range of emission of two fluorophores overlap significantly and one of them is much more strongly excited than the other (Murray, 2005).

Table 1–2. Literature works using multiple stains for probing EPS or cells. (Adapted from Chen et al., 2007).

Reference	Sample	Stain(s) specificity	N_s[a]	Excitation light source(s) used (nm)					
				350–370	420	488	494–514	543–568	633–647
Neu and lawrance (1997)	Biofilm	Syto, concanavalin A, Arachis lectins	3	N/A					
Neu et al., (2001)	Biofilm	Selected lectins	3			X		X	X
Strathmann et al., (2003)	Biofilm	Syto 9, concanavalin A, wheat germ agglutinin	2			X		X	X
Bockelmann et al., (2002)	River snow	Syto 9, DAPI, selected lectins	2	X		X		X	X
Bosemann et al., (2003)	Biofilm	Aleuria aurantia lectin, Syto 60	2	N/A					
Lawrance et al., (2003)	Biofilm	Syto 9, Sypro orange, Nile red, lectins	3			X		X	X
Lawrance et al., (2004)	Biofilm	Selected lectins	3			X		X	X
Bosemann et al., (2004)	Biofilm	Aleuria aurantia lectin, Syto 60	2	N/A					
Staudt et al., (2004)	Biofilm	Syto 60, Aleuria aurantia lectin	2			X			X
Neu et al., (2004)	Biofilm	Syto 9, Syto 40, autofluorescence	3			X		X	X
Lawrance et al., (2005)	Biofilm	Syto 9, Triticum vulgaris–TRITC, Autofluorescence	3			X		X	X
McSwain et al., (2005)	Aerobic Granule	Syto 63, FITC, concanavalin A	3			X		X	X
Chen et al., (2007)	Aerobic Granule	Concanavalin A, calcofluor white, Syto 63, FITC, Syto Blue, Nile red	6	X	X	X	X	X	X

DAPI 4′,6-Diamidino-2-phenylindole, TRITC tetramethylrhodamine isothiocyanate

[a] Maximum number of stains used on the biofilm sample.

1.4. Microbial corrosion control strategies

There are two major approaches to control corrosion in oil and gas industry. One is the use of a high-grade material (higher cost) which saves on maintenance and avoiding the risk of catastrophic failure. The other is the use of a low-grade material (lower cost) along with a corrosion inhibitor. Experience has shown that the second approach is viable and emphasis on the corrosion inhibitor's performance has been assessed predictably. A corrosion inhibitor is "a chemical substance which when added in small concentrations to an environment minimizes or prevents corrosion" (Rajasekar et al., 2010). Depending on the mechanism of corrosion mitigation, liquid phase inhibitors are divided into different groups.

- **Anodic inhibitors:** Anodic inhibitors are known to facilitate formation of passive films that inhibit the anodic metal dissolution reactions. These are often termed as passivating inhibitors. These Passivizing inhibitors adsorbed to the metal surface via chemisorption.
- **Cathodic inhibitors:** They minimize corrosion rate by either decreasing the reduction rate (cathodic poisons) or by precipitating selectivity on the cathode area (cathodic precipitators).
- **Mixed inhibitors:** They are known to affect both the cathodic and anodic reactions.

About 80 % of inhibitors are organic compounds that cannot be related specifically as anodic or cathodic inhibitors. Hence they are known as mixed inhibitors. Their effectiveness is a function of their ability to adsorb at the metal/metal oxide surface.

The oil and gas industry is affected by microbial corrosion in several activities such as recovery, processing, transport and storage (Maxwell et al., 2004). Corrosion reduction or prevention can be completely achieved when corrosion inhibitor (biocide) has biocidal effect for planktonic as well as sessile microorganisms. Biocides are specific inhibitors which are able to kill or inhibit microorganisms. These substances are divided into two different classes according to their chemical reaction by acting as: (i) oxidizing agent and (ii) non-oxidizing agent. Chlorine or hypochlorite is a frequently used oxidizing biocide because it is relatively inexpensive; it can be applied on site and it can be continuously dosed at low concentrations. The inhibitive effect of oxidizing biocide is produced by oxidative stress resulting in a deterioration of DNA, lipids and cellular macromolecules (Skorko-Glonek et al., 1999). Commer-

cially available non-oxidizing biocides are generally selected active substances such as formaldehyde, glutaraldehyde, iso-thiazolones and quaternary ammonia compounds. Non-oxidizing biocides are claimed to be more effective in comparison to oxidizing biocides to control microbial corrosion. These substances have greater persistence and many of them are pH independent (Hector and Quintero, 2007). The effectiveness of non-oxidizing biocide is based on enzymes poisoning and protein denaturation.

The effectiveness of a biocide depends on the type of microorganisms in the system as well as the operating conditions of the system. Therefore, it is recommended to carry out a test run, preferably under the operating conditions of the system. If this is not possible to run the test under operating conditions, a test run is carried out under laboratory conditions to determine optimal doses of the active ingredient. Experience has demonstrated that the traditional chemical treatment regime often has limited success in large scale industrial systems, even if high biocide concentrations or long dosage periods are applied. There are a lot of reasons why traditional treatment applications often fail to eliminate microbial population especially biofilms. These need to be addressed when setting up any microbial control program (Sanders and Sturman, 2005). Planktonic bacteria are relatively easily and rapidly killed by low concentrations of traditional biocides such as chlorine or glutaraldehyde. However when bacteria grow in a biofilm, characterized by large amount of EPS, much higher concentrations are required to kill these microbes embedded in biofilms. Experience has shown that it often takes more than 10 times more of biocide amount needed to kill the sessile microbes than the same microorganisms in planktonic state. In addition, the use of only one biocide over an extended time offers the microbes a chance to get adapted to this substance via changes in outer cell membrane structure, enzymatic pathways, or metabolism. A common strategy for avoiding resistance problems is the application of weekly alternation of two products with different active chemistries (Sanders and Sturman, 2005). Another effective and often preferred strategy is to combine two or more biocides together (Wen et al., 2009). This can be achieved by intermittent biocide dose and a continuous low level dose of the second biocide.

1.4.1. Novel microbial corrosion control strategies

Conventional biocide treatment systems often fail to control microbial corrosion. This has stimulated the development of new strategies to prevent or mini-

mize microbial corrosion. These strategies depend on using substances or technologies that inhibit the microbial corrosion and/or protect the metal surface from attack.

1.4.1.1. Nitrate treatment

Nitrate (in the form of calcium or sodium nitrate) is a routinely used strategy in wastewater and sewage treatment. It is used to control nuisance smells of biogenic sulfide produced by SRB. Nitrate suppresses hydrogen sulfide production by encouraging the activity of nitrate-reducing bacteria, denitrifying bacteria, and nitrate-reducing/sulfide-oxidizing bacteria (NR-SOB) (Garcia-de-Lomas et al., 2007). Four hypotheses have been proposed to be reasonable for this rapid inhibition of sulfide by nitrate-utilizing bacteria (NUB): out -competition of SRB by NUB for the organic nutrients, production of toxic intermediates such as nitrite, biological oxidation of sulfide by NR-SOB and switching of SRB from sulfate to nitrate reduction (Nemati et al., 2001). Nitrate treatment is one of the most widespread newly developed microbial control strategies in oil fields. Full-scale and lab scale test runs have been carried out for many oil reservoirs and water injection systems (Dumsmore et al., 2006, Sunde et al., 2004). This shows great evidence of significant reductions in microbial corrosion, SRB activity and hydrogen sulfide souring accompanied by an alteration in the microbial community composition after long-term treatment (Voordouw and Telang, 1999). There is recent evidence that nitrate can contribute to increasing microbial corrosion (Voordouw et al., 2002). So the negative aspects of this treatment must be assessed to ensure that unwanted side effects do not occur.

1.4.1.2. Nitrite treatment

Nitrite is another simple inorganic compound that has been used to inhibit SRB and also chemically scavenge preexisting sulfide. Treatment of oil and gas wells with nitrite has resulted in virtual elimination of SRB in water samples as well as significant rapid reduction in H_2S (Sturman et al., 1999). While bio-competitive exclusion has been shown to be successful in laboratory and oil-field; current researches suggest that the microbial consortium does not change as a result of the treatment of short-term nitrite (Nemati et al., 2001).

1.4.1.3. Molybdate treatment

Molybdate ion is a specific metabolic inhibitor for SRB. Also, there are synergistic effects when molybdate, nitrate, and nitrite are combined together in one treatment (Percival, 1999). Molybdate is an efficient SRB inhibitor in laboratory culture studies. However its effectiveness is very dependent on the activity state of

the bacteria. It has been reported that the appropriate molybdate treatment is dependent on the growth rates of SRB in a system. Therefore it is not possible to establish a universal molybdate treatment regime since each system must be evaluated individually.

1.4.1.4. Sulfate Removal

A significant reduction in the sulfate concentration of injected water decreases the amount of sulfide produced by SRB. This leads to reduced bio-fouling, souring, and microbial corrosion. Ceramic nanofiltration membranes can be used to minimize the sulfate concentration in the process (McElhiney and Davis, 2002). A large-scale plant (treating up to 390.000 barrels of water per day) can lower the sulfate concentration from ca. 2.800 mg/L in the influent seawater stream to ca. 40 mg/L in the desulfated process stream.

1.4.1.5. Dispersant Technology

This technology acts as a biofilm-slime dispersant rather than as a bactericide. This can be achieved by forming amine film upon the wetted surfaces of the system. This film prevents biofilms development on surfaces and is effective in limiting the impact of bacterial growth on a system. The dosage regime is characterized by an injection of the dispersant at low concentrations and a short period of time to renew the film. Such treatments work best on clean systems where a good amine film can be formed. However a bio fouled system probably needs to be physically or chemically cleaned before starting the treatment. Biofilm dispersal technology through the addition of signaling molecules (such as HSLs) is a new promising research area (Dow et al., 2003).

1.4.1.6. Surface active compound (surfactant)

A surface active compound (surfactant) is defined as a substance that at low concentration adsorbed partially or completely to the interfaces in the system. Surfactant usually decreases the surface tension (the work required to extend surface by unit area) of water rather than to increase it (Rosen, 1989). Surfactant molecules usually consist of polar head and nonpolar tail. Both groups influence the surfactant phase behavior. The polar head is characterized by a hydrophilic functional group, whereas the nonpolar tails consist of a hydrophobic functional group as shown (see Figure 1–5).

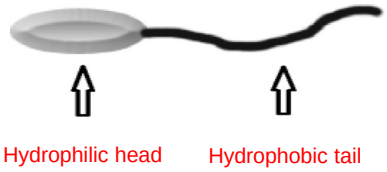

Figure 1– 5 Schematic picture of a surfactant molecule.

- **Classification of surfactant**

Surfactant can be classified by the presence of charged group on its head (Figure 1–6). A nonionic surfactant has no charged group on its head. The head of an ionic surfactant carries a net charge. If the charge is negative, the surfactant is called anionic whereas if the charge is positive, it is called cationic. While surfactant with two oppositely charged groups in its head is termed amphoteric.

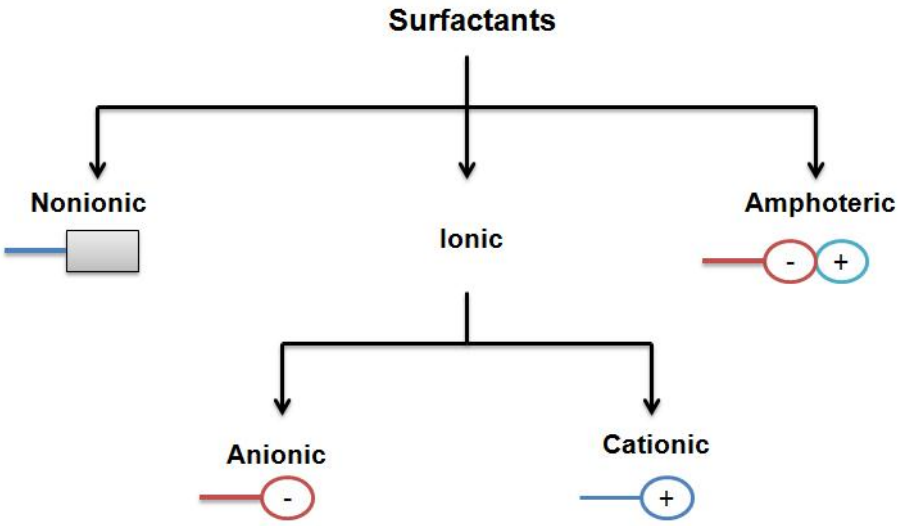

Figure 1–6. Different types of surfactant.

Nonionic surfactants: This type of surfactant is not dissociated in aqueous solutions. It plays an essential role in dispersion, floatation, tertiary oil recovery, household and industrial cleaning. Their important role is coming from their properties such as hard-water solubility, mildness, and biodegradability.

Amphoteric surfactants: In this type of surfactant, both positive and negative charges are present in the surface-active part. This type of surfactant is particularly used as personal care and household cleaning products.

Anionic surfactants: In aqueous solution, the surface-active part of these molecules is negatively charge. For instance carboxylate, sulfate, sulfonate and phosphate are the polar groups in anionic surfactants (Jonsson et al., 1998). Anionic surfactants are the most used surfactant for laundering, dish washing liquids and shampoos because of its excellent cleaning properties.

Cationic surfactants: The hydrophilic part of a cationic surfactant carries a positive charge when dissolved in aqueous solution. The majority of cationic surfactants are based on the nitrogen atom carrying the positive charge. Examples of positive polar groups are long chain fatty amines and their salts, fatty diamines, poly amines, their salts and fatty quaternary ammonium salts. The economic importance of cationic surfactants has increased significantly because of their potential to kill or inhibit the growth of many microorganisms. They are also widely used in textile industry as fabric softeners, waterproofing agents, and dye fixing agents. Because many important mineral ores and metals carry a net negative charge, the cationic surfactants are also useful in flotation processing, lubrication, and corrosion inhibition.

- **Surfactant properties**

When surfactants are added into water, surfactant molecules escape from water phase due to their hydrophobic nature. Then they move to available interfaces (Figure 1–7). The addition of surfactant decreases gradually the surface tension of water until it reaching a minimum point. If there is no more space in the solution for additional surfactant molecules to adsorb, they will aggregate in the bulk liquid phase as well near the solid-liquid interfaces. Even when additional surfactants present in the solution, they will form aggregate structure like micelles. Thus, additional surfactant (above the level needed for minimum surface tension) does not affect for more decreasing surface tension of solution. Therefore surface tension measurement is a useful tool to determine the micelle-forming concentration, termed the critical micelle concentration (C_{cmc}) (Figure 1–8) (Hunter, 2001). The surface tension of water at room temperature (72 mN/m) is normally reduced to value of 30–40 mN/m at C_{cmc} (Menger and Littau, 1993).

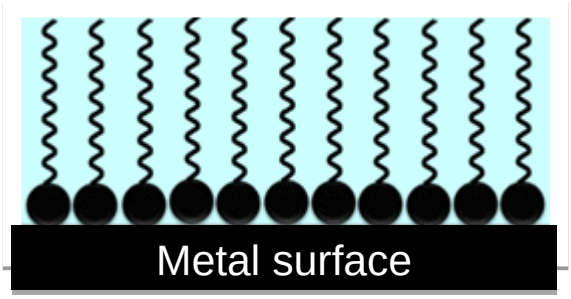

Figure 1– 7. Adsorption of surfactants molecules to the metal surface (interface)

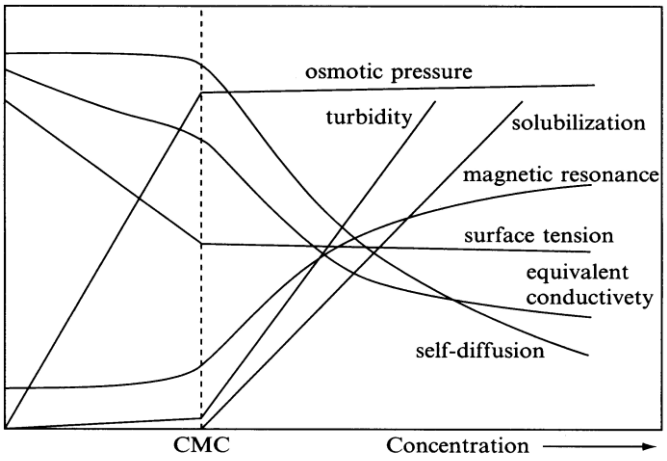

Figure 1–8 Solution properties that influencing $C_{cmc.}$

1.4.1.7. Gemini surfactants: a distinct class of self-aggregating molecules

Gemini surfactant represents a new class of surfactant. It consists of two monomeric surfactant molecules linked by a spacer chain (Maxwell et al., 2004).

- **Structure of gemini surfactants**

In contrast to conventional surfactant (see Figure1–5), a gemini surfactant is composed of a hydrocarbon chain, an ionic group, a spacer, a second ionic group and second hydrocarbon tail (see Figure 1–9). Gemini surfactant possesses two hydrophilic heads and two hydrophobic chains tails, and a variation in the nature of spacers exists (Menger et al., 2000). Spacers are short or long methylene groups, rigid (stilbene), polar (polyether), and nonpolar (aliphatic, aromatic) groups. The ionic group can be charged positive (ammonium) or negative (phosphate, sulfate, carboxylate), whereas the polar nonionic may be polyether or sugar. The majority of gemini have symmetrical structures with two identical ionic heads and two identical chain tails. The arrangement morphology of gemini monomers in polar solvent are one of the four different types shown in Figure 1–10. This morphology is depending on the structure of the molecule and its orientation.

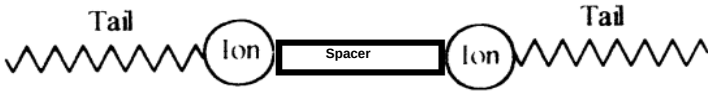

Figure 1–9. Schematic picture of a gemini surfactant.

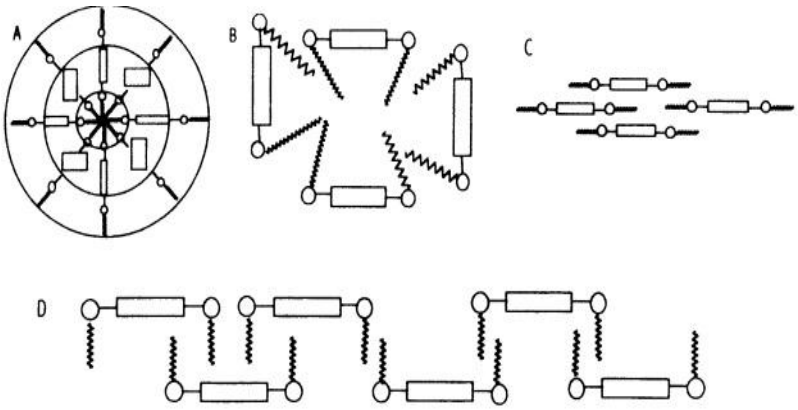

Figure 1–10. Possible morphology of gemini surfactant in the interface. Ref. (Hunter, 2001).

- **Properties of gemini surfactants**

Changes in the molecular structure of conventional surfactant for improving their properties have attracted the attention of the chemists (Almeide etr al., 2010, Wang et al., 2008). The Following parameters are responsible for the successful application of gemini surfactants:

1. Gemini surfactants have remarkably low C_{cmc} up to one to two orders of magnitude compared to the corresponding conventional surfactants of equivalent chain length (Atkin et al., 2003). The much lower C_{cmc} of gemini leads to less skin irritation which normally depends on concentration of surfactant monomer in solution.
2. Gemini surfactants are better solubilizes than conventional one due to the very low C_{cmc} values (Engberts et al., 1996). The long hydrocarbon chain increases the surface activity. Moreover, increasing hydrophobicity makes the molecule insoluble, whereas increasing hydrophilicity of the head group increase its solubility in water. Hydrophilic groups in the spacer also increase the aqueous solubility (Rosen, 1989).
3. The tighter packing of the hydrophilic head groups of gemini results in a more cohesive and stable interfacial film. The double-tailed and doubly charged gemini surfactants interact more prominently with neutral and oppositely charged surfactants.
4. Gemini surfactants are characterized by a significant surface activity, which is up to three times as large as monomeric surfactant ones (Rosen, 1989).

5. Several researches emphasize on the importance of biocide properties of gemini surfactants (Macian et al., 1996, Perez et al., 1996).
6. Gemini surfactant can be used also as a corrosion inhibitor in acidic media (Hegazy et al., 2010).
7. Gemini surfactants are safe ecologically and most gemini surfactants can be manufactured at a reasonable cost.

- **Gemini surfactant as corrosion inhibitor and biocide**

Gemini surfactant can protect the metal surface from corrosion by adsorption on the metal/solution interfaces. There are two forces favoring the adsorption process. One is the hydrophobic force causing a strong interaction between water molecules which results in a repulsion of the alkyl chain from the aqueous phase. The other is electrostatic forces by which a negatively charged surface will attract cationic surfactants and repel anionic surfactants while a positively charged surface will do the opposite. Moreover, gemini surfactant can inhibit the bacteria growth by (i) an electrostatic interaction and (ii) physical disruption. The electrostatic interaction occurs between the oppositely charged centers on the bacterial cell membrane and the positively charged head groups of the biocide molecules. While physical disruption occurs as a result of the penetration of the hydrophobic chains into the cell membrane due to the similarity in the chemical structure. The interaction between biocide molecules and cell membrane causes a strong damage of the selective permeability of these membranes which disturbs the metabolic pathway within the cytoplasm (Badawi et al., 2007).

1.5. Objectives of thesis

Although corrosion inhibitors and biocides are widely used in petroleum companies, the problem of corrosion damages is still urgent. To certain extent this is due to the fact that microbially induced pitting corrosion is responsible for all bio-damages cases of water tanks, equipment and pipelines. The corrosion problems in these companies were noticed on basis of the presence of high sulfide concentration, detection of sulfate-reducing bacteria with high viable counts and accomplished by severe corrosion in water tanks and pipelines. In this respect, the knowledge of microbial diversity is helpful to understand the interaction between the corrosive bacteria and metal surface and to provide the basic for development of new and better means for microbial corrosion prevention. Therefore, this study was focused on two main objectives. The first objective was achieved by studying the corrosion problem in basis of studying the microbial diversity and activity in the samples. In addition, the second objective was focused on the control strategy. The two objectives were studied with the following details:

1. Apply a combination of culture-dependent and culture-independent techniques to investigate the sulfidogenic microbial diversities (*Bacteria* and *Archaea*) present in the three water samples with different salinities and their related cultivated biofilms which originated from oil-field water tanks, Egypt. This approach can be achieved by using functional gene, dissimilatory sulfite reductase-β subunit (dsrβ), based on denaturing gradient gel electrophoresis (DGGE). Detect the presence of other *Archaea* such as methanogens that induce metal surface corrosion using 16S rRNA method. Determine the sulfidogenic biofilm activities over the metal surface.
2. Application of different novel synthesized surfactants to protect the metal surface from the salinities and the activities of the three environmental-sulfidogenic bacteria.

CHAPTER 2

Diversity and activity of sulfidogenic biofilms with different salinities originated from oil-field water tanks, Egypt

2.1. Objectives

The objectives of this chapter were to, (i) apply a combination of culture-dependent and culture-independent techniques to investigate the sulfidogenic microbial diversities (*Bacteria* and *Archaea*) present in three water samples with different salinities and their related cultivated biofilms which originated from oil-field water tanks, Egypt. This approach can be achieved by using functional gene (dsr) based on denaturing gradient gel electrophoresis (DGGE) method. (ii) Detect the presence of non-sulfidogenic *Archaea* diversity in the different environmental water samples using 16S rRNA technique, (iii) determine the sulfidogenic biofilms activities by measuring the sulfide production and corrosion rate. (iv) Biofilm structures and constituents (microbial cells, and EPS) were also analyzed over the metal surface.

2.2. Materials and Methods

2.2.1. Sampling enrichment and reactor setup

Three water samples with different salinity contents were collected from water tanks of Qarun Petroleum Company (QPC), and labeled Hamra, KSW, and Youmna. The Hamra water sample was the lowest salinity (NaCl) of 0.23 %. The KSW water sample was distinguished by salinity of 3.19 %. While the Youmna water sample was characterized by the highest salinity of 5.49 % (see Table 2-4). The three water samples were analyzed chemically concerning Calcium, Magnesium, Sulfate, Bicarbonate, Iron using titration method and spectroscopy HACH DR-5000. The pH of the water samples was measured using SenTix pH electrode, WTW (Weilheim, Germany). These measurements were done in the QPC-laboratories at the sampling time (March, 2009). Water samples were transferred to the laboratory under cooling and anaerobic condition for further analyses. Direct in the field, inoculation of the water samples were done in an anaerobic selective media (modified Postgate´s-B medium) according to Postgate (1984). Modification of Postgate´s medium was done by using the original water salinity (NaCl) and pH during preparation (see Table 2–1). The medium was prepared, sparged with nitrogen gas and resazurine (0.0002% w/v) was used as a redox potential indicator for anaerobic cultivation. The medium was inoculated with 10 % (v/v) water samples and incubated at 37 °C for 14 days. Medi-

um preparation and cultivation were achieved according to the modified Hungate's technique for anaerobes (Miller and Wolin, 1974). The appearance of a black precipitation (Ferrous sulfide) was used as a marker for sulfate reduction and as an indicator for the activity of sulfidogenic bacteria in culture media.

The inoculated samples were enriched three times under anaerobic conditions using modified Postgate´s-B medium to be used as inocula for four parallel two liters reactors. Each reactor contains one liter anaerobic modified Postgate's C medium (Table 2–1). A mild steel coupon with chemical composition reported in Table 2–2 (CS1018 3”x 1⁄2”x 11⁄16” strip, Cormon LTD) was used as a main iron source for the cultivated microorganisms. The four reactors were inoculated with 20 ml of the enriched sulfidogenic bacteria sample (see Table 2-3). Once a week the culture medium was exchanged completely and new medium was added for one month cultivation period at 37°C. Four parallel experiments were carried out for each sample (see Table 2–3). The first reactor (reactor A) was operated to analyze the sulfidogenic-biofilm diversity, the second reactor (reactor B) was used to determine the sulfidogenic activity weekly for one month incubation. The third reactor (reactor C) was used to visualize the biofilm formation over the metal surfaces. Moreover it was used to detect the elemental surface-microanalysis of the biofilm over the metal surface. While the fourth reactor (reactor D) was operated in order to detect the change in the biofilm structures and constituents over the metal surface. The biofilm samples of reactor D were examined at the maximum sulfidogenic activity (highest sulfide production) as explained in Figure 2–1.

Table 2–1. Composition of modified Postgate's *B* (P_B) and modified Postgate's C (P_C) media.

Composition (g/l)	**Modified P_B**	**Modified P_C**
KH_2PO_4	0.5	0.5
NH_4Cl	1.0	1.0
Na_2SO_4	1.0	4.5
$CaCl_2.6H_2O$	-	0.06
$MgSO_4.7H_2O$	2.0	0.06
Sodium lactate	3.5	4.42
Yeast extract	1.0	1.0
Ascorbic acid	0.1	-
Sodium thioglycolate	0.1	-
$FeSO_4.7H_2O$	0.5	-
Sodium citrate. $2H_2O$	-	0.3
Salinity (NaCl)*	Variable	Variable
pH**	Variable	Variable

*The water salinity was 2.3, 31.9 and 54.9 g/l for Hamra, KSW and Youmna samples respectively.

**The pH was 7.1, 6.2 and 5.7 for Hamra, KSW, and Youmna cultivated sample, respectively.

Table 2–2. Chemical composition of mild steel coupons C1018.

Chemical composition (%) (remaining: Fe)					
C	0.18	**Mo**	< 0.01	**Si**	0.02
Al	0.035	**Nb**	< 0.01	**Sn**	< 0.01
Co	< 0.01	**Ni**	0.01	**Ti**	< 0.01
Cr	0.02	**P**	0.01	**W**	< 0.01
Cu	0.02	**Pb**	< 0.01	**V**	< 0.01
Mn	0.84	**S**	< 0.005	**B**	< 0.0001

Table 2– 3 Cultivation parameters and reactor set up

	Hamra-sample	**KSW-sample**	**Youmna-sample**
Salinity	0.23 %	3.19 %	5.49 %
pH	7.1	6.2	5.7
Temperature		37°C	
Time schedule	One month experiment		
Reactor A	Used to analyze the cultivated sulfidogenic– biofilm diversity (CB)* In addition to the CB diversity analysis of reactor A sample, diversity was also analyzed in the original water sample (W)		
Reactor B	Used to determine the sulfidogenic activity in the bulk phase (weekly sample) and corrosion rate (after one month incubation)		
Reactor C	Used to visualize the sulfidogenic biofilm over the metal surface and to detect the elemental-surface microanalysis of the biofilm over the metal surface		
Reactor D	Used to detect the change in the biofilm structure and constituents over the metal surface (examined at maximum sulfidogenic activity in the bulk phase)		

*CB: cultivated biofilm

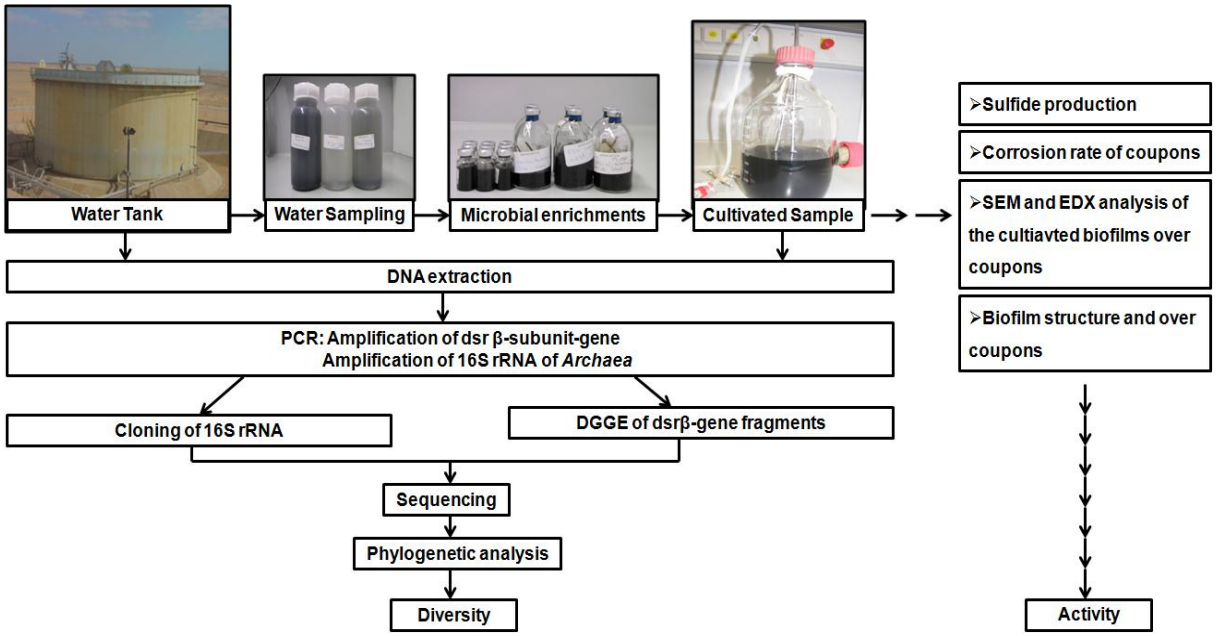

Figure 2–1. Schedule of the sampling, enrichment, cultivation, diversity, activity steps of the three different water samples (Hamra, KSW, and Youmna) collected from Qarun Petroleum Company (QPC), Egypt.

2.2.2. Sulfidogenic-bacteria and *Archaea* diversity

2.2.2.1. DNA extraction from the original water samples and the cultivated biofilms

For the extraction of genomic DNA from the water samples, one liter of the original water sample was filtrated using 0.22 µm pore size filter paper (Whatman). The filter papers were cut into small pieces and transferred to a 2 ml phosphate buffer saline (PBS, pH 7.0) then vortex and centrifuged for 10 min at 11627 g.

The cultivated biofilms (over the coupons) of reactor A were scratched from the coupons with sterile razor blades and suspended in the culture media, concentrated by centrifugation, washed two times with PBS (pH 7.0) and again concentrated by centrifugation. Genomic DNA was extracted from the prepared pellets diluted in 100 µl PBS using the Fast DNA SPIN kit for soil (Bio101; Carlsbad, CA, USA) according to the manufacturer's protocol. The extracted DNA was diluted to an adequate concentration with sterile water for subsequent PCR reactions to minimize the formation of heteroduplexe molecules and stored at -20 °C until further use.

2.2.2.2. Amplification of dsr β-subunit-gene (dsrβ)

Primer set DSRp2060F (5´ CAA CAT CGT YCA YAC CCA GGG-3`) to which a 40 bp GC-clamp (Muyzer et al., 1993) was added at the 5´ end and DSR4R

(5`GTG TAG CAG TTA CCG CA 3`) was used (White et al., 1985) to get a dsrβ-gene fragment of approximately 350 bp. PCR amplification was carried out in a Primus 96 advanced Thermocycler (Peqlab Biotechnology GmbH, Erlangen, Germany). The reaction mixture (50 µl) contained 1 µl template DNA, 25 µl hot start master mix, 1 µl from each primer (10 pmol/µl) and 22 µl biodest water (Hot Start Taq Qiagen). Thermal cycling was carried out by using an initial denaturation step of 95°C for 15 min, followed by 35 cycles of denaturation at 94°C for 1 min, annealing at 55°C for 1 min, and elongation at 72°C for 1 min. Cycling was completed by a final elongation step of 72°C for 10 min. Positive control of reference strain *Desulfovibrio desulfori-cans* (DSMZ 642) was included in PCR experiments along with negative control (No DNA added). The PCR products of dsrβ-gene fragments were purified using Qiaquick PCR purification Kit (QIAGEN GmbH, Hilden, Germany) for denaturing gradient gel electrophoresis (DGGE).

2.2.2.3. DGGE of dsrβ-gene fragments

Community pattern of the PCR amplicons of the dsrβ-gene from the water samples (W) and from the cultivated biofilm (CB) were generated using dsrβ based DGGE. DGGE was performed according to the manufacturer instruction of Bio-rad DCode system (Bio-Rad Laboratories, Hercules, CA, USA). The PCR products were loaded into 8 % (w/v) polyacrylamide gels in 1x Tris-Acetate-EDTA buffer (TAE). The polyacrylamide gel was made with a denaturing gradient ranging from 35 to 75 % (100 % denaturant contains 7 M urea and 40 % Formamide). Electrophoresis was performed in 1x TAE buffer at 100 V and at 60°C for 17 h. The gel was stained for 30 min in 1x TAE buffer containing SYBR Gold (1:1000; Molecular Probes, Eugene, OR, USA). DGGE bands of interest were excised, reamplified using the corresponding primers pairs, purified using Qiaquick PCR purification Kit (QIAGEN GmbH, Hilden, Germany) and sequenced.

2.2.2.4. Amplification of *Archaea* from the original water samples

For the analysis of *Archaea* in the original water samples, the amplification was performed using primers Arch 344F (5`ACG GGG YGC AGC AGG CGC GA 3`) and Arch 915 R (5´GTG CTC CCC CGC CAA TTC CT 3`) with an expected fragment of 590 bp. Each PCR mixture (50 µl) contained 1 µl template DNA, 25 µl hot start master mix, 1 µl from each primer (10 pmol/µl) and 22 µl biodest water (Hot Start Taq, Qiagen). Thermal cycling was carried out by using an initial denaturation step of 95°C for 15 min, followed by 35 cycles of denaturation at 95°C for 45 sec, annealing

at 65°C for 45 sec, and elongation at 72°C for 1 min. Cycling was completed by a final elongation step of 72°C for 10 min.

2.2.2.5. Cloning of *Archaea*

The eluted *Archaea* PCR products (590 bp) was ligated into the PCR -®4-TOPO ® plasmid vector and transformed into competent *E. coli* TOP 10 cells using TOPO-TA cloning kit according to the manufacturer's instructions (Invitrogen, CA, USA). Fifty colonies were randomly selected from the LB plates with ampicillin (50µl/ml) and DNA inserts were amplified with M13 forward and M13 reverse primers. Thermal cycling was carried out by using an initial denaturation step of 95°C for 15 min, followed by 35 cycles of denaturation at 95°C for 20 sec, annealing at 52.5°C for 45 sec, and elongation at 72°C for 1 min. Cycling was completed by a final elongation step of 72°C for 10 min. The PCR amplicons from the individual clones were subjected to restriction enzyme Hin PII (Hin61) and HaeIII (BsuR1) (Fermentas) digestion. Clones containing inserts that produced identical restriction patterns were grouped and then one of the different groups were purified and sequenced commercially by Eurofins (MWG GmbH, Germany).

2.2.2.6. Phylogenetic analysis

The sequences from the DGGE bands and the *Archaea* clones were analyzed using the BLAST (Page, 1996) and FASTA programs (Lipman and Pearson, 1985) of the National Center for Biotechnology Information (NCBI) in order to get phylogenetic relationships. The dsrβ sequences were translated into amino acids sequences using ExPASy-Translate tool. Sequence alignments of dsrβ and 16S rRNA *Archaea* clones sequences were performed by using the CLUSTAL X program (v.1.83). Matrices of evolutionary distance were constructed by the neighbor-joining method (Page, 1996) and the phylogenetic trees were visualized with Tree View software (Saitou and Nei, 1987). Bootstrap resembling analysis of 1.000 replicates was performed to estimate the confidence of tree topology. The sequence for dsrβ (accession no. HQ271209–HQ271254) and 16S rRNA *Archaea* sequences (accession no. HQ271186–HQ271194) have been deposited in GenBank.

2.2.3. Sulfidogenic activity

Fifty ml was taken weekly during 4 weeks cultivation from reactor B bulk phase and used to analyze dissolved sulfide according to the German Standard Methods (DEV, 1993). Afterward the biofilm was removed from the coupon by immersing each coupon in Clarke solution (1 L 36 % HCl, 20 g Sb_2O_3 and 50 g $SnCl_2$) for 10-15 sec,

washed with deionized water, ethanol and then dried in the desiccator. Subsequently the dried coupons were weighed and the weight loss was determined by comparison with the weight of the coupons after and before cultivation. The corrosion rate (g/m^2d) was calculated from weight loss results (Quraishi et al., 2002).

The metal surface in this study was examined using scanning electron microscopy (SEM) model Leica/Cambridge Stereo scan 360 at magnification ranging from 50x to 10.000x and operated at an acceleration voltage of 20 V. After cultivation, the mild steel coupons with the attached biofilms were removed from the reactor C, fixed with 3 % glutaraldehyde PBS, pH 7.3–7.4 for 4 h, washed two times with PBS (5 min each), rinsed with distilled water for another two times (5 min each) and then dehydrated using an ethanol gradient (50, 75, 95 and 99 %) for 10 min before being finally stored in the desiccator. Energy-dispersive X-ray spectroscopy (EDX) was used to analyze the chemical composition of corrosion products and biological deposits on metal surface.

Confocal laser scanning microscopy (CLSM) was used to characterize bacterial cells and EPS distribution within sulfidogenic biofilm. At maximum sulfide production the mild steel coupons with the attached biofilms were removed from the reactor D and immersed first in 0.85 % NaCl to remove the bulk phase planktonic cells. For the detection of bacterial cells the nucleic acid stain SYTO60 (Invitrogen, Eugene, USA) was used according to the protocol described by Neu (Neu, 1996). *Aleuria aurantia lectin* (LINARIS Biologische Produkte GmbH, Wertheim-Bettingen, Germany) labeled with AlexaFluor 488 (Invitrogen/Molecular Probes, Eugene, USA) was applied to stain EPS glycoconjugates (as a component of EPS). Proteins were stained with SYPRO Orange (Invitrogen /Molecular Probes, Eugene, USA) according protocol described by Lawrence et al., (2003). A Zeiss LSM510 META (Carl Zeiss Micro-Imaging GmbH, Jena, Germany) was used to create image stacks, adjusted by the AIM software (v. 3.2, Carl Zeiss Micro Imaging GmbH, Jena, Germany). For excitation two wavelengths were used: 488 and 633 nm that is related to the stain used. A 63x 0.95 numerical aperture (NA) water immersion lens was applied for in situ observation of the biofilms over the coupons. For each sample, five microscopic fields were selected randomly and scanned for nucleic acids, EPS glycoconjugates and proteins. The pinhole was adjusted for all channels with an identical value to a stack slice thicknesses of 0.79 µm (North, 2006). For Image analysis, the software ImageJ (v.1.39i, http://rsb.info.nih.gov/ij/index.html) was used. Image analysis and

calculation details are documented by Wagner et al., (2009). The coverage (C) of each single image of the image stack was quantified by the ImageJ software. The average coverage ($\bar{C}_{stack}$) was calculated for each image stack from the first slice (n=1) where average coverage equal 0.1 % to the last slice ($n=n_{max}$) where average coverage equal 0.1 % according to the following equation (Wagner et al., 2009),

$$\bar{C}_{stack} = \frac{1}{n_{max}} \sum_{n=1}^{n=n_{max}} C \qquad \text{With n =number of slice} \qquad (1)$$

Then the mean average coverage values of the five scanned microscopic fields on the same coupon were calculated and used to evaluate the change in the nucleic acids, EPS glycoconjugates and proteins distribution in different biofilms.

2.3. Results and Discussion

2.3.1. Chemical characteristics of the water samples

The water samples were yellowish-black in color. The chemical analysis of the water samples showed significant differences in their chemical properties (Table 2–4). The lowest salinity Hamra water sample was distinguished by neutral pH (7.1) with low Calcium, Magnesium, Sulfate concentration in comparison with the KSW and the Youmna water samples. While the high salinity KSW-water sample was discriminated by mild acidic pH (6.3) with high Magnesium, Sulfate, Bicarbonate and very low Iron content in comparison with the Hamra and the Youmna water samples. Moreover, the highest salinity Youmna water sample was characterized by acidic pH (5.8) and the highest Calcium and Iron concentration.

Table 2–4 Original water samples analysis of different parameters

Data	Unit	Hamra	KSW	Youmna
Calcium	mg/l	131	950	3600
Magnesium	mg/l	21	1950	1120
Sulfate	mg/l	850	1520	1300
Bicarbonate	mg/l	435	440	140
Iron	mg/l	1.69	0.51	20.0
pH		7.1	6.3	5.8
Salinity (NaCl)	mg/l	230	3190	5490
Water well temperature	°C	78	93	80
Water tank temperature	°C	37	37	37

2.3.2. Phylogenetic analysis of sulfidogenic anaerobic microbial community

The impact of sulfidogenic-biofilm activities in QPC water tanks with different salinity contents is not well understood in spite of the serious problems caused by these microorganisms over the metal surface. Changing in the chemical analysis of the water samples (Table 2–4) can predict different microbial diversities and different corrosion activities.

Detection of sulfidogenic activities in most petroleum companies relies on the inoculation of standard medium with samples (water, oil). Then after incubation period, the appearance of a black precipitation (Ferrous sulfide) was used as a marker for sulfate reduction and as an indicator for the activity of sulfidogenic bacteria in culture media. However cultivation conditions such as using lactate as a carbon source, specific nutrients contents according to Postgate (1984) and specific cultivation temperature (37°C) cannot reflect in situ field conditions (well and tank temperature). Additionally, the change of these conditions might cause a shift in the original sulfidogenic microbial diversity in the water samples. In this respect, the knowledge of microbial diversity in the cultivated biofilms and in the original water samples is helpful to understand the microbial diversity inducing metal corrosion in different salinity environments. Dsrβ (as a taxonomic marker) based DGGE was used to rapidly assess the community composition of sulfate reducers (Klein et al., 2001). The DGGE profile (Figure 2–2) demonstrated the change in the sulfidogenic diversity of the original water samples (W) with different salinities and their related cultivated

biofilms (CB). The DGGE pattern of the Hamra sample was represented in six DGGE-bands from W and seven from CB. While the KSW sample was displayed in seven DGGE-bands from W and ten from CB. Moreover, the Youmna sample results showed a reduction in microbial diversity from nine bands in W to one band in CB. The change in the DGGE pattern in W and CB might be attributed to the selective cultivation conditions which did not reflect the in situ water properties such as organic, inorganic contents and cultivation temperature (Gasol et al., 2004, Voordouw et al., 1992). Additionally, it has been reported that bacteria that compose ≤ 9 % of complex microbial communities may not be detected by DGGE (Straub and Buchholz-Cleven, 1998).

The phylogenetic sequence analysis of the excised DGGE bands of the Hamra sample (Figure 2–3a) showed that, most of sequences affiliated to the phylum *Proteobacteria*, order *Desulfovibrionales.* These sequences were represented by two genera *Desulfovibrio* and *Desulfomicrobium*. The presence of *Desulfomicrobium thermophilum* in the original water sample sequences can be attributed to the high temperature (78°C) of Hamra-water well. It has been reported that *Desulfomicrobium thermophilum* grow optimally at 55°C (Thevenieau et al., 2007). Further Hamra sequences were identified as genus *Desulfotomaculum* and *Desulfosporosinus* (phylum *Firmicutes*). The taxonomic affiliation of the genera *Desulfotomaculum* and *Desulfosporosinus, (*phylum *Firmicutes)* within the phylum *Proteobacteria* can be explained by the presence of nonorthologous *dsr*-genes in these species obtained by lateral gene transfer from species belonging to the phylum *Proteobacteria* (Geets et al., 2006, Klein et al., 2001).

The phylogenetic sequence analysis of the KSW sample (Figure 2–3b) showed that most of the analyzed DGGE band sequences were also belonging to the phylum *Proteobacteria* of the order *Desulfovibrionales.* These sequences were represented by three genera, *Desulfovibrio*, *Desulfomicrobium* and *Desulfonauticus. Desulfonauticus submarinus* was detected in the cultivated biofilm sample and this species was detected growing with optimum salinity of (2–5 % NaCl) (Mayilraj et al., 2009) similar to the salinity of KSW sample. *Desulfotomaculum acetoxidans* affiliated within the phylum *Firmicutes* was detected in this sample (as in the Hamra sample).

Phylogenetic analysis of the Youmna DGGE band sequences (Figure 2–3c) demonstrated a high similarity to the Hamra and KSW samples. Most of the DGGE band sequences were related to the phylum *Proteobacteria within* the order

Desulfovibrionales. These sequences were represented by two genera *Desulfovibrio* and *Desulfohalobium.* The *Desulfohalobium retbaense* was detected in the DGGE band sequences and the same species was isolated from Hypersaline Lake in Senegal and growing with the high salinity as in the Youmna sample (Ollivier et al., 1991). The other band sequences were attributed as uncultured bacteria. *Desulfovibrio oxyclinae* was present in both the water sample and the cultivated biofilm. It is also known this species can grow in salinity up to 10 % NaCl (Krekeler et al., 1997) similar to the salinity of Youmna sample.

Desulfovibrio spp. was the most dominant sequence in the analyzed DGGE sequence-bands of all original water samples and their cultivated biofilms. These results emphasized the important role of the genus *Desulfovibrio* in the microbial corrosion as reported in the previous studies (Chan et al., 2002, Dinh et al., 2004). Its important role is due to H_2S production which changes the medium pH and leads to precipitation of ferrous sulfide on the metal surface and hence leads to severe metal corrosion (Neria-Gonzalez et al., 2006).

The phylogenetic analysis of the DGGE band sequences showed that multiple-bands for one related species sequence, KSW (W1), KSW (W2), Hamra (CB3), Hamra (CB5) were related to genus *Desulfovibrio*. Multiple bands might be the result of degeneracy of the DSRp2060F primer resulting in two or more copies of the same dsrβ-gene with minor variation followed by heteroduplexes formation (Geets et al., 2006).

In the present study, dsrβ-gene as a functional marker was effectively applied to investigate the changes of the sulfidogenic microbial communities in the water samples with different salinities and their related cultivated biofilms. With this approach it is possible to differentiate between genus and species. Therefore is considered the best studied example of such functional and taxonomic marker as reported in the previous studies (Dhillon et al., 2003).

No sulfidogenic *Archaea* species were detected with the dsrβ-gene based DGGE. In order to assess if there is *Archaea* species present in the original water samples with corrosion activity, the 16S rRNA cloning approach was used. Only Hamra water sample produced a positive PCR result with *Archaea* specific primers. The occurrence of *Archaea* species was associated with the lower sulfate content and the lower salinity in the Hamra-original water sample in comparison to the KSW and Youmna water samples (see Table 2–4). It has been reported that the presence

of SRB in high sulfate environment (as in marine system) leads to the production of corrosive hydrogen sulfide (Jørgensen, 1993). The corrosive toxic hydrogen sulfide inhibits the growth of methane producing *Archaea* (Karkhoff-Schweizer et al., 1995). In contrast, the methanogenesis is the dominant process in the fresh water systems with low sulfate level (Lovely and Phillips, 1987) as determined in the Hamra water sample. All clone inserts within the clone libraries of the Hamra sample (Figure 2–4) associated within the phylum *Euryarchaota represented* by different methanogenic species. This result was expected due to the optimal growth conditions for these species with the Hamra water sample as explained above. The most of the clone sequences were belonged to the order *Methanobacteriales*. One clone sequence was classified within the order *Methanomicriales* and one clone sequence was affiliated with the order *Thermococcales*. Members of the orders *Methanobacteriales* and *Methanomicriales* were known to be associated with petroleum pipeline corrosion (Zhu et al., 2003). Additionally, the detected species *Methanoplanus limicola* (order *Methanobacteriales*) in the Hamra water sample was reported to be an anaerobic hydrogen consuming microorganism. The same species was isolated from Japanese oil/gas facilities (Mori et al., 2010). It is well known that the detected methanogenic *Archaea* have the capability to accelerate corrosion process by a cathodic depolarization. Therefore the presences of the methanogenic *Archaea* in addition to the sulfidogenic bacteria within the Hamra water sample help us to better understand the microbial corrosion process.

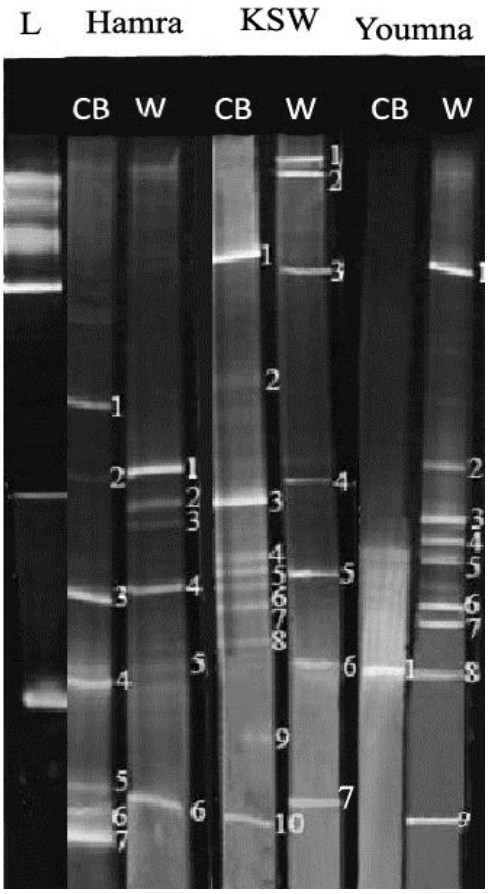

Figure 2–2. DGGE analysis of dsrβ-gene fragments amplified with GC-DSRp2060F/DSR4R (fragment length 350 bp) from three sulfidogenic microbial communities with different salinity contents (NaCl), Hamra (0.23 %), KSW (3.19 %) and Youmna (5.49 %). DGGE denaturing gradient was 35 to 75%. Numbers represent excised bands, (L) DNA ladder, (CB) cultivated biofilm and (W) original water sample.

(a)


Hamra-CB2 (HQ271232)
64
Desulfomicrobium sp. CME2 (AAK71940)
Hamra-CB7 (HQ271237)
65
Hamra-CB1 (HQ271231)
67
Hamra-W6 (HQ271230)
Desulfomicrobium thermophilum (ABE73460)
Hamra-W4 (HQ271228)
Hamra-CB6 (HQ271236)
63
Desulfovibrio aespoeensis Aspo-2 (ZP_06233090)
67
Hamra-W5 (HQ271229)
58
Desulfovibrio sp. P1B2 (AAC24108)
Phylum Proteobacteria
83
Hamra-W1 (HQ271225)
Desulfotomaculum acetoxidans(AAK82967)
83
Hamra-W2 (HQ271226)
Desulfotomaculum sp. Srb55 (BAF34616)
55
Hamra-W3 (HQ271227)
68
Desulfosporosinus sp. JG32A (AAV54527)
Phylum Firmicutes
Hamra-CB3(HQ271233)
Hamra-CB5 (HQ271235)
Desulfovibrio termitidis HI1 (BAB55578)
Hamra-CB4(HQ271234)
Desulfovibrio desulfuricans subsp. desulfuricans str. G20(YP_387023)
Phylum Proteobacteria
Archaeoglobus fulgidus DSM 4304
Pseudomonas aeruginosa
0.1

(b)


KSW-CB10 (HQ271254)
Desulfovibrio sp. CME3 (AAK71942)
KSW-W1 (HQ271238)
66
KSW-W2 (HQ271239)
Desulfovibrio aespoeensis Aspo-2(ZP_06233090)
62
KSW-W7 (HQ271244)
Bacterium LS1101 (ABD57227.1)
KSW-W4 (HQ271241)
KSW-W5 (HQ271242)
KSW-CB5 (HQ271249)
Desulfovibrio sp. P1B2 (AAC24108)
84
KSW-CB2 (HQ271246)
Sulfate-reducing bacterium AR1104(ABC60325)
78
KSW-CB7 (HQ271251)
Desulfovibrio oxyclinae(AAV35109)
KSW-CB3 (HQ271247)
66
Bacterium AR1201(ABD57229)
KSW-CB6 (HQ271250)
72
Bacterium AR1103 (ABC60324.1)
KSW-CB9 (HQ271253)
66
Desulfomicrobium thermophilum (ABE73460)
Phylum Proteobacteria
54
56
85
KSW-W3 (HQ271240)
Desulfotomaculum acetoxidans DSM 771 (AAK13056)
Phylum Firmicutes
53
66
KSW-CB4 (HQ271248)
Desulfonauticus submarinus (AAO27365)
55
KSW-CB1 (HQ271245)
65
Desulfomicrobium baculatum (YP_003156823)
Desulfomicrobium sp. ADR28(CAM35462)
Phylum Proteobacteria
KSW-CB8 (HQ271252)
KSW-W6 (HQ271243)
79
Desulfovibrio salexigens (YP_002990393.1)
Archaeoglobus fulgidus DSM 4304
Pseudomonas aeruginosa
0.1

(c)

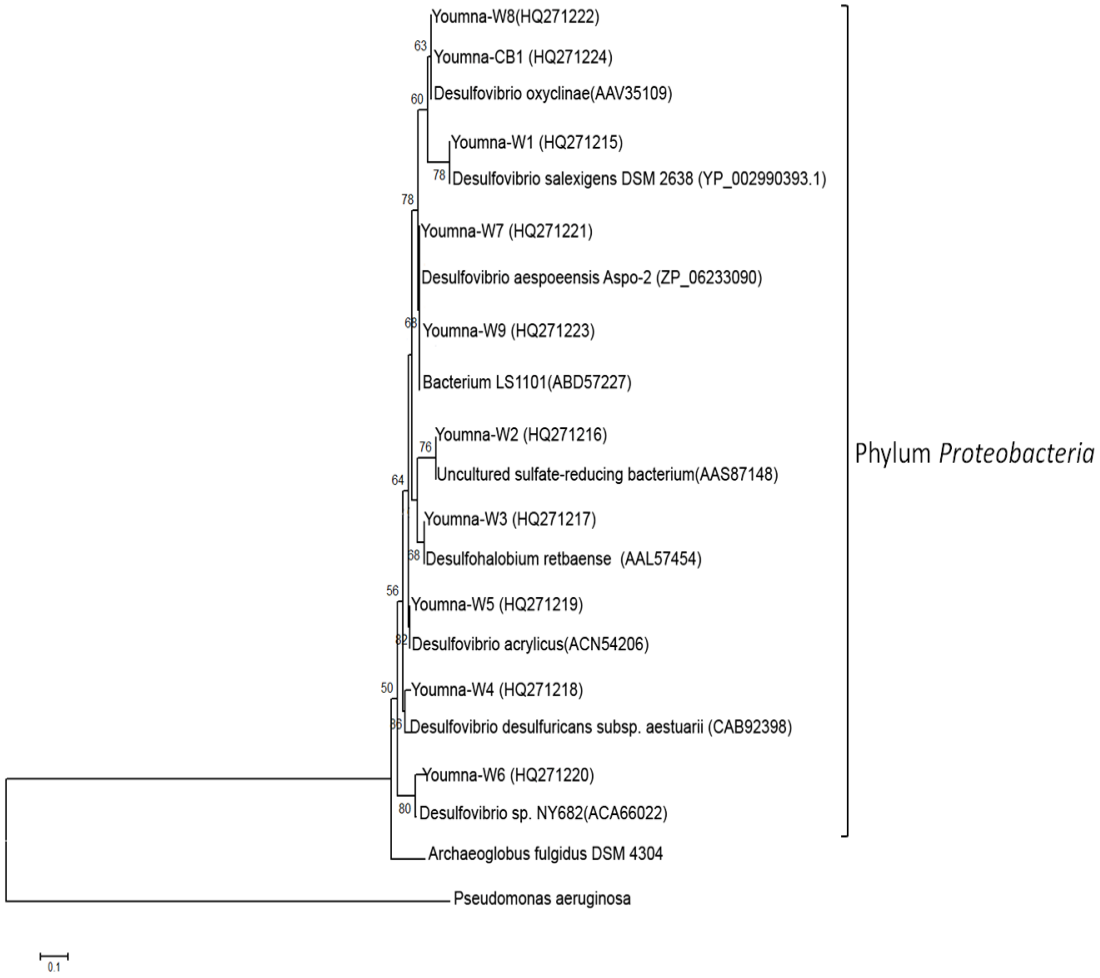

Figure 2–3. Neighbor-joining phylogenetic tree of partial the dsrβ protein sequence (350 bp) from DGGE bands. Original water sample (W) and related cultivated bacteria (CB). (a) Hamra, (b) KSW and (c) Youmna samples. Bootstrap values (1000 replicates). Gene bank accession numbers of DGGE band sequences and closely related bacteria are shown in parentheses, scale bar represents 10 % estimated sequence divergence.

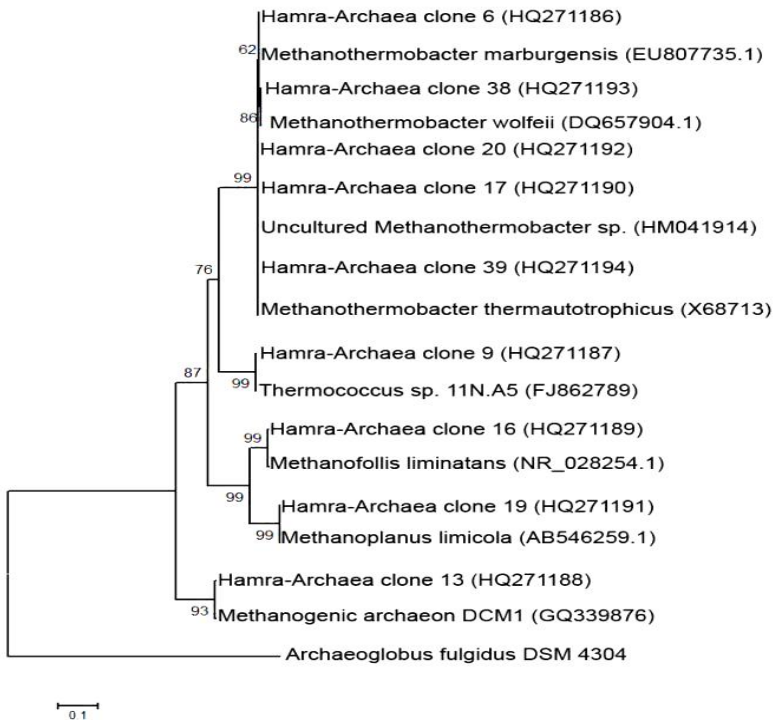

Figure 2–4. Neighbor-joining phylogenetic tree based on 16S rRNA gene (590 bp) partial sequence of *Archaea* clone library detected in the Hamra original water sample. Bootstrap values (1000 replicates). Gene bank accession numbers of the Hamra *Archaea* clones and related *Archaea* are shown in parentheses, scale bar represents 10 % estimated sequence divergence.

2.3.3. The sulfidogenic biofilm activity

Sulfide concentration was measured in all reactors as a metabolic end product of sulfidogenic process (Figure 1–4). All sulfidogenic biofilms attached to the metal surface (coupon) were able to produce sulfide in the bulk phase as an indication of very active bacterial consortia over the metal surface. Sulfide concentrations in all reactors were increased from the beginning followed by a decline after two weeks cultivation (Figure 2–5). These observations indicated that the produced sulfide inhibited further sulfate reduction activity as was also reported by Utgikar and co-workers (Utgikar et al., 2002). The Hamra-sulfidogenic biofilm showed the highest sulfide production in comparison to the KSW and the Youmna-sulfidogenic biofilms. This result was attributed to strong bacterial consortia over metal surface that were represented by seven DGGE band sequences (see Figure 2–2). In addition Hamra-sulfidogenic activity-result can predict microbially-influenced corrosion (MIC) effect

over the metal surface. However Youmna-sulfidogenic biofilm was the lowest microbial diversity, it is showing high sulfide production in comparison to KSW-sulfidogenic biofilm with high diversity composition.

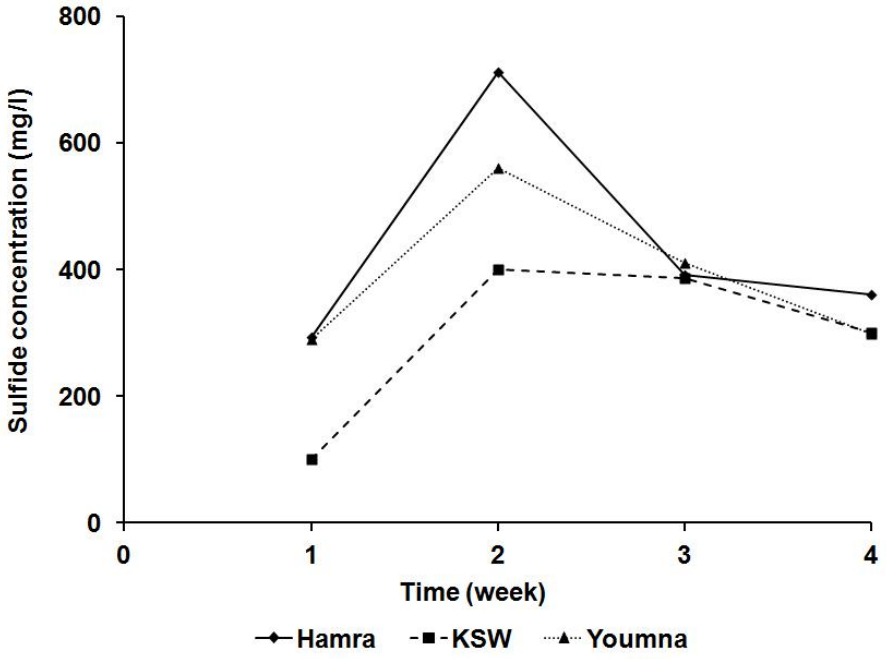

Figure 2–5. Sulfide concentrations (mg/l) in the bulk phase of the three reactors (Hamra, KSW, and Youmna) during cultivation.

At the end of one month cultivation, the weight loss of the coupon was measured and metal corrosion rate was calculated (Table 2–5). The results demonstrated a positive correlation between the metal corrosion rate and the salinity of the cultivated biofilms in the KSW and Youmna-sulfidogenic biofilms. The KSW and the Youmna-sulfidogenic biofilms with high medium salinities showed higher metal corrosion rate than in the Hamra-sulfidogenic biofilm with a low medium salinity. This result can be attributed more to the different medium salinity than the sulfidogenic biofilm activity. In contrast, the Hamra-sulfidogenic biofilm metal corrosion rate was related more to the sulfidogenic activity than the medium salinity (see Figure 2–5) in comparison to Youmna and KSW-sulfidogenic biofilms.

The metal corrosion rate of the cultivated sulfidogenic-bacteria (at different medium salinities) was attributed to three main factors. (1) Medium salinity (NaCl %) that is considered as one of an important factors increasing the metal corrosion rate especially in KSW and Youmna samples in comparison to Hamra sample. Chloride anion increases the solubility of the corrosion products and rises significant-

ly the conductivity of the electrolyte layer over the metal surface. Thus it destroys the passive film existing on the metal surface and produce pits and crevices corrosion (Giudice and Amo, 1996, Skolink et al., 2000) (More details were provided in chapter 3). (2) Corrosiveness of hydrogen sulfide (H_2S) which produced from the cultivated sulfidogenic-bacteria (Figure 2–5). Sulfide can accelerate corrosion of metals by being source of bound protons and by precipitation of Fe^{2+} as FeS (Lee et al., 1995) (Figure 1–4). It has also been proposed that the iron sulfide layers that forms over the metal surface plays an important role in the initiation of pitting corrosion (Rickard, 1969). King et al., (1973) demonstrated that weight loss of the metal was proportional to the concentration of sulfide (More details were provided in chapter 3). (3) The cultivated sulfidogenic-bacteria facilitate corrosion process by attaching themselves to the metal surface, trapping corrosive metabolites products such as sulfide in close to the metals surfaces and thus initialized localized corrosion (Geesey et al., 2006, Jones and Amy, 2002). It has been hypothesized that EPS have the ability to entrap metal ions by binding carboxylic groups of the exopolysaccharides and phosphate groups of the nucleic acids to the metal ions. Hence, it increased the overall metal-binding capacity of EPS (Beech and Gaylarde, 1999). This binding would influence the electrochemical behavior of a metal through formation of metal corrosion cells and galvanic coupling (Braissant et al., 2007). The detection of biofilm, sulfide and sodium chloride will be confirmed later from SEM and EDX analysis.

Table 2–5 Corrosion rate for each sulfidogenic coupons attached in the reactors.

Sample	**Hamra**	**KSW**	**Youmna**
Corrosion rate (g/m^2 d)	0.73	0.92	3.29

To visualize the biofilm formation over the metal surfaces, SEM was used. Results clearly confirmed that the sulfidogenic biofilms colonized the metal surface (Figure 2–6a). SEM combined with EDX detects the elemental surface-microanalysis of the biofilm over the metal surface. EDX analysis (Figure 2–6b) revealed that sulfide as a sulfidogenic metabolic end product was present in all samples over the metal surface. Sulfide ions can be bound with ferrous forming ferrous sulfide deposited on the metal surfaces as FeS or $Fe(OH)_2$ and initiated the pitting corrosion. Sulfide itself showed anodic properties substance that play important role in metal dissolution (Hamilton, 1985). Sodium and chloride can also be identified in the biofilm matrices

over the metal surface. The presence of chloride anion beneath the biofilm matrix is likely due to the medium salinity. It can be obviously recognized in the Youmna and the KSW sample in comparison to the Hamra and the control sample. The EDX results confirmed the corrosion rate data, the role of metabolic products of sulfidogenic biofilms and harmful chloride anion for inducing severs corrosion on the metal surface.

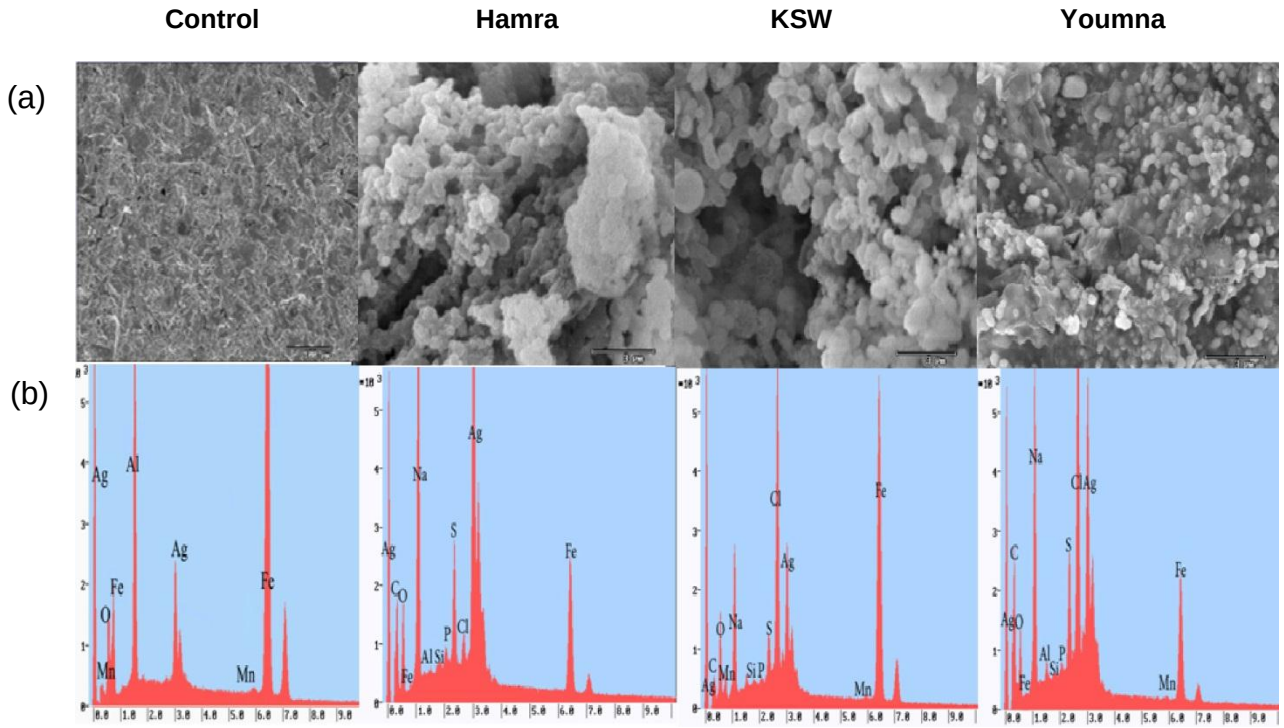

Figure 2–6. SEM image of sulfidogenic biofilms on the mild steel coupons, the Hamra-sulfidogenic biofilm (a) and EDX spectra (b). Control coupons=coupons without bacteria, Hamra= coupons with Hamra-sulfidogenic biofilm at salinity of 0.23 %, KSW=coupons with the KSW-sulfidogenic biofilm at salinity of 3.19 % and Youmna=coupons with the Youmna-sulfidogenic bacteria at salinity of 5.49 %. Scale bar = 3 µm.

2.3.4. Biofilm structure

Fully hydrated biofilms (Hamra, KSW, and Youmna) were investigated with CLSM and staining protocol to determine their structure concerning the distribution of the EPS and the microbial population over the coupons (Figure 2–7 and Figure 2–8). Results represented in Figure 2–7 showed the distribution of nucleic acids/EPS glycoconjugates (slice coverage %) across the biofilm thickness (µm) of the cultivated biofilms (Hamra, KSW and Youmna) which cultivated at different medium salinities and showed different diversities Figure 2–2 and activities Figure 2–5 and Table 2–5.

Most of the biomass of the sulfidogenic biofilms is mainly located in the upper regions of the biofilm, near to the bulk phase. The Hamra and KSW-sulfidogenic biofilms showed thicker and developed biofilms in comparison to Youmna-sulfidogenic-biofilm. This result can be attributed to the diversity of the cultivated biofilm matrix.

The distribution of nucleic acids, EPS glycoconjugates and proteins for five microscopic fields on the same coupons were detected. The results (Figure 2–8) revealed that the heterogeneity of the biofilms and the bacterial density over the metal surface can also be correlated to high EPS-compounds with metal surface interactions (Gu et al., 2000). The Hamra-sulfidogenic biofilm which was cultivated with low salinity medium (0.23 % NaCl), seven DGGE band sequences and highest sulfide production showed similar average coverage of the bacterial population and EPS compounds over the metal surface. While the cultivated KSW-sulfidogenic biofilm with a medium salinity (3.19 % NaCl), ten DGGE band sequences and lowest sulfide production demonstrated most excessive biofilm development over the metal surface. KSW-sulfidogenic biofilm tend to produce EPS glycoconjugates rather than protein. The cultivated Youmna-sulfidogenic biofilm with the highest salinity (5.49 % NaCl) and only one DGGE band sequence showed the lowest biofilm development over the metal surface. The Youmna-sulfidogenic biofilm showed also the tendency to produce EPS glycoconjugates rather than protein as in the KSW-sulfidogenic biofilm. This can be explained by the sensitivity of the proteins to salinity that leads to denaturation of the proteins. The salt ions bind to ionic "R" groups of the protein and then disrupt the ionic salt bridges which stabilize the tertiary and quaternary protein structure.

(a)

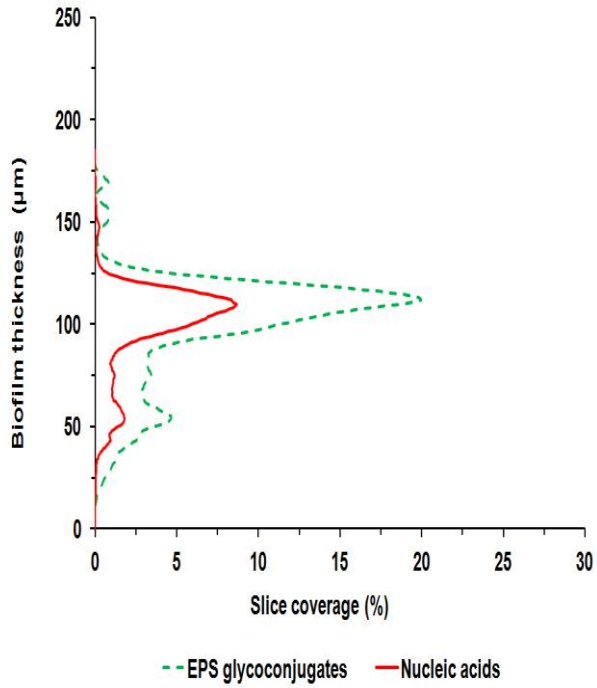

Nucleic acids/EPS glycoconjugates

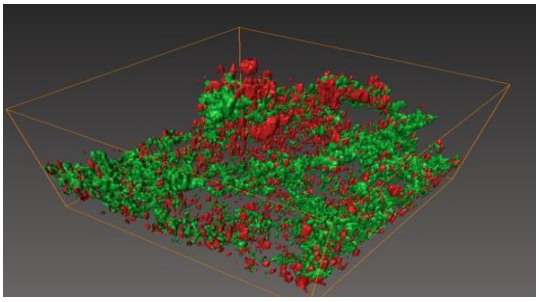

Nucleic acids/Proteins

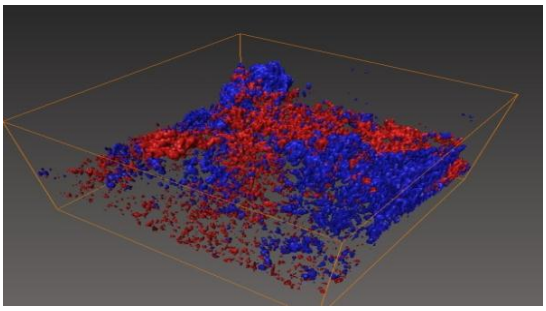

(b)

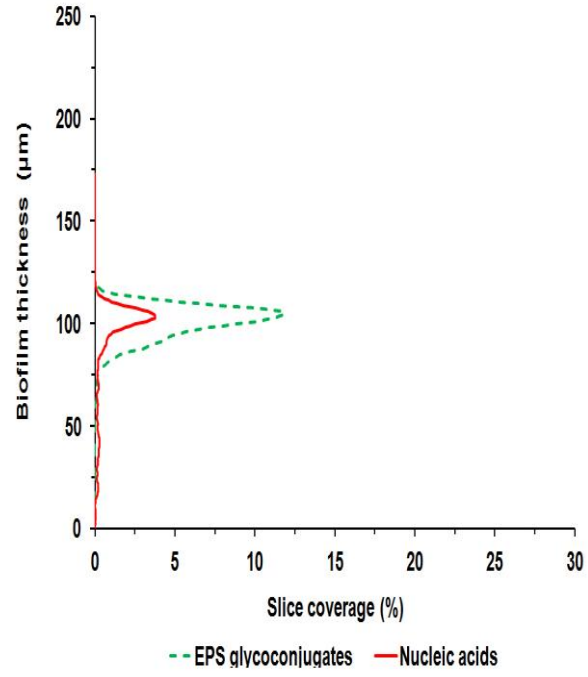

Nucleic acids/EPS glycoconjugates

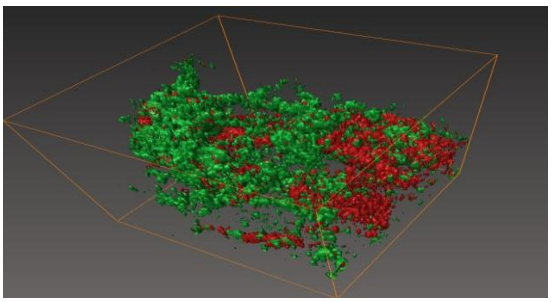

Nucleic acids/Proteins

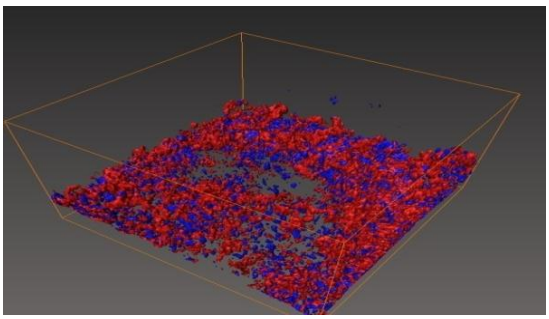

(c)

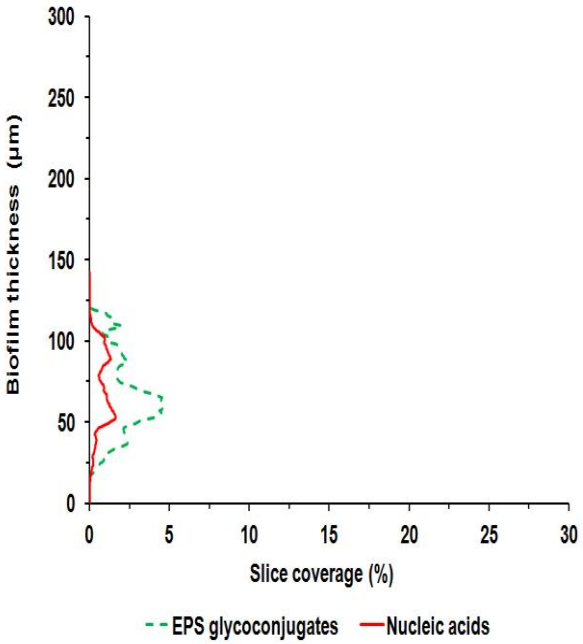

Nucleic acids/EPS glycoconjugates

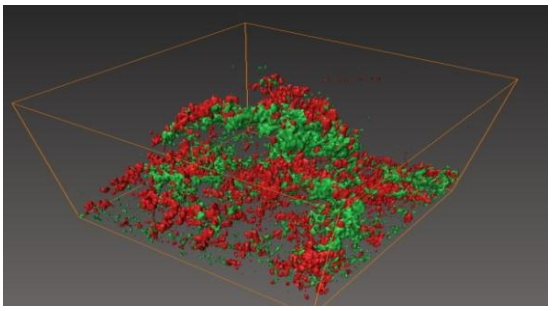

Nucleic acids/Proteins

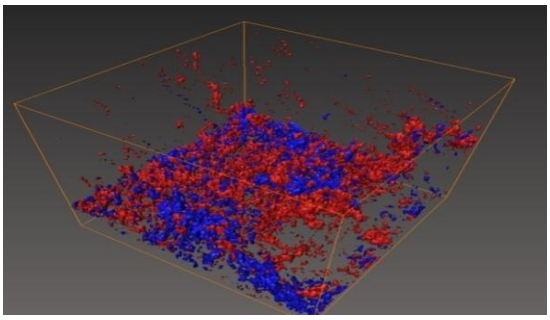

Figure 2–7 Distribution of nucleic acids/EPS glycoconjugates (represented as slice coverage %) across the biofilm thickness (µm) of three different biofilms. The left graphs showing (a) Hamra-sulfidogenic biofilm, (b) KSW-sulfidogenic biofilm and (c) Youmna-sulfidogenic biofilm. Zero marks the position of the substratum (coupon surface). The right graphs showing the corresponding 3D reconstruction of the CLSM stacks of the cultivated biofilms. Green color indicates EPS glycoconjugates, red color indicates Nucleic acids, and blue color indicates proteins.

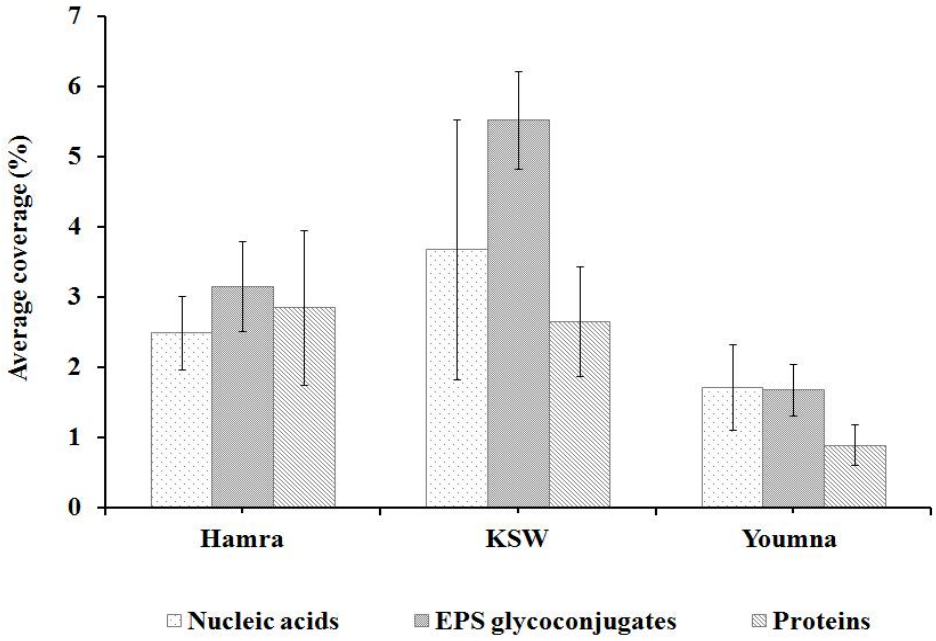

Figure 2–8. Distribution of nucleic acids, EPS glycoconjugates and proteins of the three different biofilms inoculated with the enriched sulfidogenic bacteria from Hamra, KSW and Youmna samples. The figures showed the average coverage of five randomly selected areas of the cultivated biofilms with corresponding standard deviation.

Summary

Chapter 2 showed a comparison between three water samples with different salinities on the basis of diversity and microbial/metal corrosion activity. Diversity was examined in the original water samples (w) as well as after enrichment and biofilms cultivation (CB).

The dsrβ (as a functional and taxonomic marker) gene-based DGGE approach. Microbial activity was detected on the basis of sulfide production, changes in the biofilm structure and constituents, and metal corrosion rate. The dsrβ gene-based DGGE approach was successfully used to assess the sulfidogenic diversities. Hamra sample, which was characterized by a low salinity (0.23 % NaCl), was represented in six DGGE-bands from original water samples (W) and seven from cultivated biofilm (CB). While, KSW sample, which had a salinity of 3.19 % NaCl was displayed in seven DGGE-bands from W and ten from CB. In addition, Youmna sample, which had a high salinity of 5.49 % NaCl, showed a reduction in microbial diversity from nine bands in W to one band in CB. No sulfidogenic-*Archaea* were detected in the DGGE-bands. In order to assess if there is *Archaea* species present in the original water samples with corrosion activity, the 16S rRNA cloning approach was used. Methanogenic-*Archaea* were only detected in water having a low salinity and sulfate concentration (Hamra).

Hamra-sulfidogenic biofilm showed the highest sulfide production in the bulk phase. In addition, it was marked by a compact and well developed biofilm structure with similar average coverage of the bacterial population and EPS compounds over the metal surface. Therefore, the metal corrosion activity of the cultivated biofilm was correlated to the sulfidogenic microbial activity on the metal surface. In comparison, KSW-sulfidogenic biofilm (the highest cultivated biofilm diversity) showed the lowest sulfide production in the bulk phase. KSW-sulfidogenic bacteria tend to produce thicker biofilms which mainly due to the highest microbial diversity. As a result of low sulfidogenic activity and thicker biofilm, the metal corrosion rate was related in this case more to the medium salinity than to the microbial activity. The thicker biofilm protected the metal surface from the cultivated medium salinity. Moreover, Youmna-sulfidogenic biofilm (the lowest cultivated biofilm diversity) produced more sulfide than KSW-sulfidogenic biofilm. A thinner biofilm developed on the metal surface and metal corrosion was related to the cultivated medium salinity in addition to microbial activity.

CHAPTER 3

Inhibiting mild steel corrosion from sulfidogenic biofilms using synthesized surfactants

3.1. Objectives

In this chapter, a cationic monomeric surfactant (CMS-I) and two cationic gemini surfactants (CGS-II, CGS-III) were synthesized and characterized. The activity and effectiveness of the synthesized surfactants (corrosion inhibitors and biocides) was studied concerning protect the metal surface from medium salinity and activity of sulfidogenic bacteria originated from Qarun Petroleum Company (QPC) water tanks (Hamra, KSW, and Youmna). Comparison of the inhibitory effect of CMS-I and CGS-II was done on the basis of protecting the metal surface from medium salinity (3.19 % NaCl) and activity of the KSW-sulfidogenic bacteria. CGS-II was also applied to inhibit the Hamra-sulfidogenic bacteria grown at low salinity habitat (0.23 % NaCl). In order to protect the metal surface from high salinity (5.49 % NaCl) and activity of Youmna-sulfidogenic bacteria CGS-III was used. The activity of all surfactants was discussed in terms of sulfide production, redox potential, cultivated biofilm constituent and metal corrosion rate (see Figure 3-1).

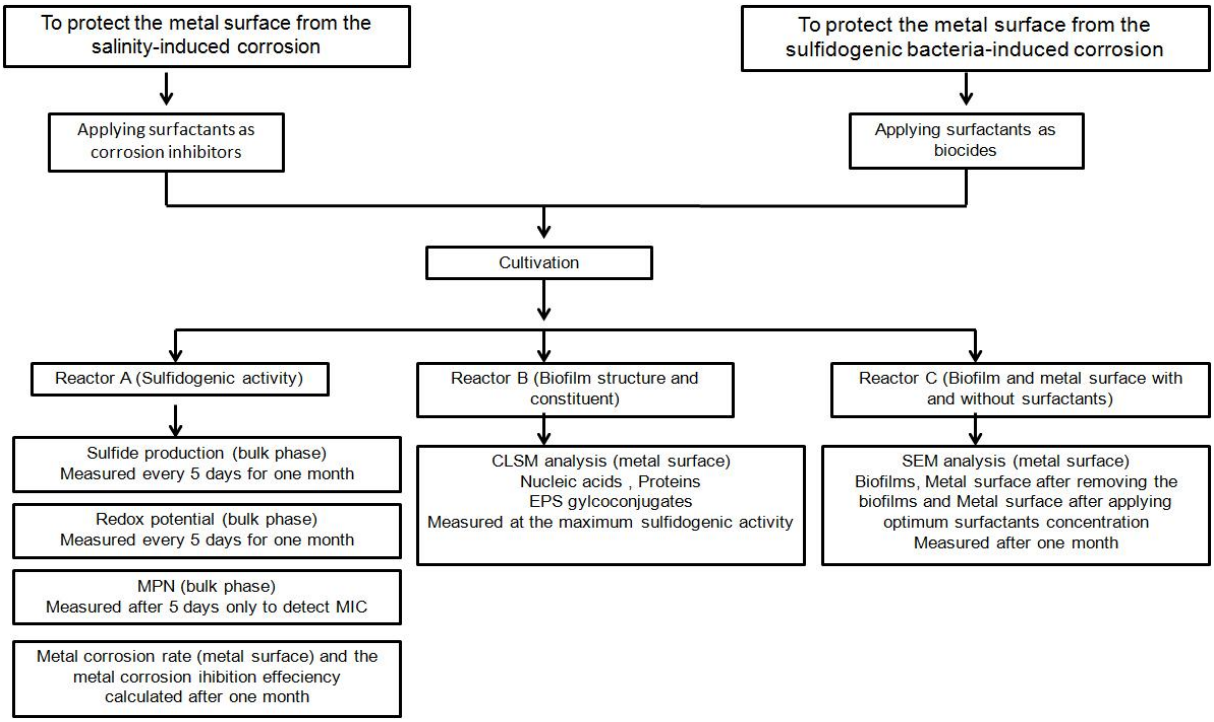

Figure 3-1 Schematic diagram showing the reactor setup and studied experiments.

3.2. Materials and Methods

3.2.1. Synthesis of the surfactants

All surfactants were synthesized and provided by M.A. Hegazy (Egyptian Petroleum Research institute, Cairo, Egypt).

3.2.1.1. Synthesis of a cationic monomeric surfactant (CMS-I)

The CMS-I in this study was synthesized by two steps. The first step involves the preparation of the surfactant molecule by quaternization reaction between 1 mol of N, N-dimethylpropan-2-amine and 1 mol of 1-bromododecane (Hegazy et al., 2011). The reactants were allowed to reflux in ethanol for 12 h at 70^{o}C. Then the reaction mixture was cooled to room temperature. In the second step, 1 mol of the reactant was allowed to react with 1 mol of potassium hydroxide. Afterward, it was refluxed in ethanol for 2 h at 70°C. The reaction mixture was left to cool for 1 h, then filtrated and concentrated by ethanol evaporation. At the end, the obtained white precipitate was then recrystallized twice from ethanol. The synthesis steps and chemical structure of the synthesized surfactant are shown in Figure 3–2.

3.2.1.2. Synthesis of two cationic gemini surfactants (CGS-II, CGS-III)

The both cationic gemini surfactants in this study were synthesized by three steps. The first step was quaternization reaction between 1 mol of 2-(dimethylamino) ethanol and 1 mol of 1-bromododecane in ethanol for 12 h at 70^{o}C. The mixture was left to cool and precipitate. Then the obtained white precipitate was purified by diethyl ether and afterward recrystallized by ethanol. The second step was esterification reaction between 2 mol of N-(2-hydroxyethyl)-N,N-dimethyldodecan-1-aminium bromide and 1 mol of phthalic acid or phosphoric acid (in the presence of toluene as solvent and p-toluene sulfonic acid as dehydrating agent) for CGS-II and CGS-III, respectively The reaction was completed after the water was removed from the reaction system and it was concentrated up to 2 mol. Afterward, the reaction mixture was distilled under vacuum to completely remove the solvent. The third step, 1 mol of the resulted products was allowed to react with 2 mol of potassium hydroxide. Then reflux in ethanol for 2 h at 70^{o}C. The reaction mixture was left to cool for 1 h and then filtrated and concentrated by ethanol evaporation. At the end the obtained pale brown precipitate was recrystallized twice from ethanol (Figure 3–2).

The chemical structure of all synthesized surfactants was confirmed by fourier transform infrared (FTIR) and nuclear magnetic resonance (NMR) spectroscopy (Bruker, Vortex 70 and Bruker, 400 MHZ NMR spectrometer, Avance DRX 400 for FTIR and NMR, respectively). The CGS-III was more confirmed by ^{31}P NMR using Jeol ECA 500 NMR spectrometer at 500 MHZ.

3.2.2. Surface tension and conductivity analysis

The surface tension of the synthesized surfactants was analyzed at different concentrations using a Du Nouy Tensiometer (Kruss Type 6). The measurements were done in distilled water (with surface tension 72 mN /m) at 25°C. For the conductivity analysis conduktometer (LF 191 WTW) was used.

3.2.3. Application of the synthesized surfactants as inhibitors

3.2.3.1. Sulfidogenic consortia

As it has been mentioned in the chapter 2, the sulfidogenic bacteria (Hamra, KSW, and Youmna) were originated from QPC, water tanks, Egypt.

3.2.3.2. Reactor setup, cultivation conditions and evaluation of the sulfidogenic activity

In order to investigate the effect of different synthesized surfactants on the sulfidogenic community, batch reactor experiment was carried out using modified Postgate´s-C medium see Table 2–1. A mild steel coupon with a chemical composition reported in Table 2–2 (CS1018 3”x 1⁄2”x 11⁄16” strip, Cormon LTD) was used as the main iron source for cultivated bacteria. Parallel reactor set ups were used for all experiments. Inhibition experiments were evaluated using different concentrations of the synthesized surfactants. In addition two control approaches were carried out (i) blank (medium without bacteria) and (ii) control (cultivated sulfidogenic bacteria without surfactant).

Three batch reactors (150 ml working volume) were inoculated with 3 ml enriched sulfidogenic bacteria (see Figure 3–1 and Table 3–1). The first reactor (reactor A) was operated in order to determine the sulfidogenic activity in the reactor bulk phase. A separate reactor (reactor B) was implemented to evaluate the biofilm constituents using confocal laser scanning microscopy (CLSM) and staining procedure. Moreover, an additional reactor (reactor C) was operated for one month to examine the biofilm, the metal surface (after removing the biofilm) and the metal sur-

face inoculated with the enriched sulfidogenic bacteria and the optimum biocide concentration using scanning electron microscopy (SEM).

Samples from the bulk phase of reactor A were taken every five days for one month cultivation time to detect the sulfidogenic activity by measuring sulfide concentration according to the German Standard Methods (DEV, 1993) and redox potential using SenTix ORP electrode, WTW. The minimum inhibitory concentration (MIC) of the synthesized surfactants against the sulfidogenic-bacteria was detected. MIC is defined as the lowest concentration of antimicrobial agent that inhibits the development of visible microorganism growth (Singare and Mhatre, 2012). Samples were taken from the reactors (reactor A) bulk phase after 5 days cultivation and tested for viable bacterial counts using most probable number (MPN) method (Anonymous, 1998). At the end of one month incubation, the coupons were taken from reactors A and immersed in Clarke solution (1 L 36 % HCl, 20 g Sb_2O_3 and 50 g $SnCl_2$) for 10–15 sec, washed with deionized water, ethanol and finally dried in the desiccator. Afterward, the dried coupons were weighed and the weight loss was determined by comparison the weight of the coupons after and before the inhibition experiments. Metal corrosion rate (g/m^2d) (Quraishi et al., 2002) and inhibitory efficiency (Khaled and Amin, 2009) were calculated from the weight loss results.

CLSM with staining protocol was used to detect the change in bacterial cells and EPS distribution within the sulfidogenic-biofilm matrix in the presence and absence of the synthesized surfactants. At the highest sulfide value in the bulk phase, the mild steel coupons with the attached biofilms were removed from the reactor B and immersed first in 0.85 % NaCl to remove the planktonic cells. For the detection/quantification of bacteria, the nucleic acid stain SYTO9 (Invitrogen, Eugene, USA) was used according to the protocol described by Neu (1996). *Aleuria aurantia lectin* (AAL, LINARIS Biologische Produkte GmbH, Wertheim-Bettingen, Germany) labeled with AlexaFluor 633 (Invitrogen /Molecular Probes, Eugene, USA) was applied to stain EPS glycoconjugates. Proteins were stained with SYPRO Orange (Invitrogen /Molecular Probes, Eugene, USA) according to the protocol described by Lawrence et al., (2003). The method and calculation were described in details in chapter 2.

The biofilms, metal surfaces (after removing the biofilms) and the metal surfaces with the optimum biocide concentration (reactor C) in this study were examined using SEM model Leica/Cambridge Stereo scan 360 at magnification rang-

ing from 50x to 10.000x and operated at an acceleration voltage of 20 V. After one month incubation time, the coupons were removed from reactor C, fixed with 3 % glutaraldehyde PBS, pH 7.3–7.4 for 4 h, washed two times with PBS (5 min each), rinsed with distilled water for more two times (5 min each) and then dehydrated using an ethanol gradient (50, 75, 95 and 99 %) for 10 min before being finally stored in the desiccator.

3.2.4. Antibacterial activity of the synthesized surfactants

The biocidal activity of the synthesized surfactants was tested against different bacterial strains (DSMZ: Deutsche Sammlung von Mikroorganismen und Zellkulturen) as follows: Gram-positive bacteria (*Staphylococcus aureus* DSM 3463) and Gram-negative bacteria (*Pseudomonas aeruginosa* DSM 50071, *Escherichia coli* DSM 30083). The antibacterial activity of the synthesized surfactants was determined by a modified agar well diffusion method (Perez et al., 1990). In this method, nutrient agar plates were seeded with the tested microorganism by streaking over the agar plates. A sterile 10 mm borer was used to cut three wells of equidistance in each of plates; 0.2 ml of synthesized surfactants was introduced into the wells. The plates were incubated at 37 ^{o}C for overnight. The antibacterial activity was evaluated by measuring the diameter of zones of inhibition (in mm). In addition standard tetracycline solution (0.025 g/10 ml) was used as a positive control and sterile water was used as a negative control.

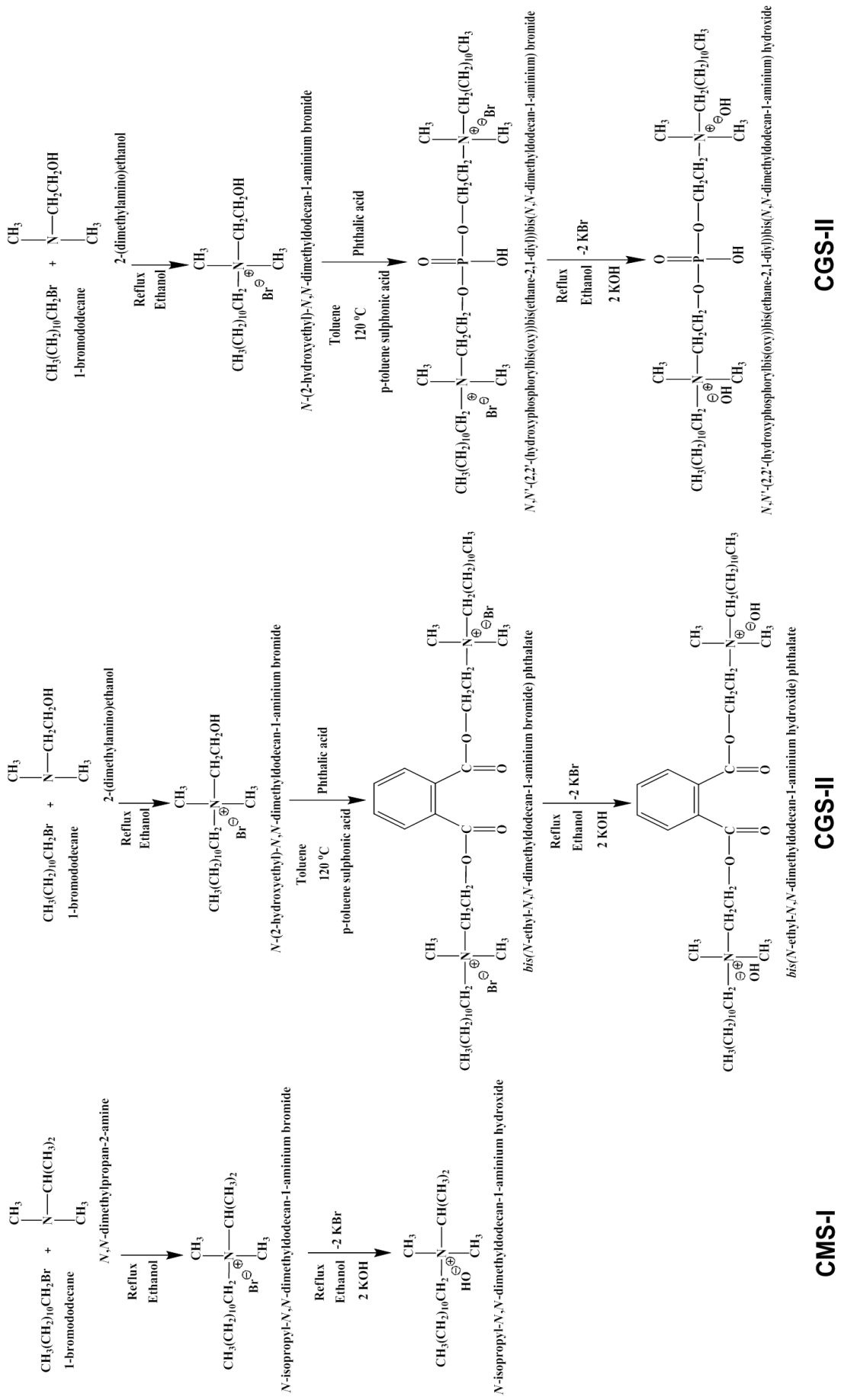

Figure 3–2. The chemical reaction pathways for the synthesis of the investigated surfactants

Table 3–1.Reactors operation mode

	Reactor A	Reactor B	Reactor C
Temperature	37 °C	37 °C	37 °C
Shaking	100 rpm	100 rpm	100 rpm
Experiment	Sulfidogenic activity	Biofilm constituents	Biofilm and metal surface analysis
Analysis	- Sulfide - Redox potential - MPN - Corrosion rate	CLSM with staining protocols to detect nucleic acids, proteins and EPS glycol-conjugates in the cultivated biofilms	SEM to detect the biofilm, metal surface (after removing the biofilm), and metal surface with optimal biocide.
Sampling day	- Every five days: sulfide and redox potential - MPN: after 5 days - Corrosion rate: after one month.	At maximum sulfidogenic activity (high sulfide concentration in the bulk phase).	After one month cultivation

Table 3–2. Structure and the applied inhibition experiments of the synthesized surfactants

	Cationic monomeric surfactant (CMS-I)	Cationic gemini surfactant (CGS-II)	Cationic gemini surfactant (CGS-III)
Structure	-One alkyl group	-Two alkyl groups	-Two alkyl groups
	-One ammonium group	-Two ammonium groups	-Two ammonium groups
	-one hydroxide ion	-Two hydroxide ions	-Two hydroxide ions
	-No spacer	-Two ester groups and benzene ring	-One phosphorous and three oxygen atoms
The applied experiment	CMS-I in comparison to CGS-II with KSW-sulfidogenic bacteria at salinity of 3.19 % NaCl	- CGS-II in comparison to CMS-I with KSW-sulfidogenic bacteria at salinity of 3.19 % NaCl - CGS-II with Hamra- sulfidogenic bacteria at salinity of 0.23 % NaCl.	CGS-III with Youmna-sulfidogenic bacteria at salinity of 5.49 % NaCl.

3.3. Results and Discussion

3.3.1. Confirmation of chemical structures of the synthesized surfactants

The chemical structure of the all synthesized surfactants was elucidated and confirmed by FTIR and NMR spectroscopy.

3.3.1.1. FTIR spectra

The FTIR spectra confirmed the expected functional groups in the synthesized surfactants (see Figure A–1).

3.3.1.2. NMR spectra

- **^{1}H NMR**

The data of ^{1}H NMR spectra confirmed the expected hydrogen proton distribution in the synthesized surfactants with indication of no by product (see Figure A–2).

- **^{13}C NMR**

The data of ^{13}C NMR spectra confirmed the expected carbon distribution in the synthesized surfactants (see Figure A–3).

- **^{31}PNMR**

The data of ^{31}P NMR spectra of the synthesized surfactant (CGS-III) demonstrated characteristic signal (see Figure A–4).

3.3.2. Surface active properties of the synthesized surfactants

3.3.2.1. The surface tension (γ)

The change of the surface tension (γ) values of the synthesized surfactants in the solution (at different concentrations) is represented in Figure 3–3a, b, c. A significant decrease in the surface tension was observed with increasing surfactant concentration. Afterward, the curves break rapidly at relatively low surfactant concentration and continue to slowly decrease as the concentrations increase. The critical micelle concentration (C_{cmc}) values were determined from the break points in the γ–log C plots of the synthesized surfactants (Lee et al., 1995). This behavior shown by the surfactant molecule in solution is common and is used to determine its purity and C_{cmc} values. CGS-II and CGS-III displayed very low C_{cmc} values compared to CMS-I. Lowering C_{cmc} leads to better solubility which normally depends on the concentration of the surfactant monomer in solution (Engberts et al., 1996). Moreover, both gemini showed high significant surface activity compared with monomeric surfactant as previously reported (Rosen, 1989). The results can be attributed to the increased

number of alkyl chain in the synthesized gemini surfactants compared to the monomeric one (see Figure 3-2).

(a)

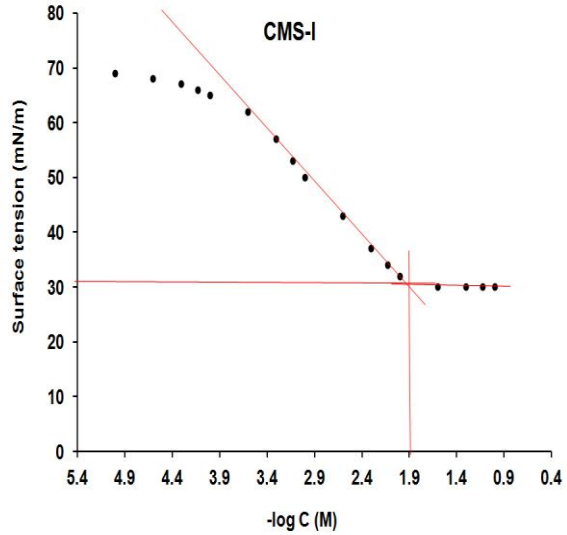

(b)

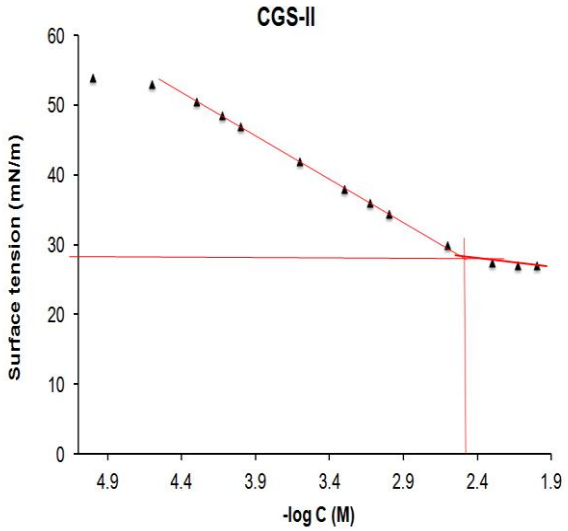

(c)

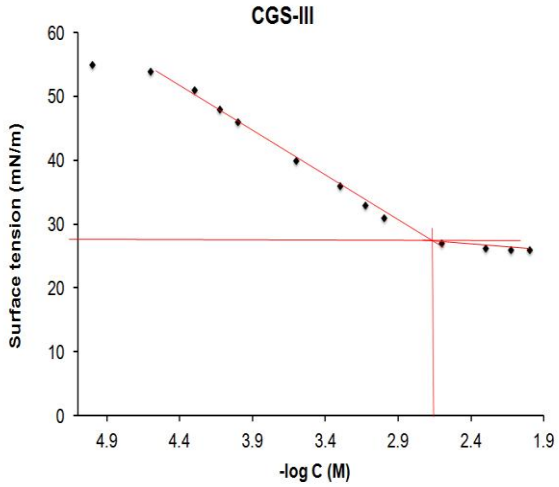

Figure 3–3. The surface tension of the synthesized surfactants at different concentrations in water at 25 ^{o}C. The critical micelle concentration (C_{cmc}) values were determined from the break points. (a) CMS-I, (b) CGS-II and (c) CGS-III.

3.3.2.2. The effectiveness (Π_{CMC})

The surface tension values (γ) at C_{cmc} points were used to calculate the surface pressure (effectiveness) values according to the following equation (Khaled and Hackerman, 2003):

$$\Pi_{CMC} = \gamma_o - \gamma_{cmc} \quad (1)$$

where γ_o and γ_{cmc} are the surface tension of pure water and surface tension at C_{cmc}, respectively. The effectiveness of the synthesized surfactants seems to be good for lowering the surface tension of water to the present values (see Table 3–2). The most effective surfactant is the one that gives the largest reduction of surface tension at the critical micelle concentration (C_{cmc}). Results listed in Table 3–2 indicated that the gemini surfactants are more effective at the C_{cmc} point than the monomeric surfactant. The effectiveness of the synthesized CMS-I (41 mN/m) is good in comparison to other cationic monomeric surfactants (32–36 mN/m) (Tawfik et al., 2012). In addition the synthesized cationic gemini surfactants (44, 45 mN/m for CGS-II ad CGS-III respectively) showed also higher effectiveness in comparison to other cationic gemini surfactants (28.2–33.7 mN/m) at the C_{cmc} point (Hegazy, 2009).

3.3.2.3. The surface excess (Γ_{max})

The surface excess is calculated according to Gibb´s adsorption equation (Samakande et al., 2008):

$$\Gamma_{max} = - (1/nRT) (d\gamma/ d \ln C) \quad (2)$$

where Γ_{max} is the surface excess concentration of surfactant ions, R is the gas constant, T is the absolute temperature, γ is the surface tension at a specific concentration, n is the number of species of ions in solution and C is the concentration of surfactant. A surfactant substance that decreases the surface energy is thus present in excess or near the surface. This means that the surface tension decreases with increasing activity (concentration) of a surfactant molecule. The Γ_{max} data (Table 3–2) showed that by increasing the hydrophobic chain length, as is the case for the synthesized gemini surfactants, the hydrophobicity increases. Thus, the synthesized surfactant molecules are directed to the interface and therefore, the surface energy of the solution decreases. This leads to an increase in the maximum surface access.

3.3.2.4. The minimum surface area per molecule (A_{min})

The minimum surface area (A_{min}) is defined as the area occupied by a molecule in nm^2 at the interface. A_{min} of the adsorbed surfactants increases with increasing length of the hydrophobic part. A_{min} was calculated according to the following equation (Gamboa and Olea, 2006):

$$A_{min} = 10^{16} / \Gamma_{max} N_A \quad (3)$$

where N_A is the Avogadro's number and Γ_{max} (mol/m^2) is the maximal surface excess of the adsorbed surfactant molecules to the interface. Results listed in Table 3–2 revealed that the surface pressure (Π_{cmc}) of the synthesized surfactants increased with decreasing the minimum surface area (A_{min}) of the adsorbed surfactant molecules.

Table 3–2. Critical micelle concentration (C_{cmc}), surface tension (γ_{cmc}) effectiveness (Π_{cmc}), maximum surface excess (Γ_{max}), minimum area (A_{min}), the degree of counter ion dissociation (β) and free energy of micellization (ΔG_{mic}) of the synthesized surfactants at 25°C

Surfactant	**C_{cmc} (mol/ dm^3)**	**γ_{CMC} (mN/m)**	**Π_{cmc} (mN/m^1)**	**Γ_{max} x 10^{10} (mol/cm^2)**	**A_{min} (nm^2)**	**β**	**ΔG_{mic} (kJ/mol^1)**
CMS-I	1.5x 10^{-2}	31	41	6.19	0.27	0.24	-18.28
CGS-II	4.3x10^{-3}	28	44	6.29	0.26	0.30	-22.89
CGS-III	2.3x10^{-3}	27	45	6.31	0.26	0.26	-23.18

3.3.2.5. The specific conductivity (K)

Specific conductivity (K) measurements were performed for the synthesized surfactants at 25°C in order to evaluate the C_{cmc} value and the degree of counter ion dissociation (β). It is well known that the specific conductivity is linearly correlated to the surfactant concentration in both the premicellar and the postmicellar region as represented in Figure 3–4a, b, c. The slope at the premicellar region is greater than in the postmicellar region (Mata et al., 2005). The intersection point between the two lines gives the C_{cmc} value. The ratio between the two slopes gives the β value as listed in Table 3–2. The C_{cmc} values calculated from the specific conductivity figure were in agreement with those obtained using surface tension results. It is obvious that the difference between the synthesized CGS-II and CGS-III as compared to the CMS-I is due to the increase in cation bulkiness.

(a)

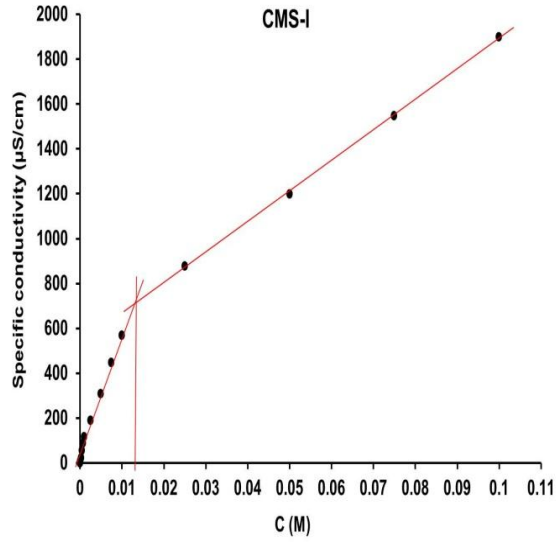

(b)

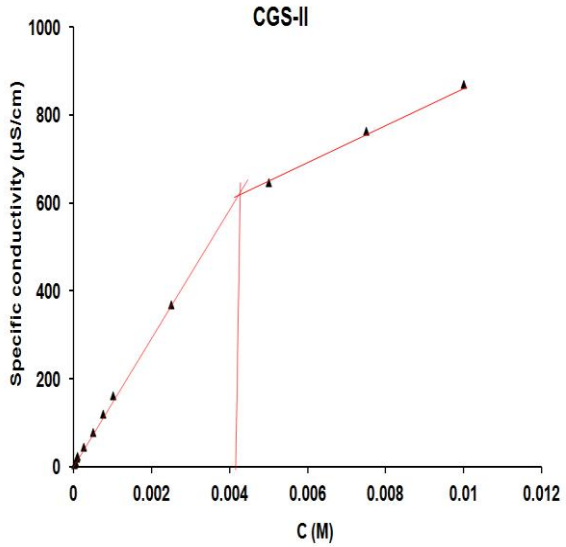

(c)

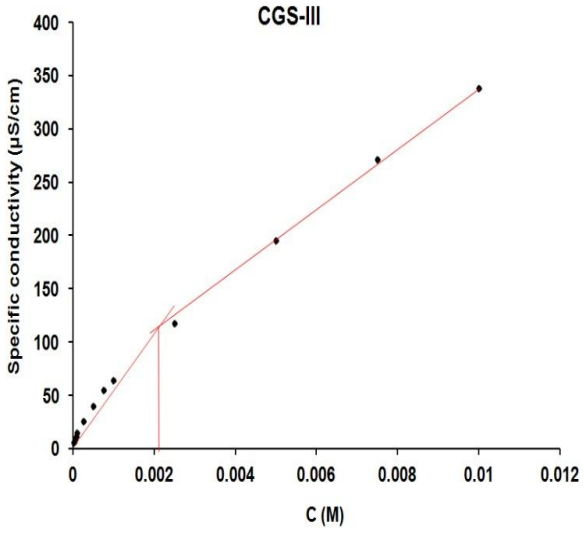

Figure 3–4. Electrical conductivity of the synthesized surfactants at different concentrations in water at 25°C. The critical micelle concentration (C_{cmc}) values were determined from the break points. (a) CMS-I, (b) CGS-II and (c) CGS-III.

3.3.2.6. The standard free energy of micellization ($\Delta G^{o}_{mic.}$)

In the charged pseudo-phase model of micellization, the standard free energy micellization (ΔG^{o}_{mic}) per mole of the synthesized surfactants was calculated according to the following equation (Samakande et al., 2008):

$$\Delta G^{o}_{mic} = (2 - \beta)\, RT \ln (CMC) \qquad (4)$$

where β is the degree of counter ion dissociation, R is the gas constant, T is the temperature, and CMC is expressed in the molarity of the surfactant. The negative values of ΔG^{o}_{mic} of the all synthesized surfactants (Table 3–2) indicated that there is a tendency of the synthesized surfactant molecules to be adsorbed at the interface (Badawi et al., 2007). In addition there is an increase in ΔG^{o}_{mic} negative value of CGS-II and CGS-III in comparison to CMS-I. This result means that the synthesized cationic gemini surfactants adsorbed at the interface faster than the cationic monomeric surfactant.

3.3.3. An overview of the sulfidogenic bacterial activities inhibition using novel cationic monomeric and cationic gemini surfactants

The previous results (Chapter 2) demonstrated that the sulfidogenic communities of the three water samples having different salinities and related cultivated biofilms are highly diverse and showed severe corrosion activity over the metal surface. The results were discussed on the basis of two processes inducing corrosion (chemical and biological). Chemical corrosion was induced by the medium salinity (NaCl %). The metal corrosion rate increased significantly in the presence of chloride anions at different concentrations beneath the sulfidogenic-biofilm matrices as in the KSW and the Youmna-sulfidogenic biofilms in comparison to the Hamra-sulfidogenic biofilm. Biological corrosion induced by the activities of the sulfidogenic bacteria in the bulk phase and over the metal surface.

In order to protect the metal surface from salinity and activity of the present sulfidogenic bacteria, three surfactants were synthesized and characterized: CMS-I “N-isopropyl-N,N-dimethyldo- decan -1-aminium hydroxide”, CGS-II “bis(N-ethyl-N,N-dimethyl- dodecan-1-aminium hydroxide) phthalate” and CGS-III “N,N'-(2,2'-(hydroxyl-phosphoryl bis(oxy)) bis (ethane-2,1-diyl)) bis (N,N-dimethyl dodecan-1-aminium) hydroxide”.

In the present study, comparison between CMS-I and CGS-II was investigated to protect the metal surface from high divers microbial community (KSW-sulfidogenic bacteria) cultivated at a high medium salinity (3.19 % NaCl) (see Table 3-2). Comparison was investigated to study the difference in the metal corrosion inhibition efficiency which related to their structure, surface active properties, adsorption mechanism and biocidal activity. The synthesized monomeric surfactant consists of one ammonium group and one alkyl group. While the gemini (CGS-II) consists of two ammonium

groups and two alkyl groups linked by spacer containing two ester groups and benzene ring. The CGS-II was also used to protect the metal surface from the activity of the Hamra-sulfidogenic bacteria at low salinity (0.23 % NaCl) and to confirm the metal corrosion inhibition efficiency that detected at high salinity (3.19 % NaCl) (see Table 3-2). In order to inhibit the activity of the Youmna-sulfidogenic bacteria and to protect the metal surface from their high salinity medium (5.49 % NaCl) (see Table 3-2), CGS-III was used. The synthesized CGS-III contains two ammonium groups and two alkyl groups linked by spacer containing one phosphorous and three oxygen atoms.

According to the C_{cmc} values of the synthesized surfactants (see Table 3–2), the inhibitor concentration ranges were selected. The C_{cmc} value for CGS-II (4.3 $x10^{-3}$ mol/dm^3) and for CGS-III (2.3 x 10^{-3} mol/dm^3) were lower than for CMS-I (1.5 x 10^{-2} mol/dm^3). Therefore lower inhibitor concentrations for both gemini surfactants as (0.01, 0.1, 1 and 5 mM) than for the monomeric surfactant (0.01, 0.1, 1, 10 mM) were chosen. The enriched inoculated samples had start MPN counts of 4.6 x 10^7 /ml and 1.5 x 10^8 /ml for the KSW-sulfidogenic bacteria for both reactors applied with CMS-I and CGS-II, respectively. MPN was 2.4 x 10^7 /ml for Hamra-sulfidogenic bacteria reactors with CGS-II and 2.9 x 10^8 /ml for the Youmna-sulfidogenic bacteria reactors with CGS-III. The activity of sulfidogenic bacteria was determined by measuring the sulfide concentration in the bulk phase as the end metabolic products of the sulfidogenic bacteria. The sulfide results were confirmed by measuring the redox potential in the bulk phase. MPN was measured in the bulk phase after 5 days cultivation in order to detect the minimum inhibitory concentration of the synthesized surfactants in the bulk phase. Moreover the biofilm structures and constituents were analyzed and the metal corrosion rate was estimated.

3.3.3.1. The inhibitory effect of CMS-I and CGS-II on the KSW-sulfidogenic bacteria, CGS-II on the Hamra-sulfidogenic bacteria and CGS-III on the Youmna-sulfidogenic bacteria

Results represented in Figure 3–5a, b, c, d showed that there was strong sulfide production in the control reactors and the sulfidogenic-reactors treated with a low surfactant concentration of 0.01 mM. Sulfide production was gradually decreased by increasing concentrations of the biocides throughout the experiment. The sulfide production indicates the growth of the sulfidogenic bacteria which growing by either oxidizing organic compounds or utilizing hydrogen as an electron donor with sulfate being reduced to hydrogen sulfide (Muyzer and Stams, 2008). At 0.1 mM of

CGS-II, the KSW-sulfidogenic activity was inhibited at the beginning, but after 5 days it started to resist the biocide effect (Figure 3–5b). While the Hamra-sulfidogenic activity was inhibited at concentration of 0.1 mM CGS-II during cultivation but after 20 days it started to resist the biocide effect but with a very low increasing rate (Figure 3–5c). At this concentration the CGS-II showed strong effect on the Hamra-sulfidogenic bacteria. While at 0.1 mM of CGS-III, the Youmna-sulfidogenic activity was inhibited at the beginning, but after 5 days it started to resist the biocide effect (Figure 3–5d). Reactor inoculated with the KSW and the Hamra and Youmna-sulfidogenic bacteria showed no sulfide production at high concentrations of the biocide (1, 10mM CMS-I, 1, 5mM CGS-II and 1, 5mM CGS-III). No sulfide production means that there is no sulfidogenic activity in the bulk phase or over the metal surface. The inhibition of sulfide production is an important factor to protect the metal surface from its corrosion. Hydrogen sulfide can accelerate corrosion of metals by being source of bound protons and by precipitation of Fe^{2+} as FeS (Lee et al., 1995, Wang et al., 2008). It has also been proposed that the nature of the iron sulfide film that forms on the metal surface plays an important role in the initiation of pitting corrosion over the metal surface (Cheung and Beech, 1996). In this respect, applying the synthesized surfactants at high concentrations (1, 10 mM CMS-I, 1, 5 mM CGS-II and 1, 5 mM CGS-III) protect the metal surface from the sulfidogenic bacterial activity.

The measured redox potential in the different reactors is in agreement with the sulfidogenic activity determined by sulfide production. It is well known that most sulfidogenic bacteria are strictly anaerobes and start to reduce the sulfate with redox potential below -100 mV (Postgate, 1984). For the control reactors and the reactors treated with 0.01, 0.1 mM CMS-I, CGS-II or CGS-III, the redox potential measured was optimal for sulfidogenic bacteria independent of inocula type and medium salinity (see Figure 3–6a, b, c, d). While at high surfactant concentrations of 1 and 10 mM CMS-I, 1 and 5 mM CGS-II and 1 and 5 mM CGS-III, the redox potential measured increased up to -100 or even higher for the KSW, the Hamra and the Youmna-sulfidogenic bacteria, respectively. The sulfide and redox potential results demonstrated that at a high concentration of all synthesized surfactants, the sulfate reduction reaction was completely inhibited causing no sulfide production and a considerable drop in the redox potential in the bulk phase.

(a) KSW-sulfidogenic bacteria-CMS-I

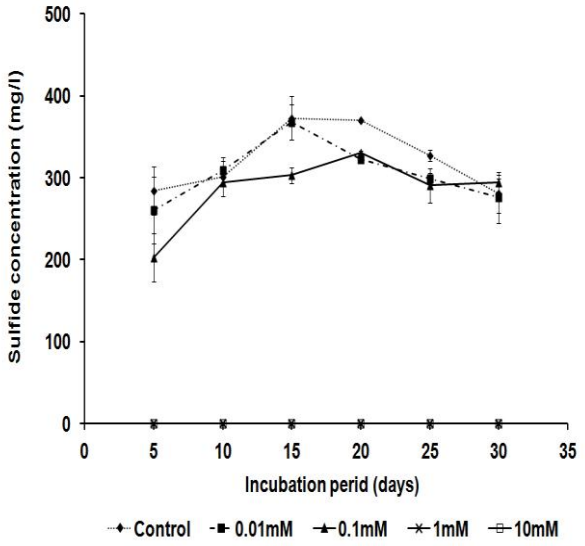

(b) KSW-sulfidogenic bacteria-CGS-II

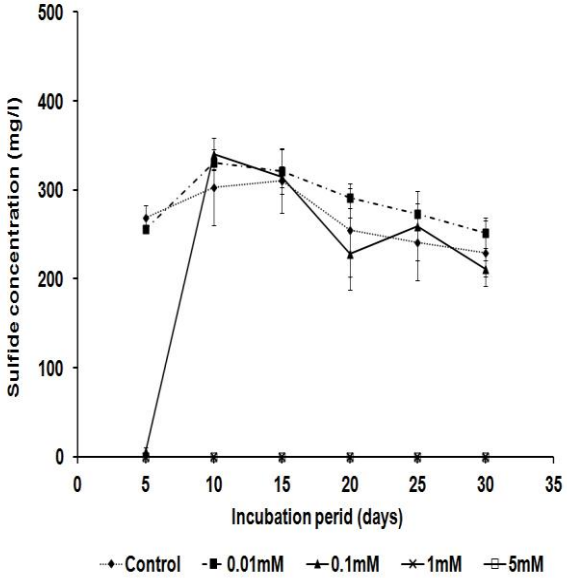

(c) Hamra-sulfidogenic bacteria-CGS-II

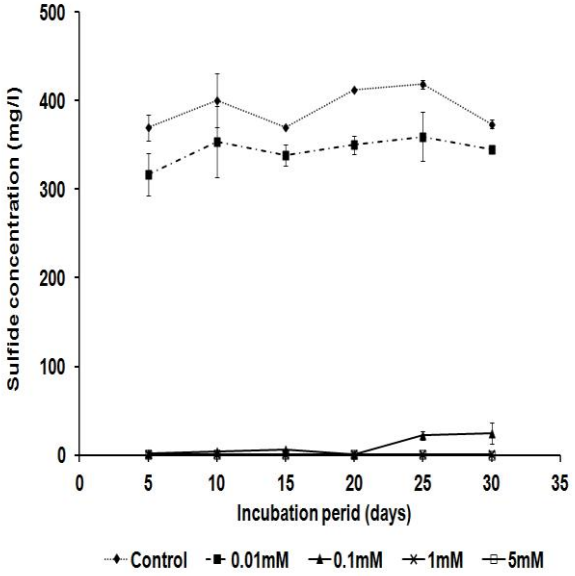

(d) Youmna-sulfidogenic bacteria-CGS-III

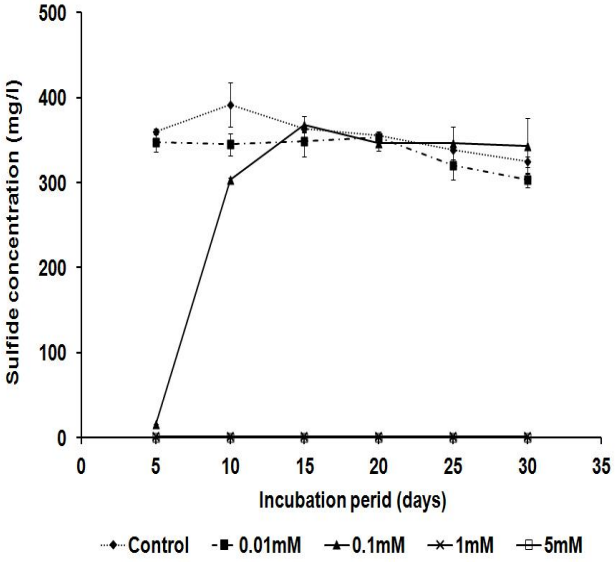

Figure 3–5. Sulfidogenic bacteria activities shown on the basis of sulfide production for the different reactors (a) CMS-I, (b) CGS-II inoculated with the enriched KSW-sulfidogenic bacteria, (c) CGS-II inoculated with the enriched Hamra-sulfidogenic bacteria and (d) CGS-III inoculated with the enriched Youmna-sulfidogenic bacteria. The results shown are mean values of duplicates with corresponding standard deviation.

(a) KSW-sulfidogenic bacteria-CMS-I

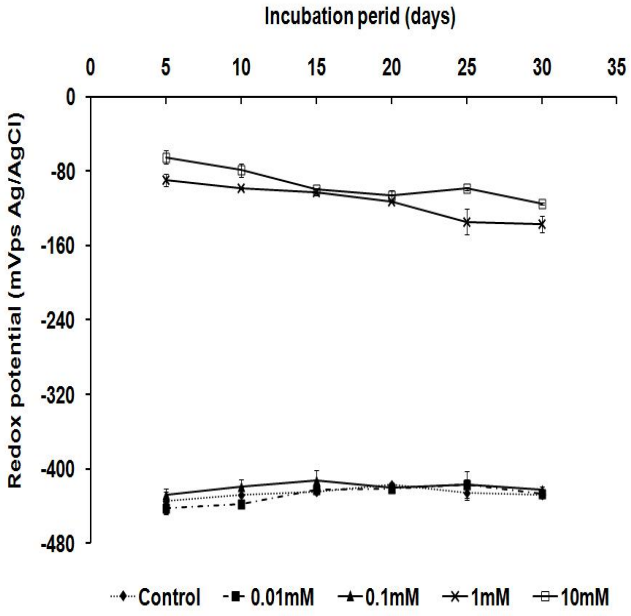

(b) KSW-sulfidogenic bacteria-CGS-II

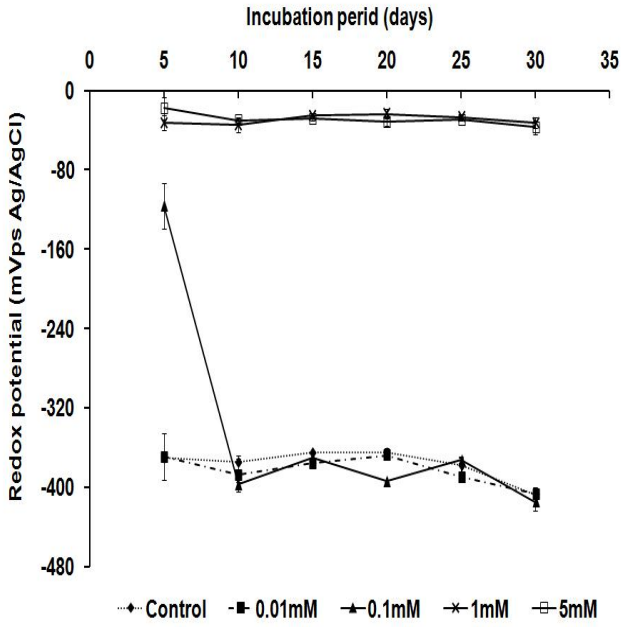

(c) Hamra-sulfidogenic bacteria-CGS-II

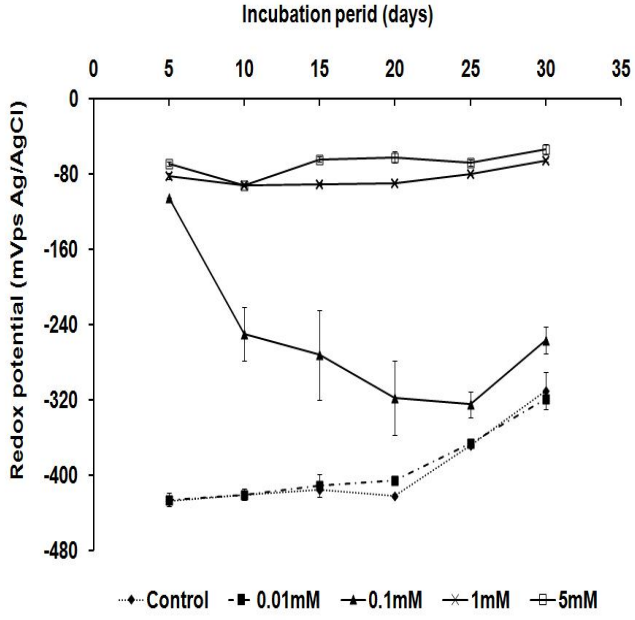

(d) Youmna-sulfidogenic bacteria-CGS-III

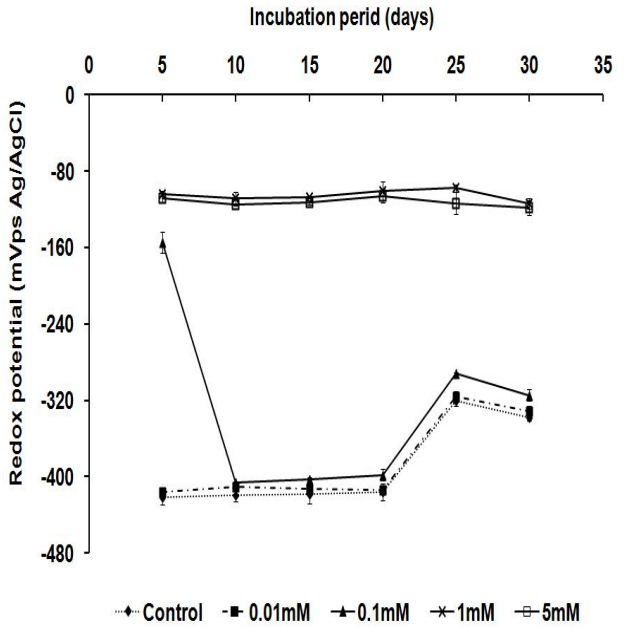

Figure 3–6. Sulfidogenic bacteria activities shown on the basis of changing of redox potential for the different reactors (a) CMS-I, (b) CGS-II inoculated with the enriched KSW-sulfidogenic bacteria, (c) CGS-II inoculated with the enriched Hamra-sulfidogenic bacteria and (d) CGS-III inoculated with the enriched Youmna-sulfidogenic bacteria. The results shown are mean values of duplicates with corresponding standard deviation.

Results represented in Table 3–3 showed that the minimum inhibitory concentration (MIC) of all synthesized surfactants against the cultivated sulfidogenic bacteria (KSW, Hamra and Youmna). The minimum inhibitory concentration is detected at concentrations of 1 mM. At higher concentrations (10 mM CMS-I, 5 mM CGS-II and CGS-III) no sulfidogenic bacterial growth was detected. At lower concentrations of 0.01, 0.1mM of CMS-I, no significant biocidal effect against KSW-sulfidogenic bacteria was detected. However gemini surfactants at concentration of 0.1 mM showed partial inhibition in the growth of KSW, Hamra and Youmna-sulfidogenic bacteria. In general, the biocidal activity of the synthesized surfactant depends on the alkyl chain length which increased in the synthesized gemini surfactants in comparison to the synthesized monomeric surfactant (see Figure 3-2). The biocidal effect took place at concentrations of surfactant at the C_{cmc} and is dependent on the individual molecules not the aggregates (Singare and Mhatre, 2012).

The synthesized surfactants have a nonspecific antibacterial activity (see Table 3-4). The synthesized surfactants (CMS-I, CGS-II, and CGS-III) showed antibacterial activity (biocidal) not only against environmental sulfidogenic bacteria but also against Gram-positive (*Staphylococcus aureus*) and Gram-negative (*Escherichia coli* and *Pseudomonas aeruginosa*) species. The synthesized CGS-II and CGS-III showed higher antimicrobial activity than the synthesized CMS-I. The difference in the biocidal activity depends on the ammonium groups (NH_4^+) and hydrophobic alkyl groups of the synthesized surfactants. It has been reported that increasing the hydrophobicity as in the gemini surfactants lead to increasing the biocidal activity (Rosen et al., 2001). The synthesized CMS-II showed strong biocidal activity in comparison to other synthesized cationic surfactants especially on *Staphylococcus aureus* and *Escherichia coli* as previously reported (Muyzer and Stams, 2008).

The hypothesized biocidal effect of the synthesized surfactants against bacterial cell can be explained as an electrostatic interaction and physical disruption. Electrostatic interaction between the negatively charged cell membrane (lipoprotein) and the positively charged CMS-I ammonium group (NH_4^+) and CGSII and CGS-III two ammonium groups (NH_4^+). A physical disruption occurs when hydrophobic chains (alkyl groups) penetrate into the bacterial cell membrane. That happens because of similarity of the cell membrane constituents and the hydrophobic chains of the synthesized surfactants. Penetration of the cell membrane leads to damage of the selective permeability of the cell, disturb the metabolic pathway within the cytoplasm

and then inactivation of the microorganism as has been reported before (Brunt, 1987, Hugo and Snow, 1981). Moreover, the spacer of the synthesized gemini surfactants play an important role in the biocidal activity. The synthesized CGS-II contains two ester groups and benzene ring spacer. It has been reported the biocidal effect of the benzene ring containing compounds on the microbial activity and in the corrosion inhibition (Azzam et al., 2012). The synthesized CGS-III contains one phosphorous and three oxygen atoms spacer. It has been reported that phosphorus containing compounds are commonly used to inhibit metals corrosion in aqueous environment (Ashassi-Sorkhabi and Asghari, 2009, Refaey, 2005). Their using is related to risk free due to their low toxicity (Li et al., 2004, Gonzalez et al., 2005).

Table 3-3 Evaluation of most probable number (MPN) of the cultivated reactors for minimum inhibitory concentration (MIC) detection.

Cultivated reactors	**MPN cell/ml**
KSW-sulfidogenic bacteria with CMS-I	
Control	2.4×10^8
0.01mM	2.8×10^7
0.1mM	6.2×10^7
1mM	No growth
10mM	No growth
KSW-sulfidogenic bacteria with CGS-II	
Control	2.65×10^8
0.01mM	1.1×10^8
0.1mM	7.8×10^4
1mM	No growth
5mM	No growth
Hamra-sulfidogenic bacteria with CGS-II	
Control	1.43×10^8
0.01mM	1.2×10^9
0.1mM	1.42×10^4
1mM	No growth
5mM	No growth
Youmna-sulfidogenic bacteria with CGS-III	
Control	2.6×10^9
0.01mM	2.4×10^9
0.1mM	1.1×10^5
1mM	No growth
5mM	No growth

Table 3-4. Antimicrobial activity of the synthesized surfactants

Biocide	Concentration	*Staphylococcus aureus* (DSM 3463) (mm)	*Pseudomonas aeruginosa* (DSM 50071) (mm)	*Escherichia coli* DSM 30083) (mm)
Tetracycline	0.025 g/ 10 ml	35 ± 0	28 ± 0.5	35 ± 0
CMS-I	0.01mM	15.5 ± 0.7	0	0
	0.1mM	16 ± 0	0	0
	1mM	29.5 ± 0.7	20 ± 0	15.5 ± 0
	5mM	35.5 ± 0.7	20.75 ± 0.3	25.75 ± 0.3
	10mM	38.2 ± 0.35	24.75 ± 0.3	28.1 ± 0.2
CGS-II	0.01mM	0	0	0
	0.1mM	17.1 ±0.2	0	0
	1mM	30.8 ±0.2	25 ± 0	20.5 ± 0
	5mM	37.5 ± 0	28 ± 0	25.5 ± 0
	10mM	38.1 ± 0.28	30.1 ± 0.2	30 ± 0
CGS-III	0.01mM	0	0	0
	0.1mM	15.8 ± 0.2	0	0
	1mM	28 ± 0	23 ± 0	15.3 ± 0.5
	5mM	39 ± 0	24.8 ± 0.2	28 ± 0
	10mM	40 ± 0	29.1 ± 0.2	31 ± 0

The sulfidogenic activities shown were detected in the bulk phase, not over the metal surface. Therefore, in order to characterize the possible changes in the biofilm structures and constituents over the metal surface after surfactant application, CLSM and staining procedures were used. Biofilms were developed and detected in the control reactors and the reactors exposed to the CMS-I, CGS-II and the CGS-III at concentrations of 0.01, 0.1 mM of CMS-I and 0.01 mM of CGS-II and CGS-III (Figure 3-7a, b, c, d). The other concentrations (1, 10 mM of CMS-I and 0.1, 1, 5 mM of CGS-II and CGS-III) completely inhibited the KSW, the Hamra and the Youmna-sulfidogenic biofilm development over the metal surface. The explanation of the biofilm results, at higher concentrations 1, 10 mM of the CMS-I and 1, 5 mM of the CGS-II and CGS-III, the synthesized surfactants showed biocidal effect to the

sulfidogenic bacteria (in the bulk phase) as confirmed from no sulfide production and drop in the redox potential in the bulk phase. At concentration of 0.1 mM CGS-II and CGS-III, the surfactant showed partial inhibition effect to the metal surface and protect the metal surface from biofilm formation. While the sulfidogenic activities at the bulk phase are not completely affected. At a concentration of 0.1 mM CMS-I exhibited a partial inhibition effect on the KSW-sulfidogenic biofilm development over the metal surface. This was shown through the reduction in nucleic acids, EPS glycoconjugates and proteins. At a lower concentration (0.01 mM CMS-I), no significant changes in the KSW-sulfidogenic biofilms components (nucleic acids, EPs glycoconjugates and proteins) were observed (see Figure 3–7a). Applying CGS-II at the same concentration (0.01 mM), the KSW-sulfidogenic biofilm did not reveal significantly changes in the microbial population (nucleic acids), however the EPS glycoconjugates were reduced (see Figure 3–7b). In contrast the Hamra-sulfidogenic biofilm (see Figure 3–7c) treated with the 0.01 mM CGS-II does not reveal significant changes. The results represented in Figure 3–7d showed that, at a concentration of 0.01 mM CGS-III did not reveal significant changes in the Youmna-sulfidogenic biofilm microbial population (nucleic acids). While EPS components changed, EPS glycoconjugates were reduced and the proteins were increased. The explanation of the change in the Youmna-sulfidogenic biofilm EPS components through the application of 0.01 mM CGS-III, is a defensive behavior of the microbial population. It has been reported that the natural response of microorganisms upon exposure to toxic environments is the stimulation production of EPS. This natural response was detected when the SRB biofilm was exposed to seawater containing toxic metals. It was noticed that the biofilm produced more proteins than polysaccharides (Fang et al., 2002).

Results represented in Figure 3–8 showed the biomass of the all cultivated biofilms are mainly located in the upper regions of the biofilm, near to the bulk phase. These results can give an expectation of the ability of the cultivated biofilms to protect the metal surface from the surrounding environment corrosion effect such as salinity by making a barrier between the medium and the metal surface. On the other hand biofilms cannot protect the metal surface from sulfide as the sulfidogenic consortia present in the biofilm matrix is probably produced high sulfide. Additionally, the planktonic cells produced sulfide which is easily entrapped within the biofilm matrix (Geesey et al., 2000).

(a) KSW-sulfidogenic bacteria-CMS-I

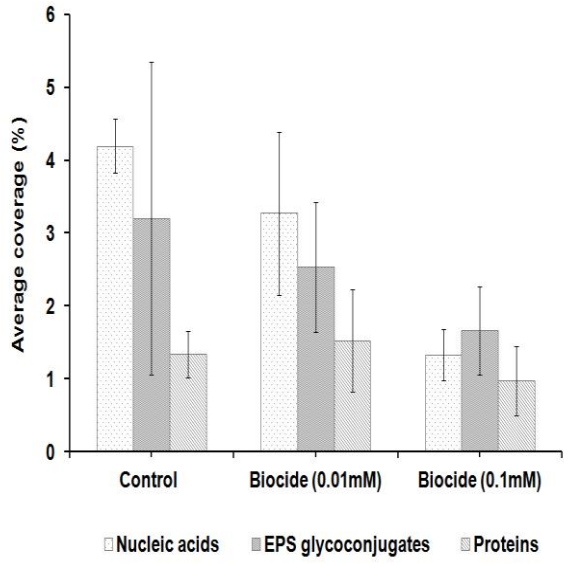

(b) KSW-sulfidogenic bacteria-CGS-II

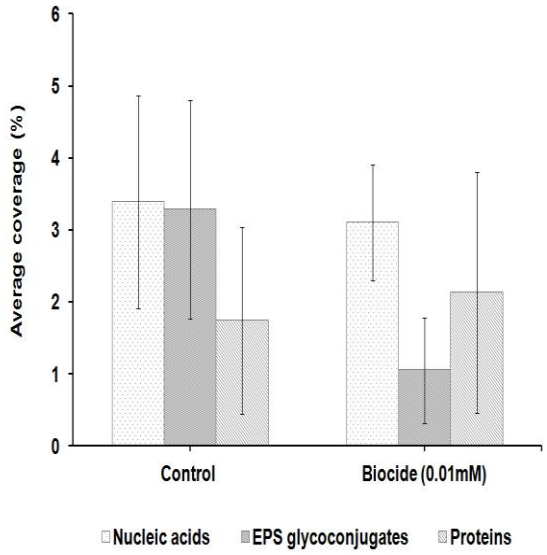

(c) Hamra-sulfidogenic bacteria-CGS-II

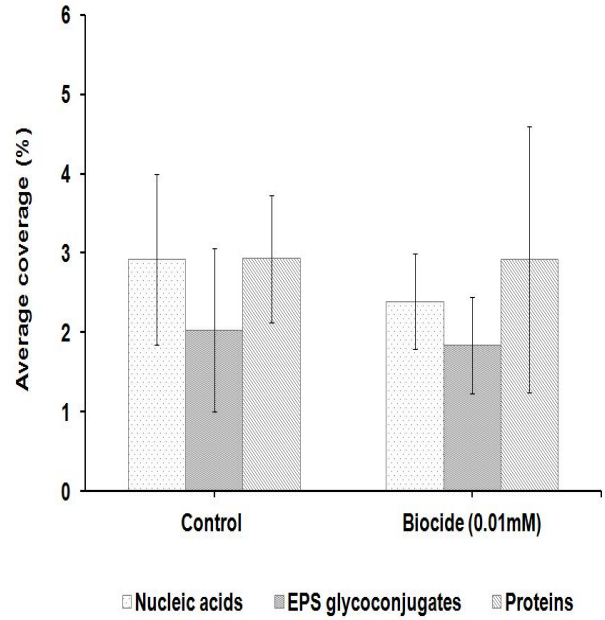

(d) Youmna-sulfidogenic bacteria-CGS-III

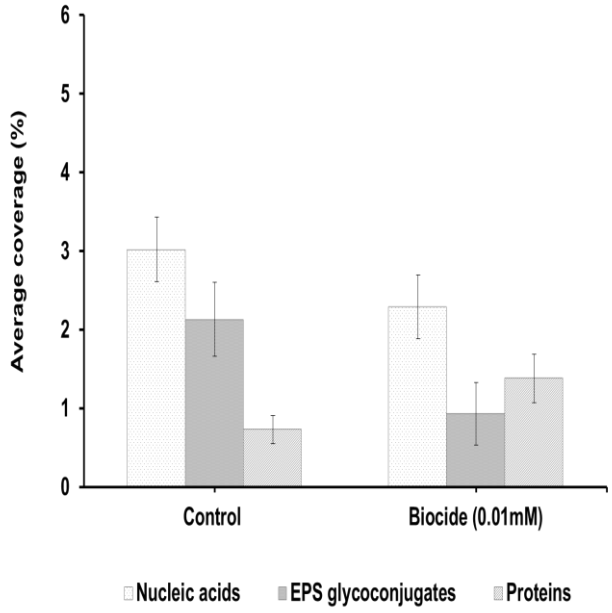

Figure 3–7. The changing of nucleic acids, EPS glycoconjugates and proteins of the sulfidogenic biofilms control reactor and the surfactants reactors. (a) CMS-I and (b) CGS-II inoculated with the enriched KSW-sulfidogenic bacteria and examined after 15 days incubation period, (c) CGS-II inoculated with the enriched Hamra-sulfidogenic bacteria and examined after 10 days incubation period and CGS-III inoculated with the enriched Youmna-sulfidogenic bacteria and examined after 10 days incubation period. The figures show the average coverage of five randomly selected areas of the cultivated biofilms with corresponding standard deviation.

(a) KSW-sulfidogenic control-biofilm

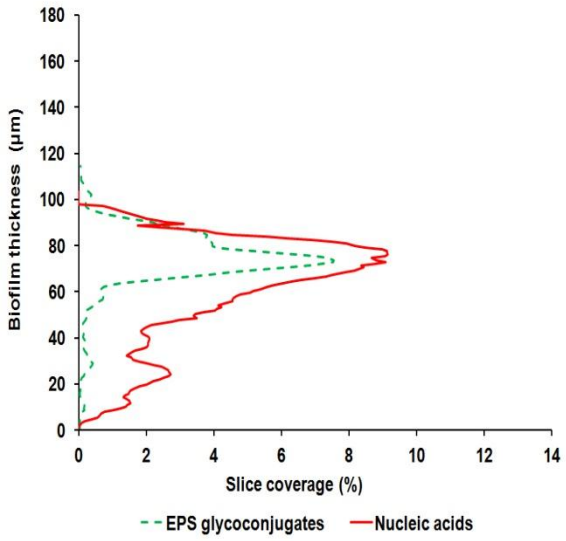

(b) KSW-sulfidogenic control-biofilm

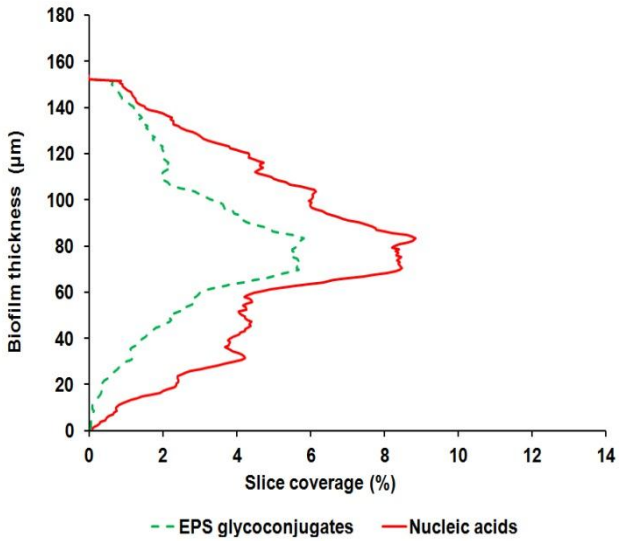

(c) Hamra-sulfidogenic control-biofilm

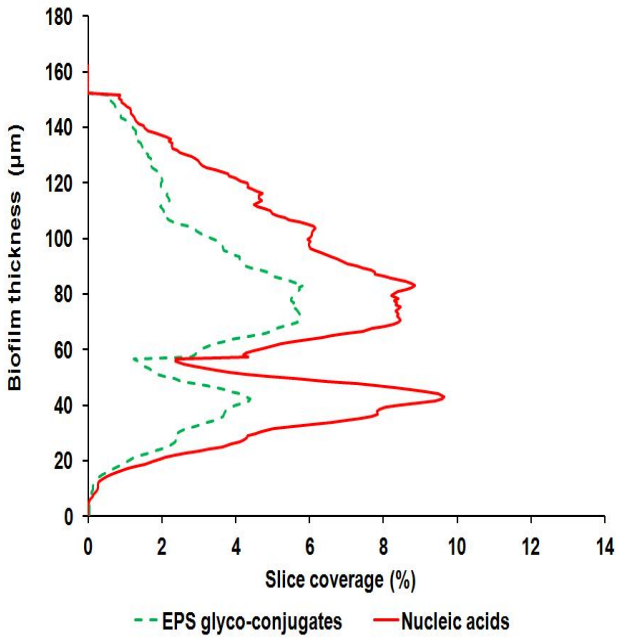

(d) Youmna-sulfidogenic control-biofilm

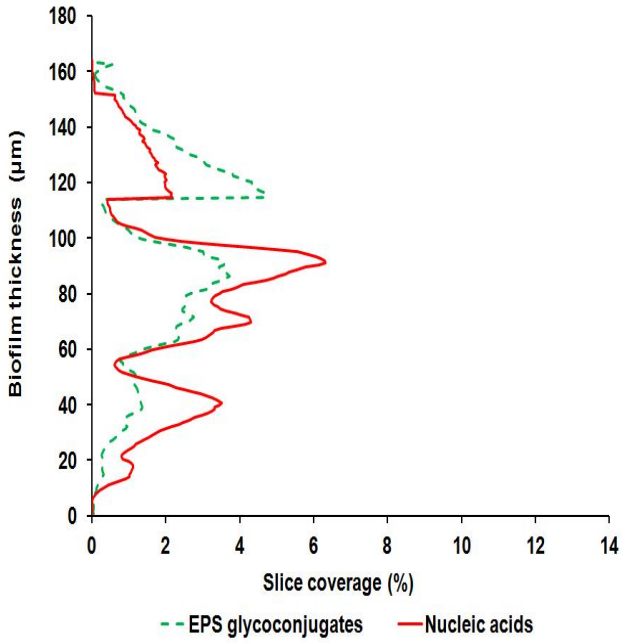

Figure 3–8 Distribution of nucleic acids/EPS glycoconjugates (represented as slice coverage %) across the biofilm thickness (µm) of control biofilms. (a) KSW-sulfidogenic biofilm (control), (b) KSW-sulfidogenic biofilm (control). KSW biofilms were examined after 15 days incubation period. (c) Hamra-sulfidogenic biofilm (control) examined after 10 days incubation period, and Youmna-sulfidogenic biofilm (control) examined after 10 days incubation period. Zero marks the position of the substratum (coupon surface).

At the end of one month cultivation, the metal corrosion rates of the coupons were calculated (Figure 3–9a, b, c, d). The blank-reactors (without biomass) metal corrosion rate results demonstrated a positive correlation between the metal corrosion rates and the different medium salinities. The metal corrosion rate of the Youmna-blank reactor (0.94 g/m^2 d), which was operated with medium salinity of 5.49 % NaCl, was higher than the KSW-blank reactor (0.44 g/m^2 d), which was operated with medium salinity of 3.19 % NaCl, and higher than the Hamra-blank reactor (0.16 g/m^2 d), which operated with medium salinity 0.23 % NaCl. It is evident (Vashi and Kadiya, 2009 and Gaylarde and Videla, 1987) that the metal corrosion rate increased by increasing medium salinity (NaCl).

Beech and Campbell, (2008) reported a metal corrosion rate of steel structure in a marine environment (salinity of 3.5 % NaCl) of 1.08 g/m^2 d. This value is in the range of the obtained results. The metal corrosion rate measured under field conditions are reported to be higher (Gubner, 1998). While, the metal corrosion rate of artificial-seawater was achieved at 0.13 – 0.17 g/m^2 d (Zhao, 2008).

Metal surface corrosion in an aqueous medium containing NaCl proceeds by chemisorption of chloride ions on the metal surface. There are two theories of chloride anion/ metal surface interaction. The first theory is the oxide film, chloride anion penetrates the oxide film through pores or defects easier than do other ions. In addition it may colloidally disperse the oxide film and increase its permeability. On the other hand, according to the adsorption theory, chloride anion adsorbs on the metal surface. Once in contact with the metal surface, chloride anion favors hydration of metal ions and increases the ease with which metal ions enter into solution. In other words, adsorbed chloride ions increase the exchange current (decrease overvoltage) for metal dissolution (Revie and Ulig, 2008). Then the adsorbed chloride ions lead to pit and crevice corrosion (Skolink et al., 2000).

Thangavel and Rengaswamy, 1998 and Tsuru, 1991 proposed the mechanism of iron corrosion in the chloride-containing solutions as follow:

$$Fe \rightarrow Fe^{2+} + 2e^{-} \quad (1)$$

$$Fe^{2+} + 2Cl^{-} \rightarrow FeCl_2 \quad (2)$$

$$Fe\,Cl_2 + 2H_2O \rightarrow Fe(OH)_2 + 2Cl^{-} + 2H^{+} \quad (3)$$

The role of chloride is unique. It can be reused again and again and hence even a small amount of chloride anion can sustain the metal corrosion process. Thus the

iron-chloride reaction is self-perpetuating and the free chloride acts as a reaction catalyst (Thangavel and Rengaswamy, 1998).

The KSW and the Youmna-sulfidogenic biofilms protected the metal surface from different medium salinities. The sulfidogenic bacteria (control-reactors) induced lower metal corrosion rate in comparison to their blank-reactors as postulated before (Lee et al., 1995, Pedersen and Hermansson, 1991). This result is supported by the previous biofilm results (Figure 3–8). In which, the cultivated biofilms were developed and mainly located near the bulk phase. Therefore biofilms protect the metal surface from the salinity effect. On the contrary, Kuang et al., (2007) showed the SRB biofilm (control) increases the metal corrosion rate of carbon steel largely comparing with that in pure seawater (blank) as a result of their high microbial activity on the metal surface.

The proposed metal–surface protection mechanism by biofilm development is by altering the transport of chemical species from or toward the metal surface. The biofilm accumulates on the metal surface and forms a protective barrier for the chemical species (Vidal and Herrera, 2005).

On contrary, in natural seawater-pipeline the interaction between biofilms and metal surface proposed different mechanisms (Mattila et al., 1997, Videla, 2003). In this environment many microorganisms can synergistically form biofilm structures. This structure provides a variety of potential growth niches for microorganisms by their ability to modify their surrounding medium. Then it results in a local gradient of many conditions such as oxygen, pH, redox potential, nutrients and flow rate (Sanders and Sturman, 2005). Since the biofilm tends to create non-uniform surface conditions (heterogonous), localized attack that might start at points on the surface leading to localized corrosion (usually in the form of pitting). Anodic area found in the thicker part of biofilm whereas the cathodic area is found in non-colonized area or in the area where biofilm is thin. Different conditions in two locations on the metal surface leads to an electrical potential and consequently corrosion current. That means when the metal surface is partially covered by biofilm it leads to higher corrosion (pitting) compared to a surface which is completely covered with biofilm (uniform corrosion). Therefore, the microorganisms in the biofilm can accompany and/or enhance the detachment of protective passive layers on the metal surface, leading to a patchy distribution of the deposits and inducing differential cell effects. This Non-uniform or patchy colonization by bacteria results in the formation of localized corrosion cell.

In contrast to the KSW and Youmna-sulfidogenic bacteria, the Hamra- sulfidogenic bacteria cultivated at a low salinity (0.23 % NaCl) induce more metal corrosion than that in the blank reactor. This result can be explained by low salinity of the blank-reactor in addition to the effect of the Hamra-sulfidogenic activity on metal corrosion. The Hamra-sulfidogenic bacteria present in the bulk phase (planktonic) or attached to the metal surface (biofilm), produce higher sulfide (with maximum sulfide peak at 418 mg/l) than the KSW (with the maximum sulfide peak at 341 mg/l) and higher than the Youmna (with maximum sulfide peak at 363 mg/l). Therefore the highest metal corrosion rate of the Hamra-control reactor was related to the maximum sulfidogenic activity in the bulk phase, or trapped within the biofilm matrices near the metal surface. This result is in agreement with results represented by Peng and Park, (1994). King et al., (1973) demonstrated that weight loss of the metal was proportional to the concentration of sulfide.

It has been reported the metal corrosion induced by SRB, isolated from an aquatic system, was ranged from 0.29 to 0.52 g/m^2 d which were 1.5-2.5 times greater than those obtained in the sterile solution (0.16 – 0.21 g/m^2 d). Bernardez et al., 2007 reported that the metal corrosion rate of steel (AISI 304) exposed to seawater (sterile medium) was 0.13 g/m^2d in comparison to medium inoculated with SRB was 0.216 g/m^2d. While the metal corrosion rate was not changed from the sterile medium to the SRB inoculated medium with steel (SAF 2507) with the same metal corrosion rate of 0.07 g/m^2d.

The mechanisms of metal corrosion in the presence of sulfidogenic bacteria in the bulk phase and over the metal surface (control reactors) are complex. In an anaerobic environment, sulfidogenic bacteria utilize hydrogen as an electron donor with sulfate (an electron acceptor) is being reduced to sulfide. In this respect, Von Wolzogen Kuhr and Van der Vlugt (1934) suggested the following reactions occurring:

$4Fe \rightarrow 4Fe^{2+} + 8e^-$	(anodic reaction)	(4)
$8H_2O \rightarrow 8OH^- + 8H^+$	(water dissociation)	(5)
$8H^+ + 8e^- \rightarrow 8H$ (ads)	(cathodic reaction)	(6)
$SO_4^{2-} + 8H$ (ads) $\rightarrow S^{2-} + 4H_2O$	(bacterial consumption)	(7)
$Fe^{2+} + S^{2-} \rightarrow FeS$	(corrosion products)	(8)
$4Fe + SO_4^{2-} + 4H_2O \rightarrow 3Fe(OH)_2 + FeS + 2OH^-$	(overall reaction)	(9)

This overall process is described as cathodic depolarization. Based on this theory, sulfidogenic bacteria increase the metal corrosion by continuous consume the atomic

hydrogen that accumulated at the cathode by a hydrogenase enzyme. Therefore, it leads to increasing the metal dissolution. Some researchers (Little et al., 1992 and Sanders and Hamilton, 1986) suggested that the metal corrosion rates increase due to the cathodic reduction of H_2S:

$$H_2S + 2e^- \rightarrow H_2 + S^{2-} \quad (10)$$

and the anodic reaction is accelerated by the formation of iron sulfide:

$$Fe + S^{2-} \rightarrow FeS + 2e^- \quad (11)$$

In addition, sulfidogenic bacteria facilitate the corrosion process by the attachment of cells to the metal surface and the binding of metal ions by EPS and/or lipopolysaccharides (LPS) (Koch et al., 2002). The sulfidogenic biofilms facilitate corrosion by trapping corrosive sulfide in close proximity to metal surfaces (Geesey et al., 2000). It has been hypothesized that the biofilm would influence the electrochemical behavior of a metal through formation of metal corrosion cells and galvanic coupling (Braissant et al., 2007).

Many authors reported the metal corrosion rates induced by SRB activity at different medium salinities, which are relevant to the obtained metal corrosion rate, (KSW-sulfidogenic bacteria was 0.2 g/m^2 d, Hamra-sulfidogenic bacteria was 0.3 g/m^2 d and Youmna-sulfidogenic bacteria was 0.5 g/m^2 d). Jayaraman et al., (1999) showed the metal corrosion rate induced by SRB (*Desulfovibrio vulgaris*) was ranged from 0.2 to 1.3 g/m^2 d. In addition, the metal corrosion rate recorded in the oil field with SRB and at salinity of 2.5 % NaCl was ranged from 0.2 to 8.77 g/m^2 d (Hubert, 2004). Moreover, Ghazy et al., (2011) showed that the metal corrosion rate of SRB (isolated from Esh El-Mallaha. Petroleum Company), which were cultivated in the artificial seawater Postgate's medium, was 0.4 g/m^2 d. Nevertheless, Zhao, (2008) reported high metal corrosion rate of 1 g/m^2 d induced by SRB in the artificial seawater. Changing in the metal corrosion rate was related not only to the medium salinity but also to the microbial diversity and activity.

The application of surfactant at different concentrations leads to gradually decrease the metal corrosion rate. The lowest metal corrosion rate of the KSW reactors was achieved at 10 and 1 mM with metal corrosion inhibition efficiencies of 92 and 94 % for CMS-I and CGS-II, respectively in comparison to the metal corrosion rate of the control reactors (inoculated with KSW-sulfidogenic bacteria). The lowest metal corrosion rate of the Hamra reactors with CGS-II was achieved at the same concentration

(1 mM) was shown for KSW reactors with an inhibition efficiency of 95 % in comparison to the metal corrosion rate of the control reactor (inoculated with Hamra-sulfidogenic bacteria). The lowest metal corrosion rate of the Youmna reactors was achieved at 5 mM with an inhibition efficiency of 97 % in comparison to the metal corrosion rate of the control reactor (inoculated with Youmna-sulfidogenic bacteria). At those concentrations, the synthesized surfactants (CMS-I, CGS-II and CGS-III) displayed biocidal effects against the sulfidogenic bacteria in the bulk phase and over the metal surface. Moreover, it is inhibiting the metal surface from medium salinity. At concentration of 1 and 10 mM CMS-I, 1 and 5 mM CGS-II, and 1 and 5 mM CGS-III the sulfidogenic bacteria were completely inhibited (see Figure 3–5, Figure 3–6 and Table 3–3) as the sulfate reduction reaction was completely inhibited causing no sulfide production and a considerable drop in the redox potential in the bulk phase. In addition, no growth was detected at those concentrations in the bulk phase and over the metal surface. In this case the rest of the metal corrosion rate was related to chemically (salinity)-induced metal corrosion which clearly recorded in the blank reactors (not inoculated with sulfidogenic bacteria). That means, the synthesized surfactant molecules present at the bulk phase is completely inhibited the sulfidogenic bacteria and the molecules present at the interface covering the metal surface from the surrounding environment and finally introduced the metal corrosion inhibition efficiency.

The hypothesized explanation of inhibiting behavior of the synthesized surfactants (CMS-I, CGS-II and CGS-III) from the medium salinity is the adsorption of the inhibitor to the metal/liquid interface. It has been reported the inhibiting action of surfactant is due to the adsorption of the surfactant molecules and formation of a tight, well surfactant layer at the metal/liquid interface and not due to the micelles (Zhou et al., 2012). The surfactant layers which adsorbed to the metal surface act as an inhibitive shield and protect the metal surface from the surrounding environment as represented in (Sastri, 1998). Two types of adsorption may take place, physical and chemical. The procedure of physical adsorption requires the presence of an electrically charged metal surface and charged species in the bulk phase. Chemisorption process involves a charge transfer or charge sharing between the inhibitor molecules and the metal surface. The presence of an inhibitor molecule that has relatively loosely bound electrons or heteroatoms with lone-pair electrons together with a transition metal have vacant and low-energy electron orbital, promotes this adsorption.

The synthesized CMS-I proceeds adsorption on the metal surface by an electrostatic interaction between the ammonium group (NH_4^+) and the cathodic sites from one hand and the counter ion (hydroxide ion) on the anodic sites from the other hand. Typically, monomeric surfactant at low concentration forms a monolayer on the metal surface. The increase of the monomeric surfactant concentration results in a formation of micelles in the bulk solution. In contrast to the described processes, the adsorption of gemini surfactants on metal surface is more complicated. The CGS-II and CGS-III contain two hydrophilic groups and two hydrophobic groups linked by spacer containing two ester groups and benzene ring in CGS-II and one phosphorous and three oxygen atoms in CGS-III. This structure reflects three different types of adsorption: (1) at low gemini surfactant concentrations, the adsorption takes place by a horizontal binding of the gemini surfactant to the metal surface (Figure 3–10a). This adsorption attitude is favored by an electrostatic interaction between the two ammonium groups (NH_4^+) and the cathodic sites on the one hand and the hydroxide ion on the anodic sites on the other hand. (2) At high gemini surfactant concentration, a perpendicular adsorption occurs as a result of an inter-hydrophobic chain interaction (Figure 3–10b). (3) With further increase of gemini surfactant concentration, up to C_{cmc} value an efficiency plateau appears (Figure 3–10c) (Farhat and Quraishi, 2010).

(a) KSW-sulfidogenic bacteria-CMS-I

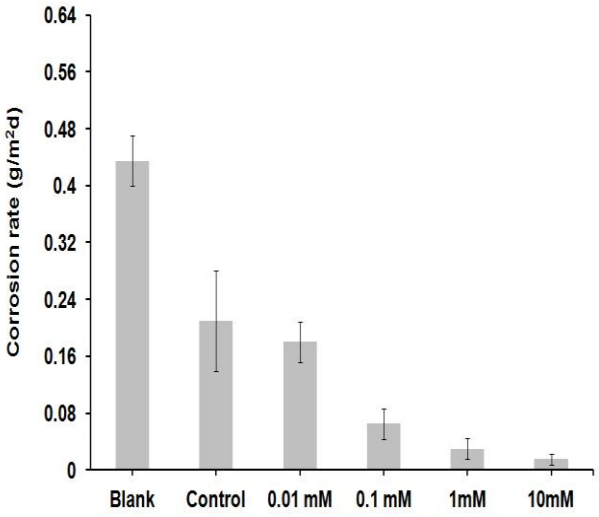

(b) KSW-sulfidogenic bacteria-CGS-II

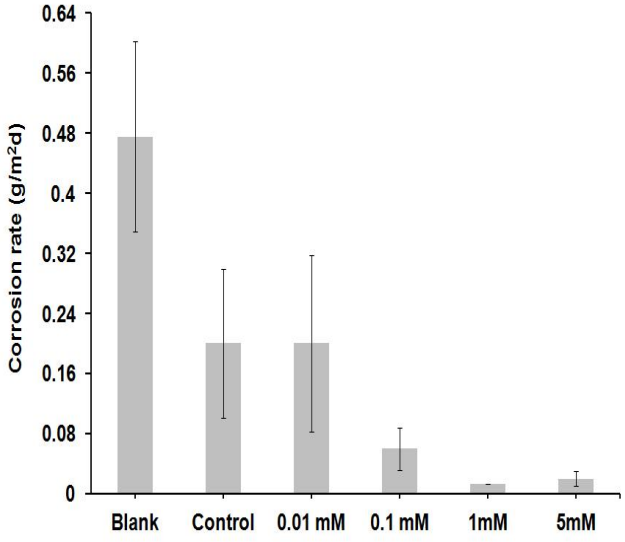

(c) Hamra-sulfidogenic bacteria-CGS-II

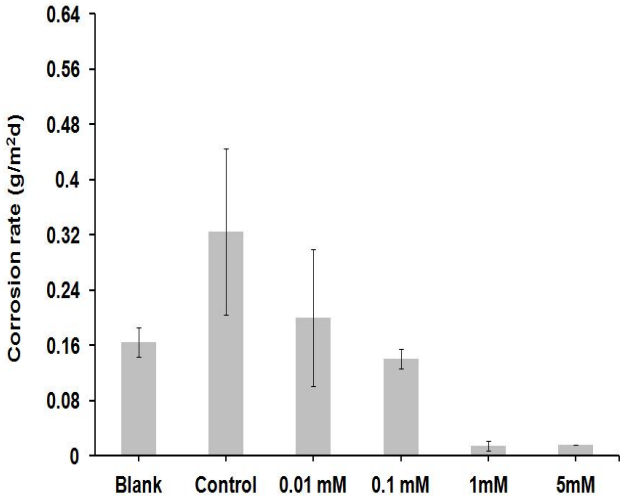

(d) Youmna-sulfidogenic bacteria-CGS-III

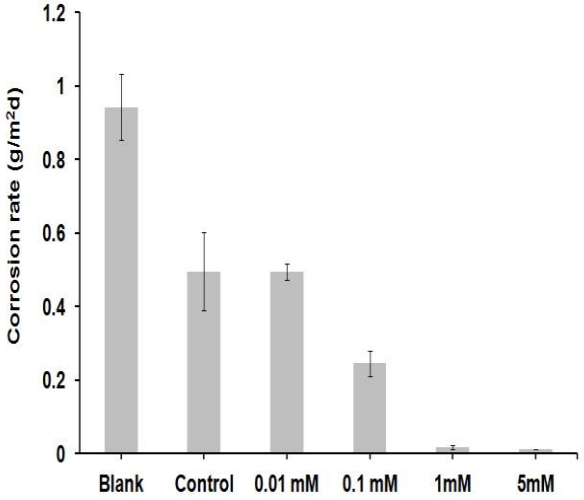

Figure 3–9. Corrosion rate of the sulfidogenic bacteria after one month incubation period are shown. Blank reactor (media without bacteria), control reactor (inoculated by sulfidogenic bacteria without surfactant) and different inhibitor concentrations (a) CMS-I and (b) CGS-II inoculated with the enriched KSW-sulfidogenic bacteria (c) CGS-II inoculated with the enriched Hamra-sulfidogenic bacteria and (d) CGS-III inoculated with the enriched Youmna-sulfidogenic bacteria. The results shown are mean values of duplicates with corresponding standard deviation.

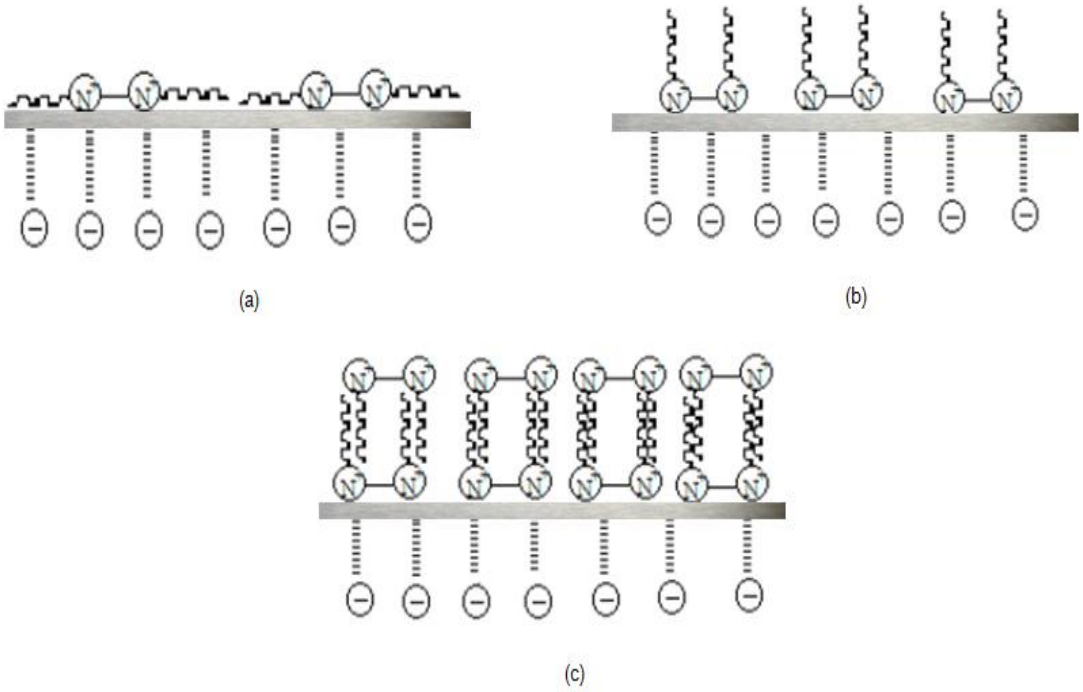

Figure.3–10 Diagram of the adsorption mechanism of cationic gemini surfactant on the metal surface. Adapted from Ref. (Farhat and Quraishi, 2010). .

The corrosion inhibition efficiency was confirmed by applying SEM to the metal surface. Figure 3-11a, b, c show SEM images of carbon steel surfaces after one month incubation with KSW, Hamra, and Youmna-sulfidogenic bacteria with different salinities. The biofilm images showed that the metal surface samples were completely covered with biofilm. After removing the biofilms, the surfaces were damaged as the effect of the cultivated biofilms at different salinities that induce metal corrosion (Figure 3–11d, e, f). However Figure 3–12a, b, c, d show the surface of another steel sample after cultivation for the same period in medium containing the best surfactant concentrations showed the highest metal corrosion inhibition efficiency, 10 mM CMS-I, 1 mM CGS-II inoculated with the enriched KSW-sulfidogenic bacteria, 1 mM CGS-II inoculated with the enriched Hamra-sulfidogenic bacteria and 5 mM CGS-III inoculated with the enriched Youmna-sulfidogenic bacteria. The SEM images revel that the surfaces are free from pits and completely covered with the inhibitors. This result indicates a good protective inhibitor film over the steel surfaces and confirms the highest inhibition efficiency of the synthesized surfactants (CMS-I, CGS-II and CGS-III). In conclusion, by applying the gemini surfactant, the metal surface was protected by lower surfactant concentrations rather than the monomeric surfactant.

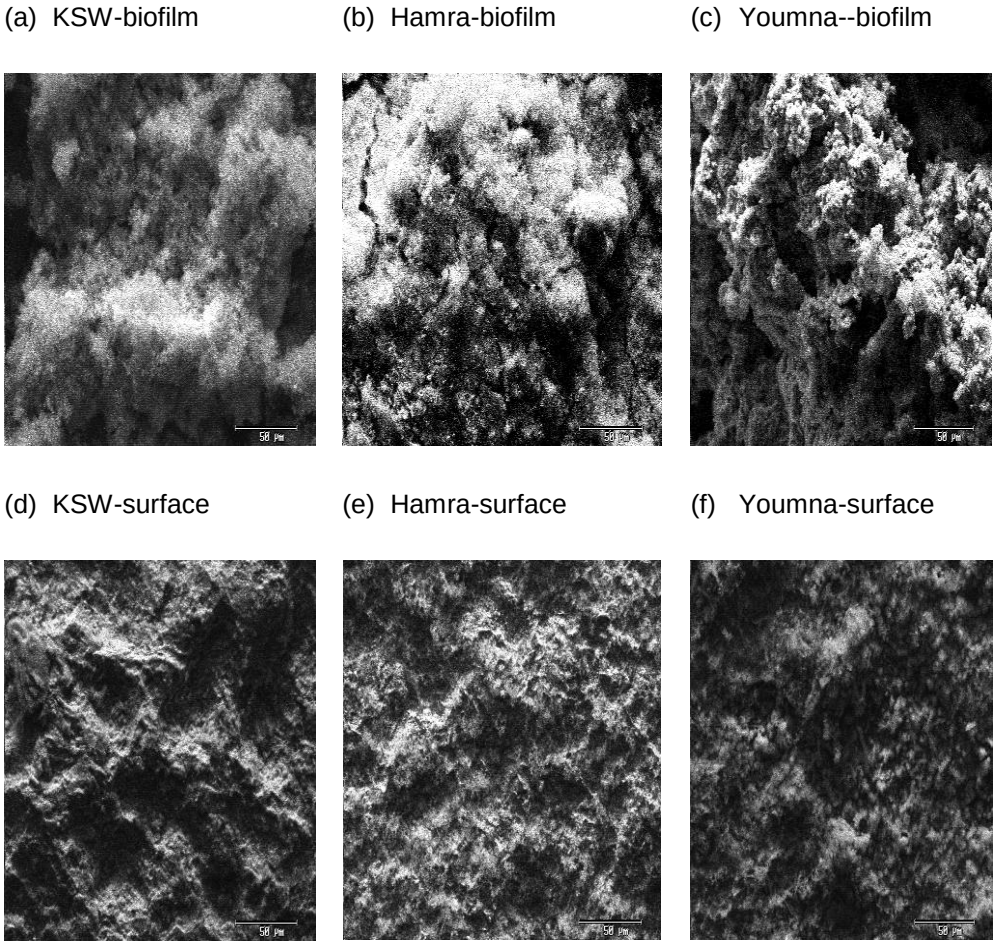

Figure 3–11. SEM images of the mild steel coupons. (a) the KSW-sulfidogenic biofilm, (b) Hamra-sulfidogenic biofilm and (c) Youmna-sulfidogenic biofilm (d) metal surface after removing the biofilm of KSW, (e) metal surface after removing the biofilm of Hamra and (f) metal surface after removing the biofilm of Youmna. Scale bar = 50 µm.

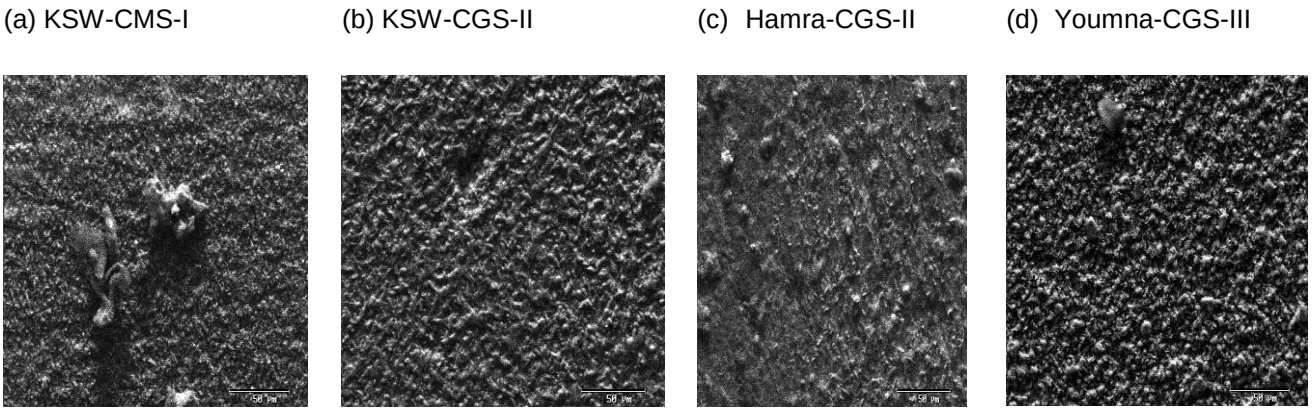

Figure 3–12. SEM images of the mild steel coupons after applying the surfactants. (a) 10 mM with the KSW sulfidogenic bacteria (b) 1 mM CGS-II with the KSW sulfidogenic bacteria (c) 1 mM CGS-II with Hamra-sulfidogenic bacteria and (d) 5 mM CGS-III with Youmna sulfidogenic bacteria. Scale bar = 50 µm

CHAPTER 4

Conclusions

The existing of metal corrosion in the three oil-field water tanks with different water salinities (0.23 %, 3.19 %, and 5.49 % NaCl) has been confined to different sulfidogenic microbial diversities and activities in addition to different cultivated salinities. The dsrβ (as a functional and taxonomic marker) gene-based DGGE approach was successfully used to assess the sulfidogenic diversities. The sulfidogenic diversities are dominating the original water samples and the water samples after enrichment and biofilms cultivation. This approach was proved to be an effective tool to rapidly detect the sulfidogenic diversity in the different environmental samples. One of unique observation in this work is the detection of sulfidogenic bacteria in the water samples used for inoculation and there absence the cultivated biofilm. This observation was related to the changing in the biofilm cultivation conditions. The presence of *Desulfovibrio spp.* as a dominant species in the original water samples and their cultivated biofilms emphasize their key role in the microbial corrosion process. Non-orthologous dsr-gene species *(*phylum *Firmicutes*) were detected within the phylum *Proteobacteria.* Those species acquired the dsr-gene by lateral transfer from species of the phylum *Proteobacteria.* Significant changes in the microbial diversity composition in the water samples and their cultivated biofilms were observed only in the sample cultivated at 5.49 % NaCl. This result might be attributed to the selective cultivation conditions which did not reflect the in situ water properties.

The sulfidogenic-biofilm metal-corrosion activities gave an indication of the involvement of chemical and microbiological corrosion-inducing processes. The chemical-induced corrosion activity is attributed to chloride anion corrosiveness that can be adsorbed on the metal surface and traps within the biofilm matrices. This attitude was clearly present in the sulfidogenic bacteria cultivated at high medium salinities (3.19 and 5.49 % NaCl). On the other hand, the microbiological-induced metal corrosion activity is related to cathodic depolarization process in addition to the sulfide (as a metabolic end product) corrosiveness effect. The microbiological-induced metal corrosion behavior was most obviously achieved in the sulfidogenic biofilm cultivated at a low medium salinity (0.23 % NaCl). In this experiment the highest sulfide production was achieved compared to the other sulfidogenic biofilms. The sulfidogenic biofilms with the higher diversity showed a thicker biofilm in comparison to a low biofilm diver-

sity that produce a thinner biofilm. The thicker biofilm protected the metal surface from the chloride anion corrosive effect.

Three novel surfactants (one cationic monomeric and two cationic gemini) were successfully synthesized and characterized. The metal corrosion rate of the blank-reactors (without biomass) demonstrated a positive correlation between the metal corrosion rates and the different medium salinities. However, the metal corrosion rate of the control-reactors (inoculated with the sulfidogenic consortia) showed different attitude. The biofilms (control-reactors) cultivated at high medium salinities exhibited protection effect to the metal surface from their high medium salinities. While the biofilm cultivated at a low medium salinity revealed a high metal corrosion rate which related to its high sulfide production (which present in the bulk phase and entrapped with the biofilm matrix). The surfactants biocidal effect was achieved by preventing the sulfide production and drop of the redox potential in the bulk phase. The synthesized surfactants not only showed biocidal activity against the environmental sulfidogenic bacterial communities but also against Gram-positive and Gram-negative bacterial standard strains and in comparison to tetracycline antibiotic. With respect to the biocidal mechanism of the synthesized surfactants, the charge of the surfactants was found to play a determining role. Biocidal mechanism was achieved by an interaction between the negatively charged cell membrane (lipoprotein) and the positively charged ammonium group (NH_4^+) of the synthesized surfactants. In addition a physical disruption occurs when hydrophobic chains (alkyl groups) penetrate into the bacterial cell membrane which in the end leads to dead of the bacterial cell.

The structures of the surfactants play an important role in determining their inhibition efficiencies. The gemini surfactants showed better surface active properties, biocidal activity, biofilm development inhibition at a low concentration in comparison to the monomeric surfactant. High metal corrosion inhibition efficiency (94 %) was achieved by applying gemini surfactant at a concentration of 1 mM on sulfidogenic bacteria (cultivated at 3.19 % NaCl) in comparison to the monomeric surfactant (92 %) at a concentration of 10 mM. The difference in the metal corrosion inhibition efficiencies between the monomeric and the gemini surfactant was related mainly to their structure. Applying the same cationic gemini surfactant on the sulfidogenic bacteria (cultivated at 0.23 % NaCl), successfully confirmed the metal corrosion inhibition efficiency of 95 % at the same concentration (1mM). In addition, another cationic gemini surfactant with different structure showed a high metal surface protection from

the sulfidogenic bacteria (cultivated at 5.49 % NaCl). The achieved high metal corrosion inhibition efficiency of 97 % was observed at a concentration of 5 mM.

The high metal corrosion inhibition efficiency of the synthesized surfactants was related to the high adsorption of the surfactant molecules to the metal surfaces and subsequent formation of protective films. The adsorption occurred by an electrostatic interaction between the ammonium group (NH_4^+) and the cathodic sites from one hand and the counter ion (hydroxide ion) on the anodic sites from the other hand.

Overall, these findings suggest that the corrosion process in this study is a synergistic effect between the metal surface, harmful chloride anions, bio-diversity (culturable and un-culturable) composition and their metabolic products in the biofilm matrices. In this respect, the synthesized surfactants successfully used to protect the metal surface from the sulfidogenic microbial growth and activities at different medium salinities. Moreover, when the metal surface and the bulk phase are free from the sulfidogenic bacteria, the synthesized surfactants successfully show corrosion-protection against the medium salinities.

References

Acha, D., and H. Hintelmann J. Yee. 2011. Importance of sulfate reducing bacteria in mercury methylation and demethylation in periphyton from Bolivian Amazon region. Chemosphere. 82: 911–916.

Almeida, J.A.S., E.F. Marques, A.S. Jurado, and A.C.C. Pais. 2010. The effect of cationic gemini surfactants upon lipid membranes. An experimental and molecular dynamics simulation study. Phys. Chem. Chem. Phys. 12: 14462–14476.

Anonymous .1998. Multiple tube fermentation technique for members of the coli form group. In: Greenberg AE, Clesceri LS, Eaton AD (eds) Standard methods for the examination of water and wastewater. American Public Health Association, American Water Works Association, and Water Environment Federation, New York, 9–51.

Ashassi-Sorkhabi H., E. Asghari. 2009. Influence of flow on the corrosion inhibition of St52-3 type steel by potassium hydrogen- phosphate. Corrosion science, 51:1828–1835.

Atkin, R., V.S.J. Craig, E.J. Wanless, and S. Biggs. 2003. Mechanism of cationic surfactant adsorption at the solid-aqueous interface. Adv. Colloid Interface Sci. 103: 219–304.

Azzam, E.M.S., R.M. Sami, N.G. Kandile. 2012. Activity inhibition of sulfate-reducing bacteria using some cationic thiol surfactants and their nanostructure. 2(3): 29-35.

Badawi A.M., M.A. Mekawi, A.S. Mohamed, M.Z. Mohamed, M.M. Khowdairy. 2007. Surface and biological activity of some novel cationic surfactants, Journal of Surfactant and Detergent. 10: 243–255.

Badawi, A.H., M.A. Hegazy, A.A. El-Sawy, H.M. Ahmed, and W.M. Kamel. 2010. Novel quaternary ammonium hydroxide cationic surfactants as corrosion inhibitors for carbon steel and as biocides for sulfate-reducing bacteria (SRB). Materials Chemistry and Physics. 124: 458-465.

Barth T., and M. Riis. 1992. Interactions between organic acid anions in formation waters and reservoir mineral phases. Org. Geodiem. 19: 455-482.

Barth, T. 1991. Organic acids and inorganic ions in waters from petroleum reservoirs, Norwegian continental shelf: a multivariate statistical analysis and comparison with American reservoir formation waters. Appl. Geochem. 6:1–15.

Barton, L.L. and F.A. Tomei. 1995. Characteristics and activities of sulfate-reducing bacteria. In: Sulfate-Reducing Bacteria (Barton, L.L., ed.), Plenum Press, New York pp1–32.

Bastin, E.S., F.E. Greer, C.A. Merritt, and G. Moulton. 1926. The presence of sulfate reducing bacteria in oil field waters. Science. 63: 21–24.

Beech, I. B., and C.C. Gaylarde. 1999. Recent advances in the study of biocorrosion an overview. Revista de Microbiologia. 30:177–190.

Beech, I.B. 2004. Corrosion of technical materials in the presence of biofilms current understanding and state-of-the art methods of study. International Biodeterioration and Biodegradation. 53: 177–183.

Beech, I.B., and S.A. Campbell. 2008. Accelerated low water corrosion of carbon steel in the presence of a biofilm harbouring sulfate-reducing and sulfur-oxidizing bacteria recovered from marine sediment. Electrochimica Acta. 54:14–21.

Beech, I.B., and S.A. Campbell. 2008. Accelerated low water corrosion of carbon steel in the presence of a biofilm harboring sulphate-reducing and sulphur oxidising bacteria recovered from a marine sediment. Electrochimica Acta, 54:14–21.

Beech, I.B., C.C. Gaylarde, J.J. Smith, and G.G. Geesey. 1991. Extracellular polysaccharides from Desulfovibrio desulfuricans and *Pseudomonas fluorescens* in the presence of mild and stainless steel. Applied Microbiology Biotechnology. 35:65–71.

Beech, I.B., J.R. Smith, A.A. Steele, I. Penegar, and S.A. Campbell. 2002. The use of atomic force microscopy for studying interactions of bacterial biofilms with surfaces. Coll Surf B: Biointerf. 23: 231–247.

Beeder, J., T. Torsvik, and T. Lien. 1995. *Thermodesulforhabdus norvegicus* gen. nov., sp. nov., a novel thermophilic sulfate-reducing bacterium from oil field water. Arch. Microbiol. 164:331–336.

Benson, D.A., I. Karsch-Mizrachi, D.J. Lipman, J. Ostell, and D.L. Wheeler. 2005. GenBank. Nucleic Acids Res., 33: D34-D38.

Bernardez, L.A. L.R.P. de Andrade Lima, and P.F. Almeida. 2007. Corrosion of stainless steels exposed to seawater containing sulfate-reducing bacteria. Brazilian Journal of Petroleum and Gas. 1(1): 51–58.

Birkeland, N-K. 2005. Sulfate-reducing bacteria and Archaea. In: Petroleum Microbiology (B. Ollivier and M. Magot), ASM Press, Washington, D.C.

Bockelmann U, W. Manz, T.R. Neu, and U. Szewzyk U. 2002. Investigation of lotic microbial aggregates by a combined technique of fluorescent in situ hybridization and lectin-binding analysis. J MicrobiolM ethods 49:75–87

Boessmann M, C. Staudt, T.R. Neu, H. Horn, and D.C. Hempel.2003. Investigation and modeling of growth, structure and oxygen penetration in particle supported biofilms. Chem Eng Technol 26 (2):219–222

Boessmann M, T.R. Neu, H. Horn, and D.C. Hempel 2004. Growth, structure and oxygen penetration in particle supported autotrophic biofilms. Water Sci Technol 49:371–377

Braissant, O., A.W. Decho, C. Dupraz, C. Glunk, K.M. Przekop, and P.T. Visscher. 2007. Exopolymeric substances of sulfate-reducing bacteria: interaction with calcium at alkaline pH and implication for formation of carbonate minerals, Geobiology. 5:401–411.

Brandt, K.K., B.K.C. Patel', and K. Ingvorsen. 1999. Desulfocella halophila gen. nov., sp. nov., a halophilic, fatty-acid-oxidizing, sulfate-reducing bacterium isolated from sediments of the Great Salt Lake. International Journal of Systematic Bacteriology. 49: 193–200.

Brennenstuhl, A.M., and P.E. Doherty. 1990. The economic impact of microbiologically influence corrosion at Ontario Hydro's nuclear plants," Microbiologically Influenced Corrosion and Biodeterioration, University of Tennessee, Knoxville, TN, pp 5–10.

Brochier-Armanet, C., B. Boussau, S. Gribaldo, and P. Forterre. 2008. Mesophilic Crenarchaeota: Proposal for a third archaeal phylum, the Thaumarchaeota. Nat. Rev. Microbiol. 6:245–252

Brunt, K.D. 1987. In: Hill HC (ed) Biocides for the oil industry. Wiley, New York, p 201

Burggraf, S., H.W. Jannasch, B. Nicolaus, and K.O. Stetter. 1990. *Archaeoglobus profundus* sp. nov., represents a new species within the sulfate-reducing *archaeobacteria*. Syst Appl Microbiol. 13: 24–28.

Castaneda, H., and X.D. Benetton. 2008. SRB-biofilm influence in active corrosion sites formed at the steel-electrolyte interface when exposed to artificial seawater conditions. Corrosion Science 50: 1169–1183.

Castro, H., K.R. Reddy, and A. Ogram. 2002. Composition and function of sulfate-reducing prokaryotes in eutrophic and pristine areas of the Florida everglades. Appl. Environ. Microbiol. 68: 6129–6137.

Caumette, P., Y. Cohen, and R. Matheron. 1991. Isolation and characterization of *Desulfovibrio halophilus* sp. nov., a halophilic sulfate-reducing bacterium isolated from Solar Lake (Sinai). Syst Appl Microbiol. 14: 33–38.

Chan, K.L., C. Xu, and HHP. Fang. 2002. Anaerobic electrochemical corrosion of mild steel in the presence of extracellular polymeric substances produced by a culture enriched in sulfate-reducing bacteria. Environmental Science Technology, 36: 1720–1727.

Chen M-Y., D-J. Lee, J-W. Tay, and K-Y. Show. 2007. Staining of extracellular polymeric substances and cells in bioaggregates. Appl Microbiol Biotechnol. 75: 467–474.

Cheung, C.W.S., and I.B. Beech. 1996. The use of biocides to control sulfate-reducing bacteria in biofilms on mild steel surfaces. Biofouling. 9:231–249.

Cord-Ruwisch, R. 1995. MIC in hydrocarbon transportation systems. Corrosion and prevention 95. Paper 7. Australian Corrosion Association, Clayton, Australia.

Cord-Ruwisch, R. 2000. Microbially influenced corrosion of steel. In: Lovley, D.R. (ed.), Environmental Microbe–Metal Interactions. ASM Press, Washington, DC, pp159–173.

Cord-Ruwisch, R., W. Kleinitz, and F. Widdel. 1986. Sulfate-reducing bacteria in an oil field. Erdol Erdgas Kohle. 102: 281–289.

Costerton, J.W, and P. Stoodley. 2003. Microbial Biofilms: Protective Niches in Ancient and Modern Geomicrobiology, In: Fossil and Recent Biofilms: A Natural History of Life on Earth,

KrumbeinWE, Paterson DM, Zavarzin GA (eds). Kluwer Academic Publishers, Dordrecht, Netherland.

Costerton, J.W. 1985. The role of bacterial exopolysaccharides in nature and disease. Dev. Ind. Microbiol. 26: 249–261.

Costerton, J.W., G.G. Geesey, and G.K. Cheng. 1978. How bacteria stick. Sci. Am. 238: 86–95.

Dahl, C., N.M. Kredich, R. Deutzmann, and H.G. Trüper. 1993. Dissimilatory sulphite-reductase from *Archaeoglobus fulgidus*: physicochemical properties of the enzyme and cloning, sequencing and analysis of the reductase genes. J. Gen. Microbiol. 139: 1817–1828.

Darkin, M.G., C. Gilpin, J.B. Williams, and C.M. Sangha. 2001. Direct Wet Surface Imaging of an Anaerobic Biofilm by Environmental Scanning Electron Microscopy: Application to Landfill Clay Liner Barriers. Scaning. 23: 346–350.

Davis, J.R. 2000. Corrosion: understanding the basics, ASM International, Materials Park, Ohio,

Detkova, E.N., G.S. Soboleva , E.V. Pikuta, and M.A. Pusheva. 2005. The effect of sodium salts and pH on hydrogenase activity of the halo Alkaliphilic sulfate-reducing bacteria. Mikrobiologiia. 74: 460–465.

DEV, Deutsche Einheitsverfahren zur Wasser. 1993. Abwasser und Schlammunter- suchung Physikalische, chemische, biologische und bakteriologische Verfahren (German Standard Methods for the Examination of Water, Wastewater and Sludge physical, chemical, biological and bacteriological methods). DIN Deutsches Institut für Normung e. V. Beuth.

Devereux, R., M. Delaney, F. Widdel, and D.A. Stahl. 1989. Natural relationships among sulfate-reducing eubacteria. J Bacteriol. 171: 6689–6695.

Dhillon, A., J. Teske, D. Dillon, A. Stahl, and M.L. Sogin. 2003. Molecular characterization of sulfate-reducing bacteria in the Guaymas Basin. Applied and Environmental Microbiology. 69: 2765–2772.

Dinh, H.Y., J. Kuever, M. Mubmann, A.W. Hassel, M. Stratmann, and F. Widdel. 2004. Iron corrosion by novel anaerobic microorganisms. Nature. 427: 829–832.

Dolla, A., M. Fournier, and Z. Dermoun. 2006. Oxygen defense in sulfate-reducing bacteria. J. of Biotechnology 126: 87–100.

Dow, J.M., L. Crossman, K. Findlay, Y.Q. He, J.X. Feng, and J.L. Tang. 2003. Biofilm dispersal in *Xanthomonas campestris* is controlled by cell-cell signaling and is required for full virulence in plants. Proc. Natl. Acad. Sci. USA. 100: 10995–11000.

Dunsmore, B.C., J. Youldon, D.R. Thrasher, and L. Vance. 2006. Effects of nitrate treatment on a mixed species, oil field microbial biofilm. J Ind Microbiol Biotechnol. 33: 454–462.

Elkins, J. G., M. Podar, D.E. Graham, K.S. Makarova, Y. Wolf, L. Ranau, B.P. Hedlund, C. Brochier-Armanet, V. Kunin, and I. Anderson. 2008. A korarchaeal genome reveals insights into the evolution of the Archaea. Proc Natl Acad Sci USA. 105: 8102-8107.

Engberts, J.B.F.N., J. Karthauser, S. Karaborni, and N.M. Van Os. 1996. Synthesis, surface properties and oil solubilisation capacity. Colloids Surf. 118: 41–49.

Fang, H.P., L.Ch.Xu,and K-Y. Chan. 2002. Effects of toxic metals and chemicals on biofilm and biocorrosion. Water Research 36: 4709–4716.

Farhat A.A, and M. A. Quraishi. 2010. Inhibitive performance of gemini surfactants as corrosion inhibitors for mild steel in formic acid. Portugaliae Electrochimica Acta. 28:321-335

Flemming, H–C. 1996. Biofouling and microbiologically influenced corrosion (MIC) an economical and technical overview, Microbial Deterioration of Materials, Springer, Heidelberg, pp 5–14.

Flemming, H-C. 2003. Role and levels of real time monitoring for successful anti-fouling strategies. Water Sci Technol. 47: 1–8.

Fukuba, T., M. Ogawa, T. Fujii, and T. Naganuma. 2003. Phylogenetic diversity of dissimilatory sulfite reductase genes from deep-sea cold seep sediment. Mar. Biotechnol. 5: 458–468.

Gamboa, C., and A.F. Olea. 2006. Association of cationic surfactants to humic acid, Effect on the surface activity. Colloids Surf. A Physicochem. Eng. Aspects 278: 241–245.

Garcia B.K.C., and J.G. Ollivier. 2000. Taxonomic, phylogenetic and ecological diversity of methanogenic archaea, Anaerobe 6: 205–226.

Garcia-de-Lomas, J., A. Corzo, M.C. Portillo, J.M. Gonzalez, J.A. Andrades, C. Saiz-Jimenez, and E. Garcia-Robledo. 2007. Nitrate stimulation of indigenous nitrate-reducing, sulfide-oxidizing bacterial community in wastewater anaerobic biofilms. Water research. 41: 3121–3131.

Garrity, G.M., and J.G. Holt. 2001. The road map to the Manual. In Bergey's Manual of Systematic Bacteriology, 2nd ed, Springer-Verlag, New York, 1: 119–166.

Gasol, J., E. Casamayor, I. Joint, K. Garde, K. Gustavson, S. Benlloch, B. Díez, M. Schauer, R. Massana, and C. Pedrós-Alió. 2004. Control of heterotrophic prokaryotic abundance and growth rate in hypersaline planktonic environments. Aquatic Microbial Ecology. 34: 193–206.

Gaylarde, C.C., and H.A. Videla. 1987. Localised corrosion induced by a marine vibrio. International Biodetetioration, 23 91–104.

Geesey, G., I. Beech, P. Bremer, B.J. Webster, and D.B. Wells. 2000. Biocorrosion. In Biofilms II Process Analysis and Applications ed. Bryers, J.D. New York: Wiley-Liss. pp. 281–325.

Geets, J., B. Borremans, L. Diels, D. Springael, J. Vangronsveld, D.V. Lilie, and K. Vanbroekhoven. 2006. DsrB gene based DGGE for community and diversity surveys of sulfate-reducing bacteria. J Microbiol Meth. 66: 194–205.

Ghazy, E.A., M.G. Mahmoud, M.S. Asker, M. N. Mahmoud, M. M. Abo Elsoud and M. E. Abdel Sami. 2011. Cultivation and detection of sulfate reducing bacteria (SRB) in sea water. Journal of American Science, 7(2): 604–608.

Giudice,C., and B.D. Amo. 1996. Corrosion Prevention and Control, pp 43–47.

Gonzalez, Y., M.C. Lafont, N. Pebere, G. Chatainier, J. Roy, T. Bouissou. 2005. A corrosion inhibition study of a carbon steel in neutral chloride solutions by zinc salt/phosphoric acid association. Corros. Sci. 37: 1823–1837.

Gu, J.H., and Mitchell. 2000. Biodeterioration. In M. Dworkin, K.H. Schleifer, and E. Stackebrandt (ed.),The prokaryotes: an evolving electronic resource for microbiology community. Springer-Verlag, New York.

Gu, J-D., T.E. Ford, and R. Mitchell. 2000. Microbial corrosion of metals. In: Review, W. (Ed.). The Uhlig Corrosion Handbook, Second ed. John Wiley & Sons, New York. 915–927.

Gubner, R.J. 1998. Biofilms and accelerated low-water corrosion in carbon steel piling in tidal waters, Ph.D. thesis, University of Portsmouth.

Hamilton, WA. 1985. Sulfate-reducing bacteria and anaerobic corrosion. Annu. Rev. Microbiol. 39: 195–217

Héctor, A.V., and L.K.H. Quintero. 2007. Biocorrosion in oil recovery systems. Prevention and protection. An update. Rev. Téc. Ing. Univ. Zulia. Edición Especial. 30: 272–279.

Hegazy M.A. 2009. Anovel Schif base-based gemini surfactants: synthesis and effect on corrosion inhibition of carbon steel in hydrochloric acid solution, Corrosion Science. 51: 2610–2618.

Hegazy, M.A., H.M. Ahmed, A.S. El-Tabei. 2011. Investigation of the inhibitive effect of p-substituted 4-(N,N,N-dimethyldodecylammonium bromide)benzylidene-benzene-2-yl-amine on corrosion of carbon steel pipelines in acidic medium. Corrosion. Science. 53:671–678.

Hegazy, M.A., M. Abdallah, and H. Ahmed. 2010. Novel cationic gemini surfactants as corrosion inhibitors for carbon steel pipelines. Corrosion Science. 52: 2897–2904.

Hille, A., T.R. Neu, D.C. Hempel, and H. Horn. 2005. Oxygen profiles and biomass distribution in biopellets of Aspergillus niger. Biotechnol. Bioeng. 92: 614–623.

Horn, H., E. Morgenroth. 2006. Transport of oxygen, sodium chloride, and sodium nitrate in biofilms. Chemical Engineering Science. 61:1347–1356.

Huber, H., M.J. Hohn, R. Rachel, T. Fuchs, V.C. Wimmer, and K.O. Stetter. 2002. A new phylum of Archaea represented by a Nano sized hyperthermophilic symbiotic. Nature. 417: 63–67.

Hubert, C.R.J. 2004. Control of hydrogen sulfide production in oil fields by managing microbial communities through nitrate or nitrite addition, Ph.D. thesis, University of Calgary, Alberta, Canada.

Hugo, W, and G. Snow. 1981. Biochemistry of antibacterial action. Chapman & Hall, London.

Hunter, R.J. 2001. Foundation of colloid science. 2nd ed., Oxford University Press. Inc., New York. pp 435–439.

Iverson, W.P. 1987. Microbial corrosion of metals. Adv. Appl. Microbiol. 32: 1–36.

Jayaraman A., P.J. Hallock, R.M. Carson, C-C. Lee, F.B. Mansfeld, and T.K. Wood. 1999. Inhibiting sulfate-reducing bacteria in biofilms on steel with antimicrobial peptides generated in situ. Appl Microbiol Biotechnol. 52:267-275.

Jeanthon, C., S.L. Haridon, V. Cueff, A. Banta, A. Reysenbach, and D. Prieur. 2002. *Thermodesulfobacterium hydrogeniphilum* sp. nov., a thermophilic, chemolithoautotrophic, sulfate-reducing bacterium isolated from a deep-sea hydrothermal vent at Guaymas Basin, and emendation of the genus Thermodesulfobacterium. International Journal of Systematic and Evolutionary Microbiology 52: 765–772.

Jones D.A., and P.S. Amy. 2002. A thermodynamic interpretation of microbiologically influenced corrosion. Corrosion. 58: 638–645.

Jonkers, H.M, M.J.E.C. VanderMaarel, H. VanGemerden, and T.A. Hansen. 1996. Dimethylsulfoxide reduction by marine sulfate-reducing bacteria. FEMS Microbiology Letters. 136: 283–287.

Jonsson, B., K. Lindmam, and B. Kronberg.1998. "Surfactants and Polymers in Aqueous Solution", John Wiley and Sons Ltd, New York.

Jørgensen, B. 1993. The microbial sulfur cycle. In W. E. Krumbein (ed.), Microbial geochemistry, Black Well Scientific, Oxford. 91–124.

Karkhoff-Schweizer, R.R., D.P.W.Huber, and G. Voordouw. 1995. Conservation of the genes for dissimilatory sulfite reductase from Desulfovibrio vulgaris and Archaeoglobus fulgidus allows their detection by PCR, Applied and Environmental Microbiology. 61: 290–296.

Khaled, K.F. and M.A. Amin. 2009. Electrochemical and molecular dynamics simulation studies on the corrosion inhibition of aluminum in molar hydrochloric acid using some imidazole derivatives. J Appl Electrochem. 39: 2553–2568.

Khaled, K.F., and N. Hackerman. 2003. Investigation of the inhibitive effect of ortho-substituted anilines on corrosion of iron in 1 M HCl solutions. Electrochim. Acta. 48:2715–2723.

King R.A., J.D.A. Miller, D.S. Wakerly. 1973. Corrosion of mild steel in cultures of sulphate-reducing bacteria; effect of changing the soluble iron concentration during growth. Br. Corros. J., 8: 89–93.

Klein, M., M. Friedrich, A.J. Roger, P. Hugenholtz, S. Fishbain, H. Abicht, L.L. Blackall, D.A. Stahl, and M. Wagner. 2001. Multiple lateral transfers of dissimilatory sulfite reductase genes between major lineages of sulfate-reducing prokaryotes. Journal Bacteriology. 183: 6028–6035.

Knoblauch, C., K. Sahm, and B.B. Jorgensen.1999. Psychrophilic sulfate-reducing bacteria isolated from permanently cold Arctic marine sediments: description of *Desulfofrigus oceanense* gen. nov., sp. nov., *Desulfofrigus fragile* sp. nov., *Desulfofabagelida gen*. nov., sp. nov., *Desulfotalea psychrophila* General nov., sp. nov. and *Desulfotalea arctica* sp. nov. Int. J. Syst. Bacteriol. 49: 1631–1643.

Koch, G.H., M.P.H.Brongers, N.G. Thompson, Y.P. Virmani, and J.H. Payer. 2002. Corrosion Costs and Preventative Strategies in the United States. Federal Highway Administration. Publication No. FHWA-RD-01-156. Printed in a supplemental to Materials Performance. NACE International.

Krekeler, D., P. Sigalevich, A. Teske, H. Cypionka, and Y. Cohen. 1997. A sulfate-reducing bacterium from the oxic layer of a microbial mat from Solar Lake (Sinai), *Desulfovibrio oxyclinae* sp. nov., Archives of Microbiology. 167: 369–375.

Kuang, F., J. Wang, L. Yan, D. Zhang. 2007. Effects of sulfate-reducing bacteria on the corrosion behavior of carbon steel. Electrochimica Acta 52:6084–6088.

Kulikova, T., P. Aldebert, N. Althorpe, W. Baker, K. Bates, P. Browne, A. Van den Broek, G. Cochrane, K. Duggan, and R. Eberhardt *et. al*., 2004. The EMBL Nucleotide Sequence Database. Nucleic Acids Res. 32: D27–D30.

Lawrence JR, G.D.W. Swerhone, G.G. Leppard, T. Araki, X. Zhang, M.M. West, and A.P. Hitchcock. 2003. Scanning transmission X-ray, laser scanning, and transmission electron microscopy mapping of the exopolymeric matrix of microbial biofilms. Appl EnvironMicrobiol 69:5543–5554.

Lawrence JR, G.D.W. Swerhone, L. Wassenaar, and T.R. Neu. 2005. Effects of selected pharmaceuticals on riverine biofilm communities. Can J Microbiol 51:655–669.

Lawrence JR, M.R. Chenier, R. Roy, D. Beaumier, N. Fortin, G.D.W. Swerhone, T.R. Neu, and C.W. Greer. 2004. Microscale and molecular assessment of impacts of nickel, nutrients, and oxygen level on structure and function of river biofilm communities. Appl Environ Microbiol 70:4326–4339.

Lee, J.P., C.S. Yi, J. LeGall, and H.D. Peck. 1973. Isolation of a new pigment, desulforubidin, from *Desulfovibrio desulfuricans* (Norway strain) and its role in sulfite reduction. J. Bacteriol. 115: 453–455.

Lee, W.C, Z. Lewandowski, P.H. Nielsen, and A. Hamilton. 1995. Role of sulfate-reducing bacteria in corrosion of mild steel: a review. Biofouling. 8: 165–194.

LeGall, J., and G. Fauque. 1988. Dissimilatory reduction of sulfur compounds, In A. J. B. Zehnder (ed.), Biology of Anaerobic Organisms. John Wiley, New York, pp 587-639.

Lewandowski, Z., and H. Beyenal. 2003. In: Wuertz S., Bishop P.L., Wildere, P.A. (eds.), Mass Transfer in Heterogeneous Biofilms. IWA Publishing, London. pp 145–172.

Li, S., L. Ni, C. Sung, L. Wang. 2004. Influence of organic matter on orthophosphate corrosion inhibition for copper pipe in soft water. Corros. Sci. 46: 137–145.

Lie, T.J., W. Godchaux, and E.R. Leadbetter. 1999. Sulfonates as terminal electron acceptors for growth of sulfite-reducing bacteria (*Desulfitobacterium* spp.) and sulfate-reducing bacteria: effects of inhibitors of sulfidogenesis. Appl Environ Microbiol. 10: 4611–4617.

Lipman, D.J., and W.R. Pearson. 1985. Rapid and sensitive protein similarity searches. Science. 227: 1435–1441.

Little, B, P. Wagner, and F. Mansfeld. 1992. An overview of microbiologically influenced corrosion. Electrochim Acta, 37: 2185–2194.

Little, B., R. Staehle, and R. Davis. 2001. Fungal influenced corrosion of post-tensioned cables. Int. Biodeter. Biodegrad. 47: 71–77.

Lovely, D.R., and J.P. Phillips. 1987. Competitive mechanism for inhibition of sulfate reduction and methane production in the zone of ferric iron reduction in sediments. Applied and Environmental Microbiology. 53: 2636–2641.

Macian, M., J. Seguer, M.R. Infante, C. Selve, and M.P. Vinardell. 1996. Preliminary studies of the toxic effects of non-ionic surfactants derived from lysine. Toxicology. 106: 1–9.

Madigan, M.T., J.M. Martinko, D.A. Stahl, and D.P. Clark. 2010. Brock Biology of Microorganisms, 13th ed., Pearson Benjamin-Cummings, San Francisco.

Magot, M., P. Caumette, J.M. Desperrier, R. Matheron, C. Dauga, F. Grimont, and L. Carreau. 1992. *Desulfovibrio longus* sp. nov., a sulfate-reducing bacterium isolated from an oil-producing well. Int. J. Syst. Bacterial. 42: 398–403.

Mara, D.D., and D.J.A. Williams. 1972. Polarization of pure iron in the presence of hydrogenase-positive microbes. II. Photosynthetic bacteria and microalgae. Corr. Sci. 12: 29–34.

Marquis, F.D.S. 1989. Strategy of macro and microanalysis in microbial corrosion. In: Sequeira, C.A.C., Tiller, A.K. (eds.), Microbial Corrosion. Elsevier Applied Science, London, pp 125–151.

Mata, J., D. Varade, and P. Bahadur. 2005. Aggregation behavior of quaternary salt based cationic surfactants. Thermochim. Acta. 428: 147–155.

Maxwell, S., C. Devine, F. Rooney, and I. Spark. 2004. Monitoring and control of bacterial biofilms in oilfield water handling systems, Paper No. 04752, Corrosion 2004, NACE International, Houston, TX.

Mayilraj, S., A. H. Kaksonen, R. Cord-Ruwisch, P. Schumann, C. Spröer, B. J. Tindall, and S. Spring. 2009. *Desulfonauticus autotrophicus* sp. nov., a novel thermophilic sulfate-reducing bacterium isolated from oil-production water and emended description of the genus Desulfonauticus, Extremophiles. 13: 247–255.

McDonnell G, and A.D. Russell. 1999. Antiseptics and disinfectants: activity, action, and resistance. Clin Microbiol Rev. 12: 147

McElhiney, J.E., and R.E. Davis. 2002. Desulfated Seawater and its Impact on t-SRB Activity: An Alternative Souring Control Methodology. In Corrosion 2002. Paper 02028. NACE international, Houston, Tex.

McSwain BS, R.L. Irvine, M. Hausner, and P.A. Wilderer. 2005. Composition and distribution of extracellular polymeric substances in aerobic flocs and granular sludge. Appl Environ Microbiol 71:1051–1057.

Menger, F.M., and C.A. Littau. 1993. Gemini Surfactants: A New Class of Self-Assembling Molecules. J. Am. Chem. SOC. 115: 10083–10090.

Menger, F.M., J.S. Keiper, B.N.A. Mbadugha, K.L. Caran, and L.S. Romsted. 2000. "Interfacial Micelles Determined by Chemical Trapping" Langmuir. 16: 9095–9098.

Miletto, M., P.L.E. Bodelier, and H.J. Laanbroek. 2007. Improved PCR-DGGE for high resolution diversity screening of complex sulfate-reducing prokaryotic communities in soils and sediments. J Microbiol Meth. 70: 103–111.

Miller T.L, and M.J. *Wolin*. 1974. A serum bottle modification of the Hungate technique for cultivating obligate anaerobes. Appl Microbiol. *27: 985–987*

Miyazaki, S., H. Sugawara, K. Ikeo, T. Gojobori, and Y. Tateno. 2004. DDBJ in the stream of various biological data Nucleic Acids Research. 32: 31–34.

Mori, K., H. Tsurumaru, and Harayama. 2010. Iron corrosion activity of anaerobic hydrogen-consuming microorganisms isolated from oil facilities, Journal of Bioscience and Bioengineering. 110: 426–430.

Murray, J.M. 2005. Confocal microscopy, deconvolution, and structured illumination methods. In: Spector D.L., Goldman R.D. (eds) Basic methods in microscopy. Cold Spring Harbor Laboratory, New York.

Muyzer, G., and A.J.M. Stams. 2008. The ecology and biotechnology of sulfate-reducing bacteria. Nature reviews. Microbiology. 6: 441–453.

Muyzer, G., E.C. De Waal, and A. G. Uitterlinden. 1993. Profiling of complex microbial populations by denaturing gradient gel electrophoresis analysis of polymerase chain reaction-amplified genes encoding for 16S rRNA, Applied and Environmental Microbiology. 59: 695–700.

Nagpal, S., S. Chuichulcherm, A. Livingston, and L. Peeva. 2000. Ethanol utilization by sulfate-reducing bacteria: an experimental and modeling study, Biotechnology and Bioengineering. 70: 533–543.

Neculita, C.M., G.J. Zagury, and B. Bussière. 2007. Passive treatment of acid mine drainage in bioreactors using sulfate-reducing bacteria: critical review and research needs, Journal of Environmental Quality. 36: 1–16.

Nemati M., T.J. Mazutinec, G.E. Jenneman, and G. Voordouw. 2001. Control of biogenic H2S production with nitrite and molybdate. JInd Microbiol Biotech 26: 350–355.

Neria-Gonzalez, I., E. T. Wang, F. Ramırez, J. M. Romero, and C. Hernandez-Rodriguez. 2006. Characterization of bacterial community associated to biofilms of corroded oil pipelines from the southeast of Mexico. Anaerobe. 12: 122–133.

Neu TR, and J.R. Lawrence. 1997. Development and structure of microbial biofilms in river water studied by confocal laser scanning microscopy. FEMS Microbiol Immunol. 24:11–25

Neu TR, G.D.W. Swerhone, and J.R. Lawrence. 2001. Assessment of lectin binding analysis for in situ detection of glycoconjugates in biofilm systems. Microbiology 147:299–313

Neu TR, S. Woelfl, and J.R. Lawrence 2004. Three-dimensional differentiation of photo autotrophic biofilm constituents by multi-channel laser scanning microscopy single-photon and two-photon excitation. J Microbiol Methods 56:161–172

Neu, T.R. 1996. Significance of bacterial surface-active compounds in interaction of bacteria with interfaces. Microbiology Reviews. 60: 151–166.

Neu, T.R. 2000. In situ cell and glycoconjugate distribution in river snow studied by confocal laser scanning microscopy. Aquat Microb Ecol. 21: 85–95.

Nga, D.P., D.T.C. Ha, T.C. Hien, and H. Stan-Lotter. 1996. *Desulfovibrio vietnamensis* sp. nov., a halophilic sulfate-reducing bacterium from Vietnamese oil fields. Anaerobe. 2: 385–392.

Nilsen, R.K., T. Torsvik, and T. Lien. 1996. *Desulfotomaculum thermocisternum* sp. nov., a sulfate reducer isolated from a hot North Sea oil reservoir. Int J Syst Bacteriol. 46: 397–402.

North, A. J. 2006. Seeing is believing? A beginners' guide to practical pitfalls in image acquisition. J. Cell Biol., 172: 9–18.

Nunoura, T., Y. Takaki, J. Kakuta, S. Nishi, J. Sugahara, H. Kazama, G.J. Chee, M. Hattori, A. Kanai, and H. Atomi. 2011. Insights into the evolution of Archaea and eukaryotic protein modifier systems revealed by the genome of a novel Archaeal group. Nucleic Acid Res. 39: 3204-3223

Ollivier, B., C.E. Hatchikian, G. Prensier, J. Guezennec, and J.-L. Garcia. 1991. *Desulfohalobium retbaense gen*. nov. sp. nov. a halophilic sulfate-reducing bacterium from sediments of a hypersaline lake in Senegal. International Journal of systematic Bacteriology. 4: 74–81.

Orphan, V.J., L.T. Taylor, D. Hafenbradl, and E.F. Delong. 2000. Culture-dependent and culture-independent characterization of microbial assemblages associated with high-temperature petroleum reservoirs. Appl. Environ. Microbiol. 66: 700–711.

Page, R.D.M. 1996. Tree View: an application to display phylogenetic trees on personal computers. Computer Applications in Biosciences. 12: 357–358.

Pedersen, A., and M. Hermansson. 1991. Inhibition of metal corrosion by bacteria. Biofouling. 3: 1-11.

Peng, C.and J.K. Park. 1994. Electrochemical mechanisms of corrosion influenced by sulfate-reducing bacteria in aquatic systems. Water Res. 28 (8): 1681-1692.

Percival, S.L. 1999. The effect of molybdenum on biofilm development. Journal of Industrial Microbiology and Biotechnology. 23: 112–117.

Perez, L., J.L. Torres, A. Manresa, C. Solans, and M.R. Infante. 1996. Synthesis, aggregation, and biological properties of a new class of gemini cationic amphiphilic compounds from arginine, bis(Args). Langmuir. 12: 5296–5301.

Pietzsch, K., and W. Babel. 2003. A sulfate-reducing bacterium that can detoxify U(VI) and obtain energy via nitrate reduction. J. Basic Microbiol. 43: 348–361.

Postgate, J.R. 1984. The sulfate reducing bacteria 2nd ed., Cambridge University Press, London and New York. 30–100.

Quraishi, M.A., F. A. Ansari, and D. Jamal. 2002. Thiourea derivatives as corrosion inhibitors for mild steel in formic acid. Mater. Chem. Phys. 77: 687–690.

Rabus, R., T. Hansen, and F. widdel. 2000. Dissimilatory sulfate and sulfur-reducing prokaryotes. In M. Dworkin, S. Falkow, E. Rosenberg, K.-H. Schleifer, and E. Stackebrandt (ed.) The prokaryotes: an Evolving electronic resource for the microbiological community. Springer-Verlag, New York.

Rabus, R., T.A. Hansen, and F. Widdel. 2006. Dissimilatory sulfate and sulfur-reducing prokaryotes, In: The Prokaryotes Vol. 2, 3ed Edition, Eds. Dworkin M., Falkow S., Rosenberg E., Schleifer K.H., Stackebrandt E., Springer Science, Singapore.

Rajasekar, A., B. Anandkumar, S. Maruthamuthu, Y.P. Ting, and P.K. Rahman. 2010. Characterization of corrosive bacterial consortia isolated from petroleum-product-transporting pipelines. Appl Microbiol Biotechnol. 85:1175–1188.

Refaey, S.A.M. 2005. Inhibition of steel pitting corrosion in HCl by some inorganic anion, Appl. Surf. Sci. 240: 396-404.

Revie, R.W., and H.H. Uhlig. 2008. Corrosion and corrosion control, an Introduction to Corrosion Science and Engineering. Fourth ed. JOHN WILEY & SONS, INC, pp 96.

Rickard, D.T. 1969. The microbiological formation of iron sulfides. Stockholm Contrib Geol. 20: 50–66.

Rosen, M. J. 1989. Surfactants and interfacial phenomena, Wiley, New York, 2ed.

Rosen, M.J., F. Li, S.W. Morrall, D.J. Versteeg. 2001. The relationship between the interfacial properties of surfactants and their toxicity to aquatic organisms. Environ. Sci. Technol. 35: 954–959.

Rosnes, J.T., T. Torsvik, and T. Lien. 1991. Spore forming thermophilic sulfate-reducing bacteria isolated from North Sea oil field waters. Appl. Environ. Microbiol. 57: 2302–2307.

Ruseska, I., J. Robbins, E.S. Lashen, and J.W. Costerton. 1982. Biocide testing against corrosion-causing oilfield bacteria helps control plugging. Oil Gas J. pp 253–264.

Saitou, N., and M. Nei. 1987. The neighbor-joining method, a new method for constructing phylogenetic trees. Mol. Biol. Evol. 4: 406–425.

Samakande, A., R. Chaghi, G. Derrien, C. Charnay, and P. C. Hartmann. 2008. Aqueous behavior of cationic surfactants containing a cleavable group. J. Colloid Interface Sci. 320: 315–320.

Sanders, P.F., and P.J. Sturman. 2005. Biofouling in the oil industry. In: Petroleum Microbiology (B. Ollivier and M. Magot), ASM Press, Washington, D.C.

Sanders, P.F., and W. A. Hamilton. 1983. Biological and corrosion activities of sulphate-reducing bacteriain industrial process plant, in Biologically Induced Corrosion, ed. S. C. Dexter (Houston, TX: NACE International, 47–68.

Sastri, V.S. 1998. Corrosion inhibitor, vol 373. Wiley, New York, pp 39-40.

Scala, D.J., and L.J. Kerkhof. 1999. Diversity of nitrous oxide reductase (*nosZ*) genes in continental shelf sediments. Appl. Environ. Microbiol. 65: 1681–1687.

Schink, B., and A.J.M. Stams. 2006. In the Prokaryotes (eds Dworkin, M., Schleifer, K-H. and Stackebrandt, E.). Springer Verlag, New York. pp 309–335.

Schmidtova, J., and S.A. Baldwin. 2011. Correlation of bacterial communities supported by different organic materials with sulfate reduction in metal-rich landfill leachate. Water Research. 45: 1115–1128.

Singare, P.U., and J.D. Mhatre 2012. Development of arginine based mono-peptides as cationic surfactants from pure amino acid, Science and Technology. 2:55–60.

Skolink, A.K., W. C. Hughes, and B. H. Augustine. 2000. A metallic surface corrosion study in aqueous NaCl solution using Atomic Force Microscopy (AFM). Chemical Education. 5: 8–13.

Skorko-Glonek, J., D. Zurawa, E. Kuczwara, M. Wozniak, Z. Wypych, and B. Lipinska. 1999. *Escherichia coli* heat shock HtrA protease participates in the defense against oxidative stress. Mol Gen. Genet. 262: 342–350.

Staudt C, H. Horn, D.C. Hempel, and T.R. Neu .2004. Volumetric measurements of bacterial cells and extracellular polymeric substance glycoconjugates in biofilms. Biotechnol Bioeng 88:585–592

Stetter, K.O., T. Huber, E. Blochl, M. Kurr, R.D. Eden, M. Fielder, H. Cash, and I. Vance. 1993. Hyperthermophilic *Archaea* are thriving in deep North-Sea and Alaskan oil reservoirs. Nature, 365: 743–745.

Steuber,J., and P.M.H. Kroneck. 1998. Desulfoviridin, the dissimilatory sulfite reductase *from Desulfovibrio desulfuricans* (Essex)-new structural and functional aspects of the membranous enzyme. Inorg. Chim. Acta. 276: 52–57.

Stoodley, P., K. Sauer, D.G. Davies, and J.W. Costerton. 2002. Biofilms as complex differentiated communities. Annu. Rev, Microbiol. 56: 187–209.

Strathmann M, J. Wingender, and H.C. Flemming .2003. Application of fluorescently labeled lectins for the visualization and biochemical characteristics of polysaccharides in biofilm *of Pseudomonas aeruginosa.* J Microbiol Methods 50:237–248.

Straub, K.L., and B.E.E. Buchholz-Cleven. 1998. Enumeration and detection of anaerobic ferrous iron-oxidizing, nitrate-reducing bacteria from diverse European sediments. Appl. Environ. Microbiol. 64: 4846-4856.

Sturman, P.J., D.M. Goeres, and M.A. Winters. 1999. Control of hydrogen sulfide in oil and gas wells with nitrite injection. SPE 56772. Society of Petroleum Engineers, Richardson, Tex.

Sunde, E., B.L.B. Lilebo, G. Bodtker, T. Torsvik, and T. Thorstenson. 2004. H_2S inhibition by nitrate injection to the Gulfaks field. In: Proceedings of corrosion, New Orleans, paper no. 04760.

Surman, S.B., J.T. Walker, D.T. Goddard, L.H.G. Morton, C.W. Keevil, W. Weaver, A. Skinner, D. Caldwell, and J. Kurtz. 1996. Comparison of microscope techniques for the examination of biofilms. Journal of Microbiological Methods. 25: 57–70.

Sutherland, I.W. 1985. Biosynthesis and composition of Gram-Negative bacterial-extracellular and wall polysaccharides, Annual Review of Microbiology. 39: 243–262.

Sutton, N.A., N. Hughes, and P.S. Handley. 1994. A comparison of conventional SEM techniques, low temperature SEM and the electroscan wet scanning electron microscope to study the structure of biofilms of *Streptococcus crista* CR3. J. Appl. Bacteriol. 76: 448–54.

Takai, K., and K. Nakamura. 2011. Archaeal diversity and community development in deep sea hydrothermal vents. Curr. Opın. Mıcrobıol. 14: 282–291

Tardy-Jacquenod, C., M. Magot, B.K.C. Patel, R. Matheron, and P. Caumette. 1998. Desulfotomaculum halophilutn sp. nov., a halophilic sulfate-reducing bacterium isolated from oil production facilities. Int. Syst. Bacterial. 48: 333–338.

Tardy-Jacquenod, C., M. Magot, F. Laigret, M. Kaghad, B.K. Patel, J. Guezennec, R. Matheron, and P. Caumette.1996. *Desulfovibrio gabonensis* sp. nov., a new moderately halophilic sulfate-reducing bacterium isolated from an oil pipeline. Int. J. Syst. Bacterial. 46: 710–715.

Tawfik M.S., A. Sayed, and I. Aiad. 2012. Corrosion inhibition by some cationic surfactants in oil fields, Journal of Surfactant and detergent.

Thangavel, K., and N.S. Rengaswamy. 1998. Relationship between Chloride/hydroxide Ratio and Corrosion Rate of Steel in Concrete Cement and Concrete Composites 20: 283–292.

Thauer, R.K., and W. Badziong. 1980. Respiration with sulfate as electron acceptor, In G. J. Knowles (ed.), Diversity of Bacterial Respiratory Systems. CRC Press, Inc., Boca Raton, Fla. 2: 65–85.

Thevenieau, F., M.L. Fardeau, B. Ollivier, C. Joulian, and S. Baena. 2007. *Desulfomicrobium thermophilum* sp. nov., a novel thermophilic sulphate-reducing bacterium isolated from a terrestrial hot spring in Colombia. Extremophiles. 11: 295–303.

Trudinger, P.A., and R.E. Loughlin. 1981. Metabolism of simple sulfur compounds. In Neuberger A., and van-Deenen L.L.M. (ed.), Comprehensive Biochemistry. Elsevier, Amsterdam, Netherlands. 19a: 165–256.

Tsukamoto, T.K., H.A. Killion, and G.C. Miller. 2004. Column experiments for microbiological treatment of acid mine drainage: low-temperature, low-pH and matrix investigations. Water Res. 38: 1405–1418.

Tsuru, T. 1991. Anodic dissolution mechanisms of metals and alloys, Mater. Sci. Eng., 146 1–14.

Utgikar, V., S. Harmon M., N. Chaudhary, H. Tabak H., R. Govind and J. R. Haines. 2002. Inhibition of sulfate reducing bacteria by metal sulfide formation in bioremediation of acid mine drainage, Wiley Periodicals, Inc.

Vashi , R.T., and H. K. Kadiya. 2009. Corrosion study of metals in marine environment. E-Journal of Chemistry, 6(4): 1240–1246.

Videla, H.A. 2000. An overview of mechanisms by which sulfate-reducing bacteria influence corrosion of steel in marine environments. Biofouling. 15:37–47.

Videla, H.A. 2001. Microbial induced corrosion: an updated overview. Int. Biodeter. Biodegrad. 48: 176–201.

Von Wolzogen Kuhr, C.A.H., and I.S. Van der Vlugt. 1934. Graphication of cast iron as an electrochemical process in anaerobic soils, Water. 18: 147–165.

Voordouw, G. and A.J. Telang. 1999. The geomicrobiological role of sulfate-reducing bacteria in environments contaminated by petroleum products. Microbial Ecology of Oil fields.

Voordouw, G., J.K. Voordouw, T.R. Jack, J. Foght, P.M. Fedorak, and D.W.S. Westlake. 1992. Identification of distinct communities of sulfate-reducing bacteria in oil-fields by reverse sample genome probing. Appl. Environ. Microbiol. 58: 3542–3552.

Voordouw, G., J.K. Voordouw, T.R. Jack, J. Foght, P.M. Fedorak, and D.W.S. Westlake. 1992. Identification of distinct communities of sulfate-reducing bacteria in oil fields by reverse sample genome probing. Appl. Environ. Microbiol. 58: 3542–3552.

Voordouw, G., S.M. Armstrong, M.F. Reimer, B. Fouts, A.J. Telang, Y. Shen, and D. Gevertz. 1996. Characterization of 16S rRNA genes from oil field microbial communities indicates the presence of a variety of sulfate-reducing, fermentative, and sulfide-oxidizing bacteria. Appl. Environ. Microbiol. 62: 1623–1629.

Voordouw, G.M., M. Nemati, and G.E. Jenneman. 2002. Use of nitrate-reducing, sulfide oxidizing bacteria to reduce souring in oilfields: interactions with SRB and effects on corrosion. In corrosion 2002. Paper 02034. NACE International, Houston, Tex.

Wagner M., A. Loy, M. Klein, N. Lee, N.B. Ramsing, D.A. Stahl, and M.W. Friedrich. 2005. Functional marker genes for identification of sulfate-reducing bacteria. Meth. Enzymol. 397: 469–487.

Wagner, M., N.P. Ivleva, C. Haisch, R. Niessner, and H. Horn. 2009. Combined use of confocal laser scanning microscopy (CLSM) and Raman microscopy (RM): Investigations on EPS-Matrix. Water Research. 43: 63–76.

Wang, Y., Y. Han, X. Huang, M. Cao, and Y. Wang. 2008. Aggregation behaviors of a series of anionic sulfonate gemini surfactants and their corresponding monomeric surfactant. Journal of Colloid and Interface Science. 319: 534–541.

Ward, D.M, and M.R. Winfrey. 1985. Interactions between methanogenic and sulfate-reducing bacteria in sediments. Adv Aquat Microbiol. 3: 141–179.

Wen, J., K. Zhao, T. Gu, and I.I. Raad. 2009. A green biocide enhancer for the treatment of sulfate-reducing bacteria (SRB) biofilms on carbon steel surfaces using glutaraldehyde: International Biodeterioration Biodegradation. 63:1102–1106.

White, D.C., P.D. Nivens, A.T. Nichols, B. D. Kergrer, J.M. Henson, G. G. Geesey, and C.K. Clarke. 1985. Corrosion of steel induced by aerobic bacteria and their extracellular polymers. In proceedings of International Workshop on Biodeterioration held at the University of La Plata, Argentina. 73–86.

Whitman, W.B., T.L. Bowen, and D.R. Boone. 1992. The methanogenic bacteria. In The prokaryotes, 2nd ed. (ed. A. Balows et al.). Springer- Verlag, New York. 1: 719–767.

Widdel, F., and F. Bak. 1992. Gram-negative mesophilic sulfate-reducing bacteria. In A. Balows, H.G. Trüper, M. Dworkin, W Harder, and K.-H. Schleifer (ed.), The prokaryotes, 2nd ed. Springer-Verlag, New York. 1: 3352–3378.

Wingender, J., T.R. Neu, and H-C. Flemming. 1999. What are bacterial extracellular polymeric substances? in Microbial Extracellular Polymeric Substances: characterization, structure and function, ed. by Wingender J., Neu T.R., Flemming H.-C, Springer, Berlin-New York. pp. 1–19.

Zhao, K. 2008. Investigation of microbiologically influenced corrosion (MIC) and biocide treatment in anaerobic salt water and development of a mechanistic MIC model. Ph.D thesis, Ohio University.

Zhou, M., J. Zhao, and X. Hu. 2012. Synthesis of Bis[N,N′-(alkylamideethyl)ethyl Triethylene-diamine bromide surfactants and their oilfield application investigation, Journal of Surfactants and Detergents. 3: 309–315.

Zhu, X., J. Lubeck, and J. Kilbane II. 2003. Characterization of microbial communities in gas industry pipelines. Appl. Environ. Microbiol., 5354–5363.

A- Appendix

FTIR

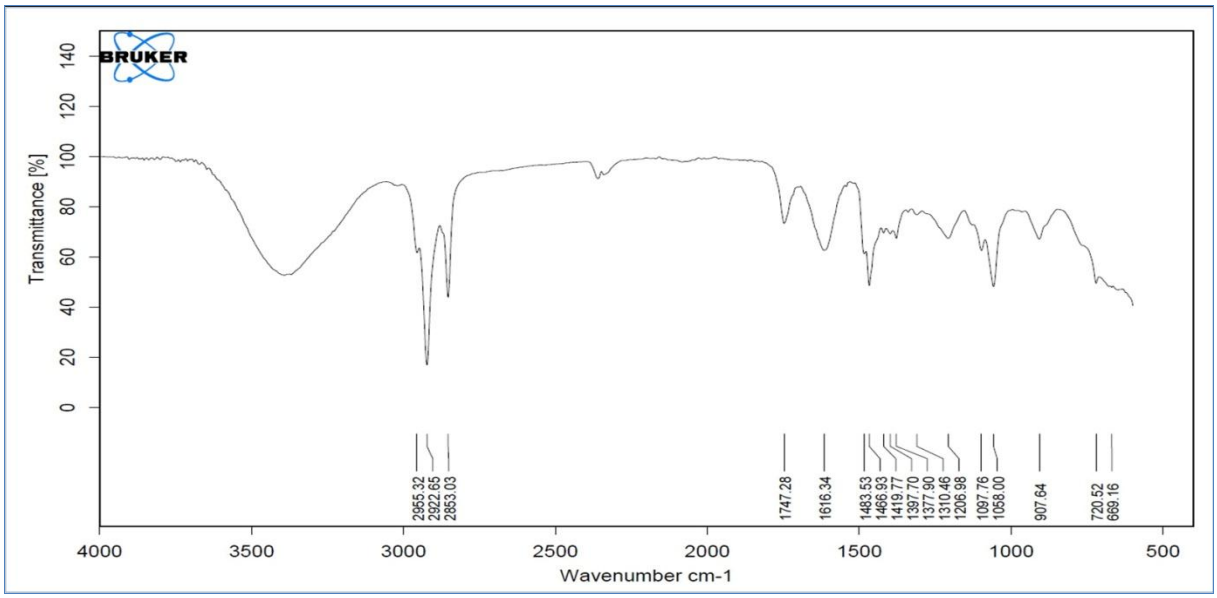

(a) FTIR spectra of the CMS-I showed that the characteristic peaks for the alkyl moiety are 2916.77 and 2849.92 cm^{-1} for asymmetric and symmetric stretching (CH) respectively. While at 1383.32 cm^{-1} for symmetric bending (CH_3), 1468.86 cm^{-1} for symmetric bending (CH_2) and 718.92 cm^{-1} for–$(CH_2)_n$– rocking. R_4N^+ appeared band at 1093.79 cm^{-1}.The FTIR spectra confirmed the expected functional groups in the synthesized cationic monomeric surfactant.

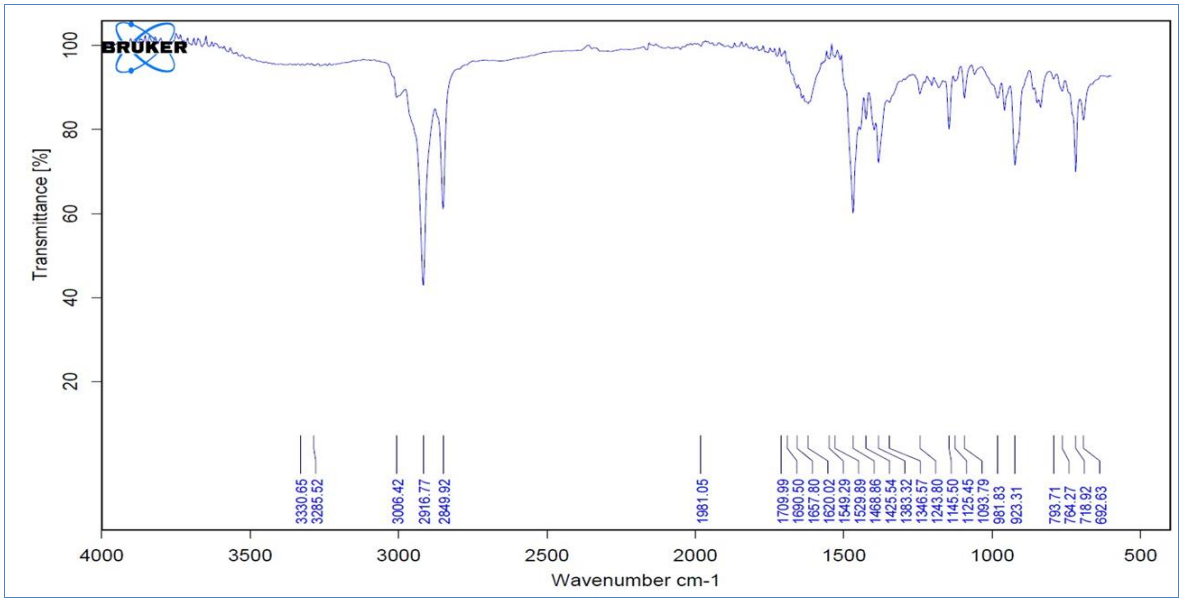

(b) FTIR spectra of the CGS displayed that the characteristic peaks for the alkyl moiety are 2916.63 and 2849.74 cm^{-1} for asymmetric and symmetric stretching (CH), respectively. While at 1383.31 cm^{-1} for symmetric bending (CH3), 1468.56 cm^{-1} for symmetric bending (CH_2) and 719.04 cm^{-1} for –(CH_2)n– rocking. For C=C ring stretching exhibited absorption band at 1549.31 cm^{-1}, =C–C stretching showed band at 1612.92 cm^{-1} and at 300.58 cm^{-1} for stretching absorption band of =C–H ring. R_4N^+ appeared band at 1059.05 cm^{-1}; while broad band at 1737.98 cm^{-1} is due to the presence of ester group. The FTIR spectra also confirmed the expected functional groups in the synthesized cationic gemini surfactant.

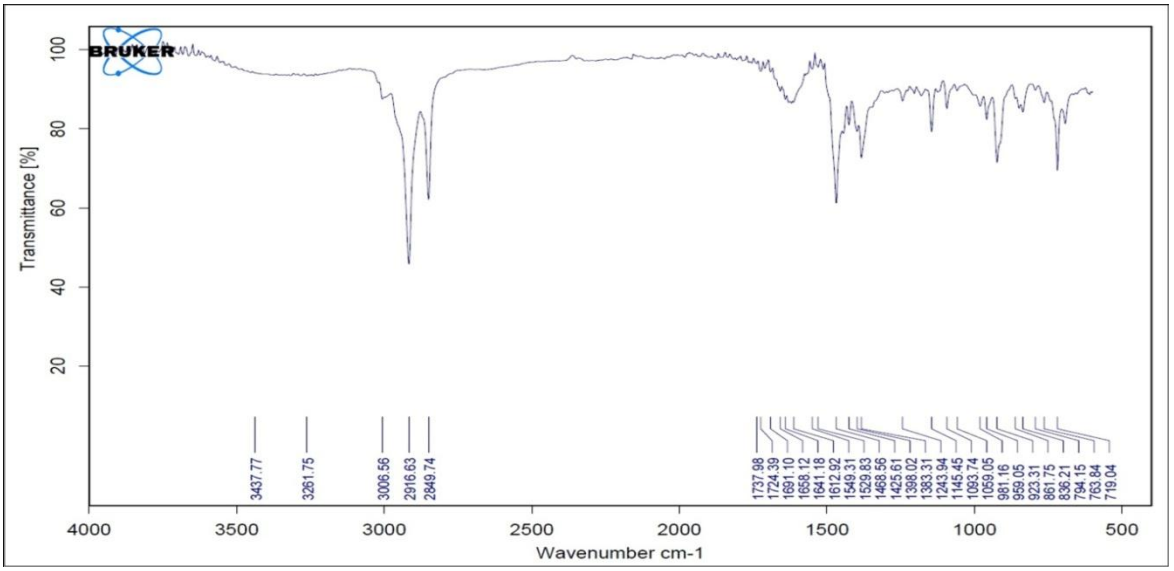

(c) FTIR spectra of the synthesized NCGS demonstrated that the characteristic bands for the alkyl moiety are 2922.65, 2853.03 cm^{-1} for asymmetric and symmetric stretching (CH), respectively. While at 1377.90 cm^{-1} for symmetric bending (CH3), at 1466.93 cm^{-1} for symmetric bending (CH2) and at 720.52 cm^{-1} for –(CH2)n–rock. R_4N^+ appeared band at 1058.00 cm^{-1}. In addition to band at 1097.76 cm^{-1} for P–O–C aliphatic and band at 907.64 cm^{-1} corresponding to ionic phosphate and at 1150. 64 cm^{-1} for P=O stretching. The FTIR spectra confirmed the expected functional groups in the synthesized cationic gemini surfactant.

Figure A–1. FTIR analyses of the synthesized surfactants are shown. (a) CMS-I, (b) CGS-II and (c) CGS-III.

^{1}H NMR

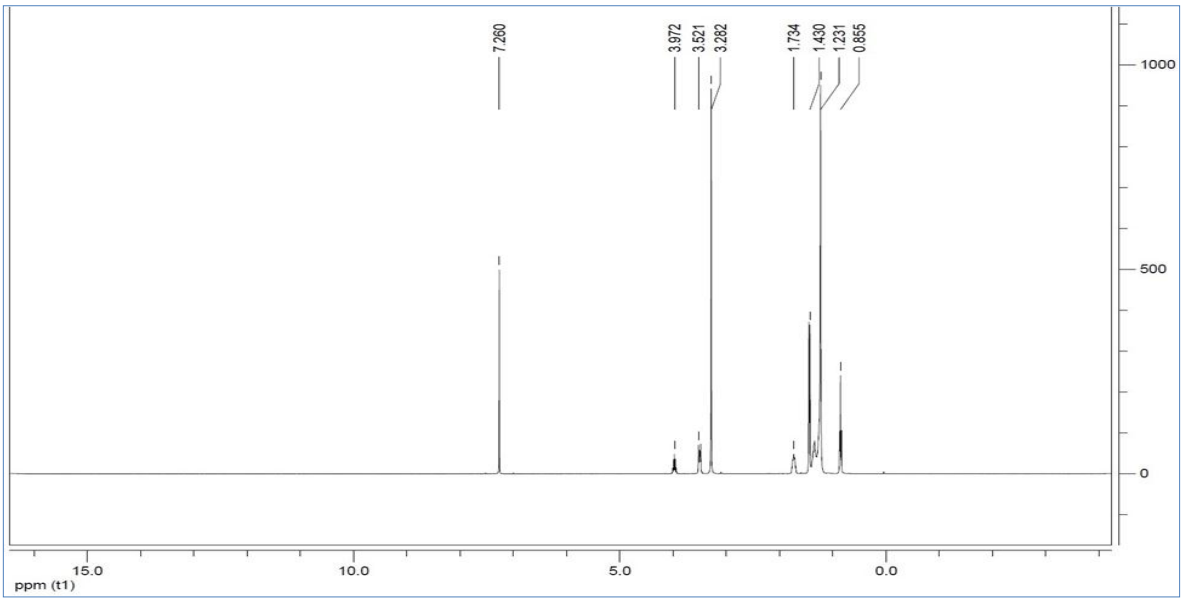

(a) ^{1}H NMR (DMSO) spectrum of the CMS-I showed different peaks at 0.85 ppm (t, 3H, $NCH_2CH_2(CH_2)_9CH_3$), at 1.23 ppm (m,16H, $NCH_2CH_2(CH_2)_9CH_3$), at 1.73 ppm (m, 2H, $NCH_2CH_2(CH_2)_9CH_3$), at 3.28 ppm (t, 2H, $NCH_2CH_2(CH_2)_9CH_3$), at 3.52 ppm (s, 3H, NCH_3), at 3.97 ppm (m, 1H, $NCH(CH_3)_2$), at 1.43 ppm (d, 6H, $NCH-(CH_3)_2$).

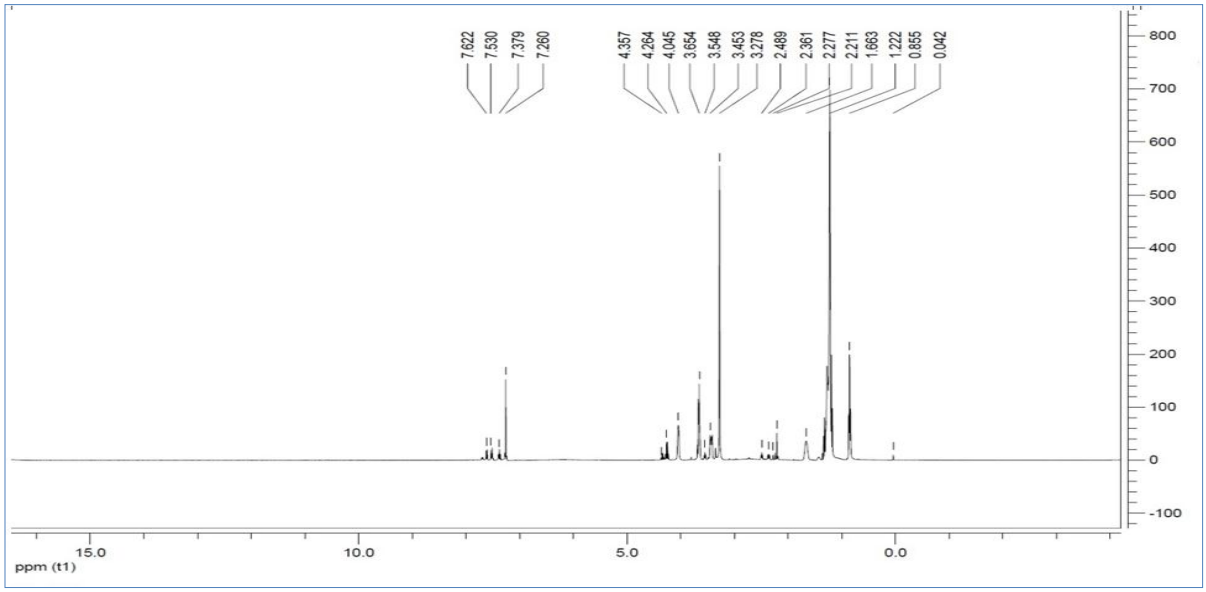

(b) ^{1}H NMR (DMSO) spectrum of the CGS-II presented different peaks at δ=0.85 ppm (t, 3H, $NCH_2CH_2(CH_2)_9CH_3$); δ=1.22 ppm (m, 18H, $NCH_2CH_2(CH_2)$ $9CH_3$); δ=1.68 ppm (m, 2H, $NCH2CH_2$-$(CH2)_9CH_3$); δ=3.27 ppm (t, 2H, NCH_2 CH_2 $(CH_2)_9CH_3$); at 3.45 ppm (s, 3H, NCH_3); δ=3.65 ppm (t, 3H, NCH_2CH_2O); δ=4.28 ppm (t, 2H, NCH_2CH_2O); δ=7.28 ppm (d, 1H, Ar-H); δ=7.53 ppm (s, 1H, Ar-H).

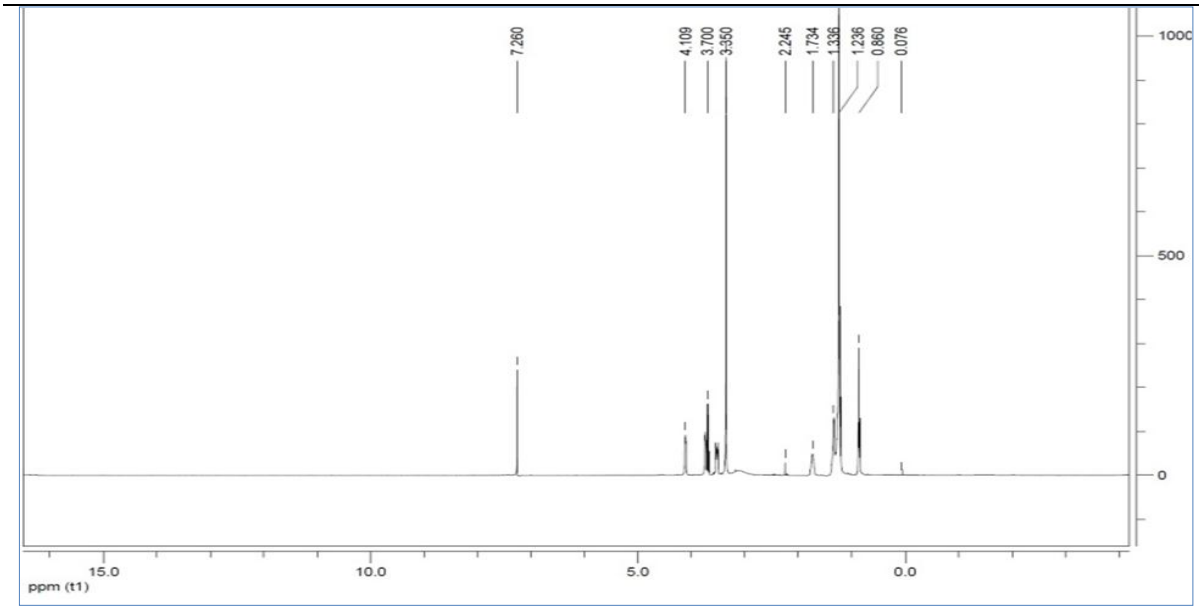

(c) ^{1}H NMR (DMSO) spectrum of the CGS-III exhibited different peaks at δ=0.88 ppm (t, 3H, $NCH_2CH_2(CH_2)_9CH_3$); δ=1.23 ppm (m, 18H, NCH_2CH_2-$(CH_2)_9CH_3$); δ=1.73 ppm (m, 2H, $NCH_2CH_2(CH_2)_9CH_3$); δ=3.35 ppm (t, 2H, NCH_2CH_2-$(CH_2)_9CH_3$); at 3.45 ppm (s, 3H, NCH_3); δ=3.70 ppm (t, 3H, NCH_2CH_2OP); δ=4.11 ppm (t, 2H, NCH_2CH_2OP).

Figure A–2. ^{1}H NMR analyses of the synthesized surfactants are shown. (a) CMS-I, (b) CGS-II, and (c) CGS-III

^{13}C NMR

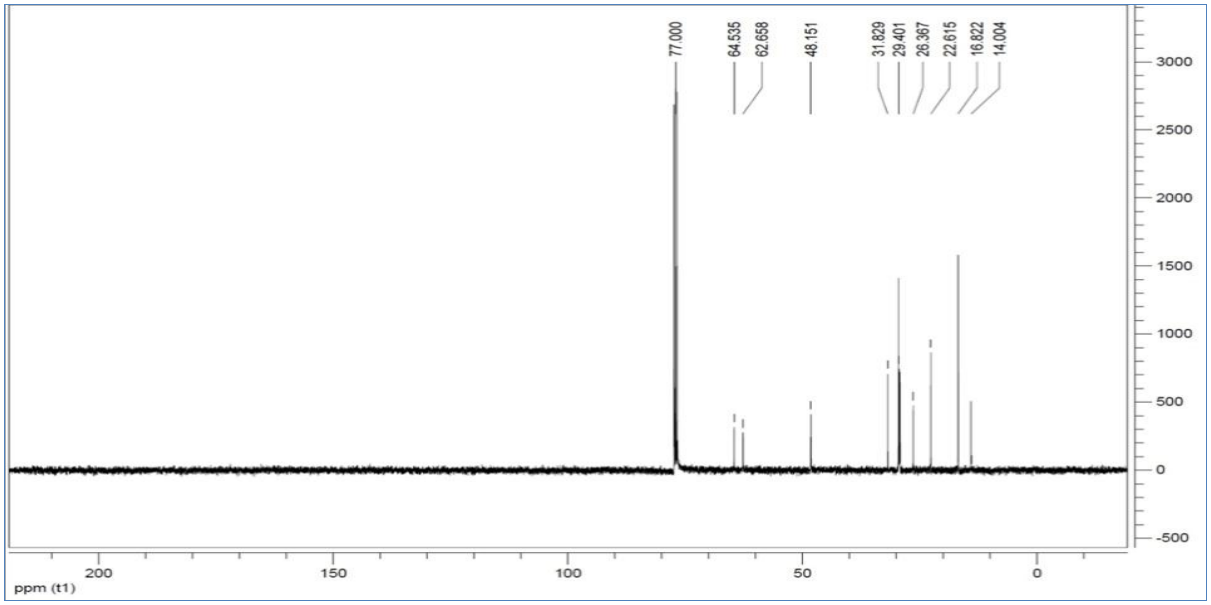

(a) ^{13}C NMR ($CDCl_3$) spectrum of the CMS-I demonstrated different peaks at δ=14.00 ppm ($NCH_2CH_2CH_2(CH_2)_6CH_2CH_2CH_3$); δ=16.82 ppm ($NCH_2CH_2$-$CH_2(CH_2)_6CH_2CH_2CH_3$); δ=22.62 ppm ($NCH_2CH_2CH_2$-$(CH_2)_6CH_2CH_2CH_3$); δ=29.40 ppm ($NCH_2CH_2CH_2(CH_2)_6CH_2CH_2$-$CH_3$); δ=26.37 ppm ($NCH_2CH_2CH_2(CH_2)_6CH_2CH_2$-$CH_3$); δ=26.37 ppm ($NCH_2CH_2CH_2(CH_2)_6$- $CH_2CH_2CH_3$); δ=64.54 ppm ($NCH_2CH_2CH_2$ $(CH_2)_6CH_2CH_2CH_3$); at δ=48.15 ppm (NCH_3); at δ=62.66 ppm ($NCH(CH_3)_2$), at δ=18.82 ppm ($NCH(CH_3)_2$).

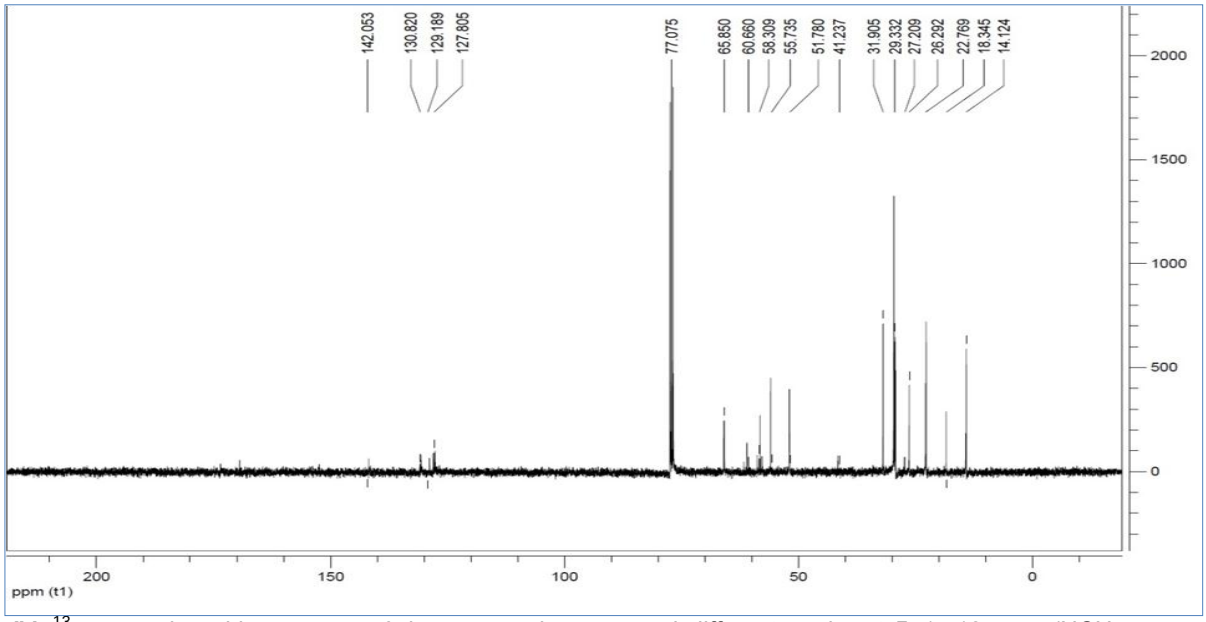

(b) ^{13}C NMR ($CDCl_3$) spectrum of the CGS-II demonstrated different peaks at δ=14.12 ppm ($NCH_2CH_2CH_2$-$(CH_2)_6CH_2CH_2CH_3$); δ=18.35 ppm ($NCH_2CH_2CH_2(CH_2)_6$ CH_2 CH_2CH_3); δ=22.77 ppm ($NCH_2CH_2CH_2(CH_2)_6CH_2CH_2CH_3$); δ=29.33 ppm ($NCH_2$ CH_2 $CH_2(CH_2)_6CH_2CH_2CH_3$); δ=27.21 ppm ($NCH_2CH_2CH_2(CH_2)_6CH_2CH_2CH_3$); δ=26.29 ppm($NCH_2CH_2$ CH_2-$(CH_2)_6CH_2CH_2CH_3$); δ=65.85 ppm ($NCH_2CH_2CH_2$ $(CH_2)_6$ CH_2CH_2 CH_3); at δ=51.78 ppm (NCH_3); δ=60.66 ppm (NCH_2CH_2O); δ=58.31 ppm (NCH_2CH_2 O) ; δ=142.05 ppm (O-C=O); δ=129.19 ppm (Ar-H); δ=127.81 ppm (Ar-H); δ=130.82 ppm (Ar-H).

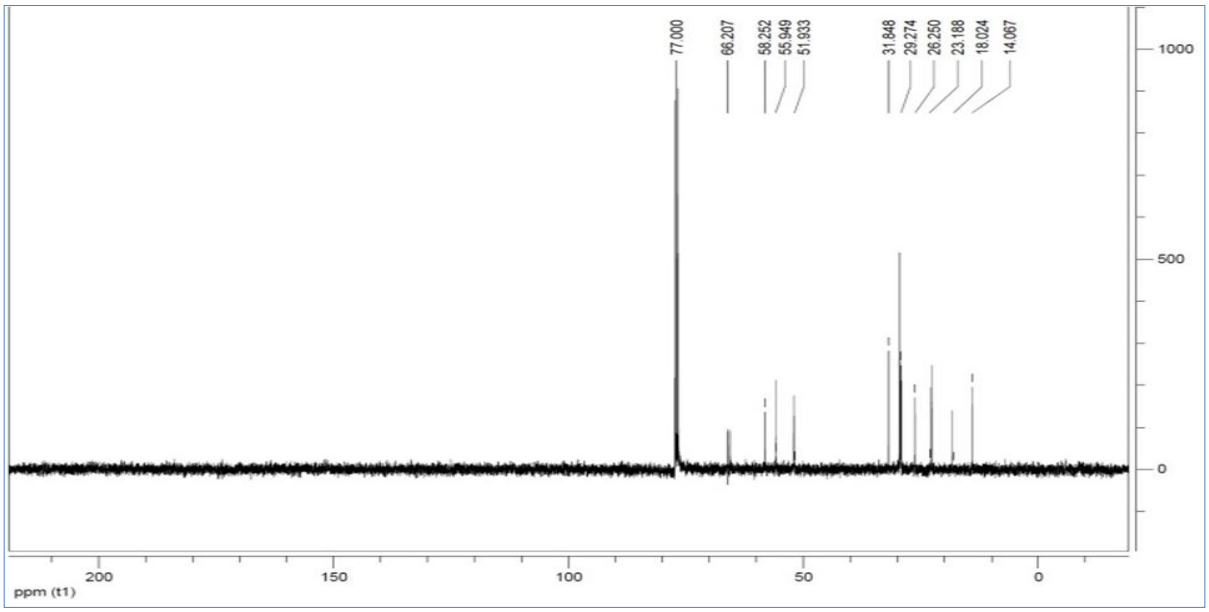

(c) ^{13}C NMR ($CDCl_3$) spectrum of the CGS-III presented different peaks at δ=14.07 ppm ($NCH_2CH_2CH_2(CH_2)_6CH_2CH_2CH_3$); δ=18.02 ppm ($NCH_2CH_2CH_2$-$(CH_2)_6CH_2CH_2$- CH_3); δ=23.19 ppm ($NCH_2CH_2CH_2(CH_2)_6CH_2CH_2CH_3$); δ=29.27 ppm ($NCH_2CH_2CH_2$-$(CH_2)_6$- $CH_2CH_2CH_3$); δ=26.55ppm ($NCH_2CH_2CH_2(CH_2)_6CH_2CH_2CH_3$); δ=23.18 ppm ($NCH_2CH_2CH_2$-$(CH_2)_6CH_2CH_2$-$CH_3$); δ=66.21 ppm ($NCH_2CH_2CH_2(CH_2)_6CH_2CH_2CH_3$) ; at δ=51.93 ppm ($NCH_3$); δ=58.25 ppm ($NCH_2CH_2O$); δ=55.95 ppm ($NCH_2CH_2O$).

Figure A–3. ^{13}C NMR analyses of the synthesized surfactants are shown. (a) CMS-I, (b) CGS-II, and (c) CGS-III.

^{31}P NMR

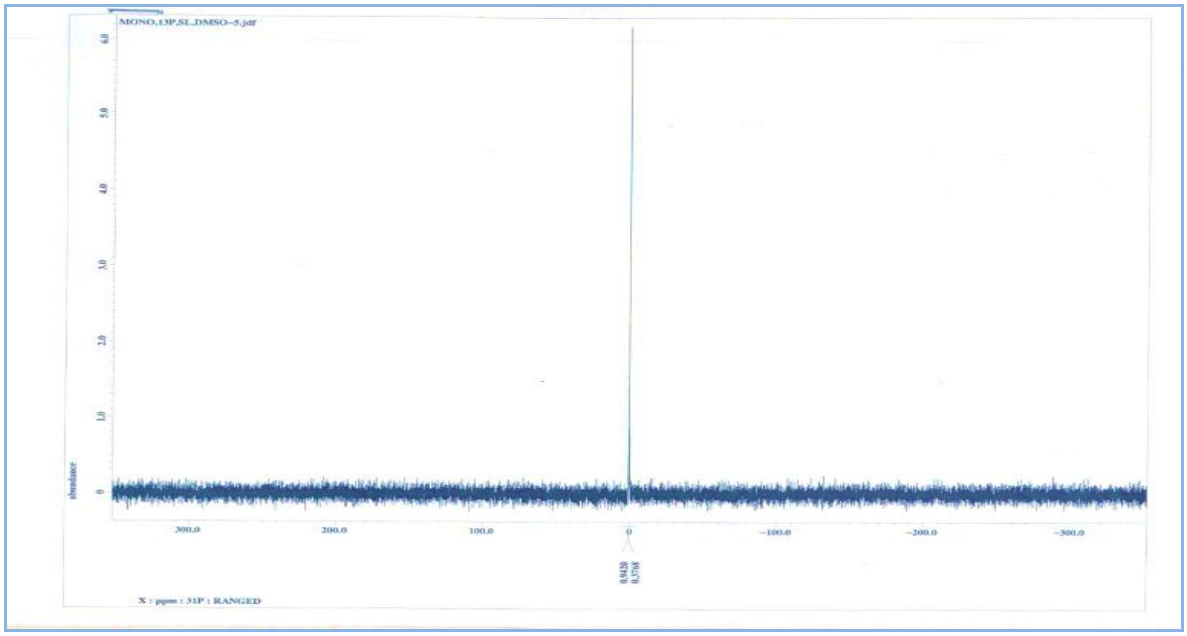

^{31}P NMR (DMSO) spectrum of the synthesized surfactants demonstrated characteristic signal at δp -0.5114 ppm

Figure A–4. ^{31}P NMR spectrum of the synthesized surfactant (CGS-III).